Fibroblast Regional Identity in the Murine Lymphoid System

by

Sarah Jayne Flavell

A thesis submitted to the School of Immunity and Infection
of the University of Birmingham
for the degree of
DOCTOR OF PHILOSOPHY

Department of Rheumatology
School of Immunity and Infection
College of Medical and Dental Sciences
University of Birmingham
B15 2TT
September 2009

ABSTRACT

Fibroblasts are the most abundant cell type of the stroma, producing extracellular matrix components which provide mechanical strength to tissues. Recent work has shown that fibroblasts are not simply passive structural cells but active participants in the immune response. Work on human fibroblasts has demonstrated distinct gene expression profiles dependent on their tissue of origin, indicating that fibroblasts impart topographical memory and positional identity to tissues.

In this study fibroblast heterogeneity within the murine lymphoid system was investigated by analysing gene and protein expression. Their functional ability to form lymphoid like structures was also assessed. Fibroblasts were isolated from a range of lymphoid and peripheral sites. Our findings show that fibroblasts grown from different sites show heterogeneous gene and protein expression and are also functionally different in their response to lymphotoxin α treatment *in vitro* and in their capacity to recruit host leucocytes *in vivo*. A novel *in vivo* functional assay has been developed using a collagen sponge as a three-dimensional structure in the kidney capsule transfer model, to assess the ability of fibroblasts to form and maintain lymphoid structures.

We conclude that murine fibroblasts isolated from lymphoid tissues, display site specific features. They are phenotypically distinct with site specific gene and protein expression profiles. These differences are reflected in functionally unique interactions with leucocytes and their cell products. This suggests that murine lymphoid fibroblasts have positional memory and help impart anatomical identity. An important implication of these findings is the effect this diversity may have in conveying site specificity to immune responses. Our work supports the hypothesis that fibroblasts help define a stromal postcode that directs leucocyte behaviour within lymphoid tissues.

Dedicated to Mum and Dad

ACKNOWLEDGEMENTS

Firstly, I would like to thank my supervisor, Professor Chris Buckley for his guidance and encouragement throughout my PhD. His enthusiasm for science is infectious and I have never failed to leave a meeting feeling positive.

Huge thanks to 'The Buckettes' (Dr Sian Lax, Dr Ewan Ross, Dr TieZheng Hou, Dr Debbie Hardie, Dr Amy Wilson, Ruth Coughlan and Fern Barrington). I hope you will always wear your T-Shirts with pride! I have loved being a member of 'Team Mouse' and I will miss working with you all immensely. Dr Sian Lax 'my first port of call' has answered numerous ridiculous questions over the years and painstakingly read my thesis. Fern Barrington (Barry/Fren/The Glue) without whom I'd be lost in a world of cell culture. Not only has she been a tremendous help in the lab but she has become one of my very best friends and is now part of 'Team Bridesmaid'.

I would like to thank Dr Dagmar Scheel-Toellner and Dr Kai Toellner with whom I first worked with on my arrival at Birmingham. They taught me essential lab skills that I have used throughout my PhD. Thanks also to Steve Kissane and Celia Menckeberg for their advice and assistance with microarray studies and Sonia Parnell for providing me with primers for my end point PCRs. The anatomy group within the IBR have been a great help in setting up the kidney capsule experiments and sourcing embryonic tissues, especially Dr Stephanie Glanville who gave us an intensive two week course in surgery and Dr Andrea White for her technical assistance. In addition, I would like to acknowledge the Medical Research Council for funding my PhD.

Also, thanks must go to many people on the 3rd floor that have helped out generally in the lab and made it such great place to work. Dr Graham Wallace, for proof reading my thesis, which was no small task! Katherine Howlett, my wife, my gym buddy, provider of the Take That chart and member of 'Team Bridesmaid'. Thankyou for my many birthday cakes, engagement desk decorations and even the occasional cuddle! Dr Peter Hampson, I forgive you for being a Man U supporter as we have had much sporting banter. Take care of little Pete and thanks for proof reading the odd chapter. Hema Chahal, without whom I would be at least two stone heavier! There is never a good enough excuse to miss one of your classes, least of all leaving the department. Alastair Denniston for our mutual sharing of stationary and race to the finish. Leigh Church who I have driven crazy for wedding advice but whose sayings I wrote this thesis by 'why say it in four words when you can say it in one'. Lorraine Yeo for her excellent muffins, I leave you the best desk in the office! Marianne Fairclough for our American road trip which was full of surprises! I look forward to meeting 'Peanut'.

Special thanks to my family for their constant love and support in everything I do. My Mum and Dad, who think nothing of visiting from 'up North' for just an evening, not least for their financial support throughout my University career, but for the knowledge that whatever happened they'd be there. My little bro, Tom, whose courage and sense of humour over the last couple of years has been inspiring and I am such a proud big sis.

Last but not least I would like to thank my fiancé Steve for his support, friendship and ability to make me smile. I look forward to being Drs Essex!

ABBREVIATIONS

Ab	Antibody
Ag	Antigen
APC	Antigen Presenting Cell
BAFF	B Cell Activating Factor
BLyS	B Lymphocyte Stimulator
BSA	Bovine Serum Albumin
Caspase	Cysteinyl Aspartic Acid Protease
CAF	Carcinoma-Associated Fibroblast
CD	Cluster of Differentiation
cDNA	Complementary Deoxyribonucleic Acid
CM	Conditioned Media
DABCO	1,4-diazobicyclo(2,2,2) octane
DAVID	Database for Annotation, Visualisation and Integrated Discovery
dH_2O	Distilled Water
DNase	Deoxyribonuclease
DC	Dendritic Cell
E	Embryonic Day
ECM	Extracellular Matrix
EDTA	Ethylene-Diamine-Tetra-Acetic Acid
EMT	Epithelial-Mesenchymal Transition
E-selectin	Endothelial Selectin
FACS	Fluorescent Activated Cell Sorter
FCS	Foetal Calf Serum
FDC	Follicular Dendritic Cell
FDR	False Discovery Rate
FITC	Fluorescein-Isothiocyanate
FRC	Fibroblastic Reticular Cell
FS	Forward Scatter
GFP	Green Fluorescent Protein
HEV	High Endothelial Venule
HLA	Human Leukocyte Antigen
HOX	Homeobox
ICAM-1	Intercellular Adhesion Molecule-1
IFN	Interferon
Ig	Immunoglobulin
IL	Interleukin
KO	Knockout
LCMV	Lymphocytic Choriomeningitis Virus
LDA	Low Density Array
LPS	Lipopolysaccharide
LT	Lymphotoxin
LTi	Lymphoid Tissue Inducer
LTo	Lymphoid Tissue Organiser
M	Molar
mAb	Monoclonal Antibody
MadCAM	Mucosal Addressin Cell Adhesion Molecule
mM	Millimolar

NALT	Nasal-Associated Lymphoid Tissue
MMP	Matrix Metalloproteinase
MOMA-1	Marginal Zone of Monoclonal Antibody-1
mRNA	Messenger Ribonucleic Acid
MSC	Mesenchymal Stem Cell
MHC	Major Histocompatibility Complex
PALS	Periarteriolar Lymphoid Sheath
PAMPs	Pathogen-Associated Molecular Patterns
PBS	Phosphate Buffered Saline
PCA	Principle Component Analysis
PCR	Polymerase Chain Reaction
PE	Phycoerythrin
PDGF	Platelet Derived Growth Factor
PNAd	Peripheral Lymph Node Addressin
PRRs	Pattern-Recognition Receptors
RA	Rheumatoid Arthritis
RT-PCR	Real Time Polymerase Chain Reaction
SAM	Significance Analysis of Microarrays
α-SMA	α-Smooth Muscle Actin
SMP	Splanchnic Mesodermal Plate
SOP	Standard Operating Procedure
SS	Side Scatter
TBS	Tris Buffered Saline
TCR	T-cell receptor
T_H cells	Helper T cells
TLR	Toll-Like Receptor
TMEV	The Institute of Genomic Research Multi-Experiment Viewer
TNF	Tumour Necrosis Factor
TRANCE	Tumour Necrosis Factor-Related Activation-Induced Cytokine
VEGF	Vascular Endothelial Growth Factor
VCAM-1	Vascular Cell Adhesion Molecule-1
VLA-4	Very Late Antigen-4

CONTENTS

LIST OF FIGURES

Chapter One: Introduction

Chapter Two: Materials and Methods

Chapter Three: Characterisation of Adult Mouse Fibroblasts from Lymphoid and Peripheral Sites

Chapter Four: *In vitro* Function of Fibroblast Populations from Different Sites

Chapter Five: *In vivo* Function of Fibroblast Populations from Different Sites

LIST OF TABLES

Chapter One

Introduction

CHAPTER ONE

Introduction

1.1 The Immune System

Pathogens are encountered routinely, but only rarely cause disease. Pathogens first face anatomic barriers such as skin and mucous membranes and physiologic barriers such as temperature, the low pH of the stomach and lysozyme in tears. Should a pathogen get past these barriers the human immune system has various methods of recognising and responding to invasion by non-self (1).

The immune system comprises many cell types which differentiate from a pluripotent haematopoietic stem cell (figure 1.1). These cells mediate an immune response which consists of two branches; the innate and adaptive systems. Innate immunity is driven by an antigen-non-specific mechanism which a host uses immediately or within several hours after exposure to an antigen. This is the initial response by the host to eradicate microbes and prevent infection. However, although it can distinguish self from non-self, it offers no memory or lasting protective immunity. Adaptive immunity is driven by an antigen-specific mechanism that takes several days to become protective. It is designed to react with and remove a specific antigen and continues to develop throughout life, providing memory against re-infection (2).

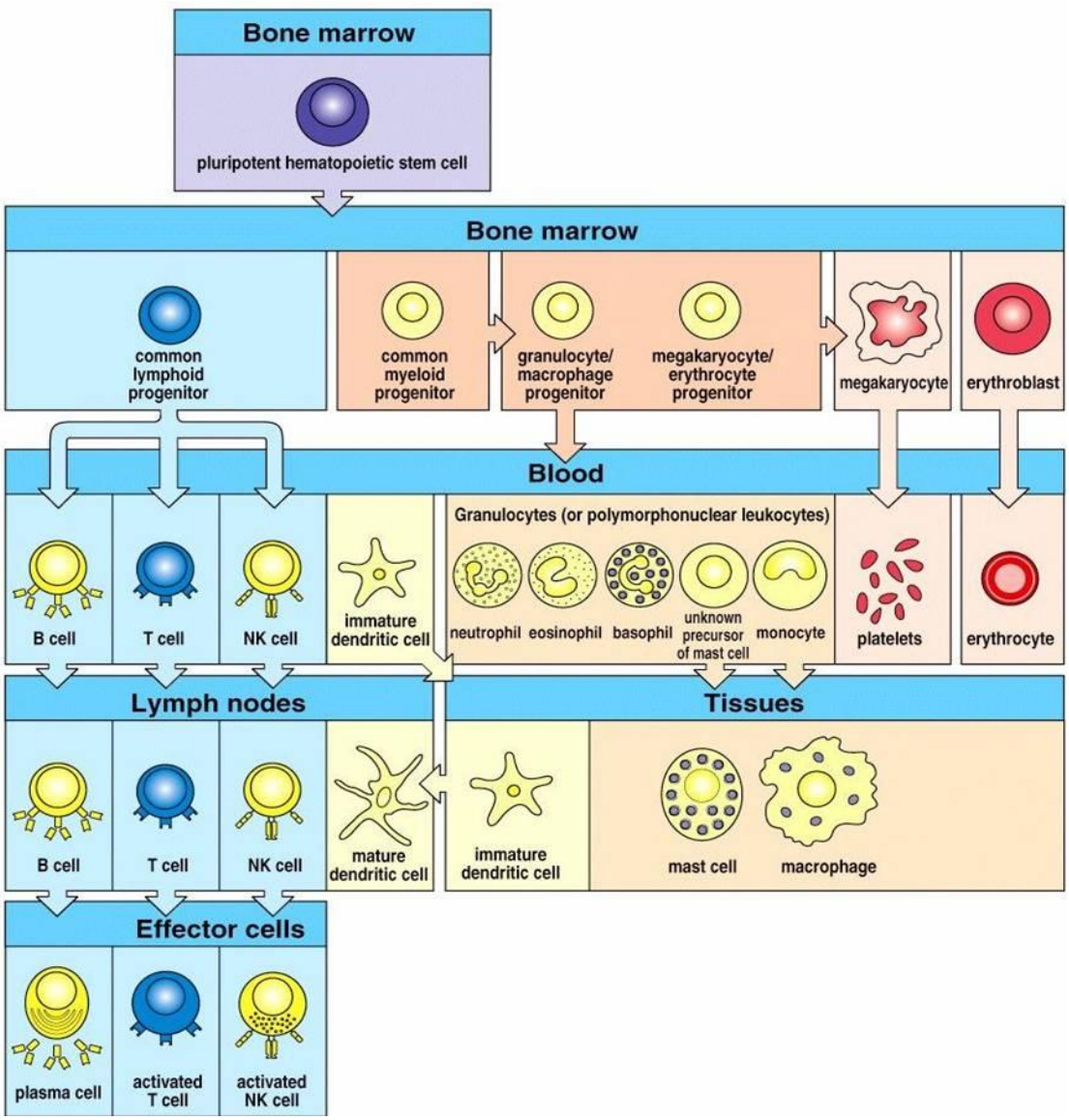

Figure 1.1 Cell lineage in the immune system
All cells arise from pluripotent haematopoietic stem cells in the bone marrow. Initially these give rise to stem cells of a more limited potential which differentiate into the many cell lineages [Taken from Janeway *et al*, 2005 (1)].

1.1.1 Innate Immunity

The cells of the innate immune system include phagocytes such as macrophages, neutrophils and immature dendritic cells (DCs), which engulf and kill invading pathogens by phagocytosis. This involves surrounding the pathogen with a phagocyte membrane and then internalising it in a membrane-bound vesicle termed a phagasome. This becomes acidified, killing most pathogens. Macrophages and

neutrophils also contain lysosomes which are membrane bound granules containing enzymes, proteins and peptides. The phagosome fuses with one or more lysosomes to form a phagolysosome, in which the lysosomal contents are released to destroy the pathogen (3). Neutrophils are short lived cells and die after completing phagocytosis, they are the most abundant leucocyte population, representing about 60% of all circulating leucocytes (4). In comparison macrophage cells are long lived and after phagocytosis continue to produce new lysosomes (3). Immature DCs, phagocytose pathogens and present their degraded proteins using major histocompatablity complex (MHC) proteins whilst simultaneously upregulating co-receptors for T cell activation such as CD80 and CD86 and also CCR7 which encourages the DC to travel to the spleen or a lymph node. Here they function as an antigen presenting cell (APC) and can induce an adaptive immune response. The DCs enter the lymph nodes as mature non-phagocytic cells which can activate antigen-specific thymus derived (T) cells (5). In addition, granulocytes such as mast cells, eosinophils and basophils release cytokines that cause dilation of blood vessels and increased vascular permeability. These cells are thought to be involved in allergic responses and defence against parasites (3).

As well as the cellular component of the innate immune system which acts mainly in the tissues, the complement system is an enzyme system activated in the blood. There are three pathways leading to complement activation: the classical pathway, the mannose binding (MB) lectin pathway and the alternative pathway (6). The classical pathway is activated by IgG or IgM antibody molecules produced by bone marrow derived (B) cells and is part of the adaptive immune response (7). The MB lectin pathway is activated by mannose and fructose residues on bacterial cell walls, and the alternative pathway by spontaneous hydrolysis of C3 from plasma to the surface of a

pathogen, both of which are innate mechanisms (8). The pathways all lead to the activation of C3, which is the central component of the cascade. The larger fragment of C3, C3b, binds to the surface of the pathogen present and activates the complement cascade which ultimately results in the formation of membrane attack complexes. These insert into the pathogen cell membrane, form a transmembrane pore and cause lysis of the bacterium (1).

A third system utilised by the innate immune system is recognition of common pathogen associated components, named pathogen-associated molecular patterns (PAMPs). These are usually components of a pathogen that they cannot survive without or cannot easily mutate without affecting their capacity to cause infection (9). The innate immune system relies on a set of germline encoded receptors called pattern-recognition receptors (PRRs) to recognise these PAMPs. Examples of these PRRs include Toll-like receptors (TLRs) of which over ten have been identified in humans that recognise different PAMPs. Examples of PAMPs include lipopolysaccharide (LPS) and peptidoglycan recognised by TLR4 and 2 respectively (10). The role of the TLRs is then to activate phagocytes and DCs to respond to the pathogens by secreting chemokines and cytokines, and to induce DC maturation (11).

The key to the innate response is its rapid onset with the peak response being just a few hours after infection. Without this, many infections would prove lethal while waiting for the body to mount an adaptive response. The innate response subsides either as an infection is resolved or as the adaptive response comes into play (12).

1.1.2 Adaptive Immunity

Many pathogens can evade the initial non-specific response, this is when the adaptive arm of the immune response comes into play. This is a specific response to a pathogen and occurs over a period of several days from when a pathogen is first encountered. The adaptive immune response requires T and B lymphocytes that recognise specific antigens presented on the surface of APCs. Both T and B lymphocytes originate in the bone marrow, but only the B lymphocytes mature there. T lymphocytes migrate to the thymus and it is here they undergo maturation and selection. Once maturation is completed both cell types enter the bloodstream, from which they traffick to lymph and peripheral lymphoid organs continuously. It is in the peripheral lymphoid organs where antigen and lymphocytes will eventually meet, triggering the adaptive immune response (1).

1.1.2.1 Lymphocytes

Lymphocytes account for 20-40% of all white cells in the circulating blood. Early in lymphocyte development their receptor genes undergo rearrangement so that each receptor is structurally diverse. There are approximately 10^{11} different lymphocytes in the human body, each with the ability to bind different antigen (1,2).

B cells produce antibodies which interact with pathogens and their toxic products in the extracellular spaces of the body. The immunoglobulin receptors of the B cell recognise antigen in its unprocessed state, the antigen-recognition molecules produced are made both as membrane bound receptors and as secreted antibodies. The majority of B cell responses, though, depend on the interaction with specialised T cells, in lymphoid tissues, for the generation of efficient high affinity antibody responses (6).

In contrast, T cells are specialised for cell-cell interaction. Antigen presented to T cells must be displayed bound to MHC proteins on the surface of the body's own cells. There are two main types of T cells, helper T cells which express CD4 and cytotoxic T cells which express CD8. $CD4^+$ T cells generally interact with peptide antigens bound to MHC class II proteins (13). These peptides are generated from exogenous antigens taken up by APCs, which process the antigen intracellularly and present the resulting peptides on MHC class II proteins in combination with co-stimulatory molecules such as CD80 and CD86 to $CD4^+$ T cells. APCs include DCs and macrophages, however only DCs are thought to be able to activate or "prime" naïve, not previously activated T cells (14). CD4 expressing T cells are split into two further subsets; Th_1 cells which are important in intracellular bacterial infections and Th_2 cells which are involved in stimulating B cells, mast cells and eosinophils and are important in parasite infections (15). More recently a new population of $CD4^+$ T cells has become apparent; these are $CD4^+CD25^+$ and have been named regulatory T cells (Tregs). The Tregs make up approximately 5-10% of the lymphocyte population and they can inhibit activation of effector T cells by secreting inhibitory cytokines, such as IL-10, which prevents IL-2 production (16). The peptides activating the Treg receptor tend to be self peptides and so it is thought they have a role in the prevention of autoimmune responses (17). Cytotoxic $CD8^+$ T cells recognise their antigen in conjunction with MHC class I proteins (18). MHC class I is expressed by most nucleated cells. MHC class I proteins generally present peptides derived from proteins produced within the presenting cell. $CD8^+$ effector T cell antigens recognise cells infected with virus or other intracellular pathogens and kill directly by inducing apoptosis of the infected cell. Some $CD8^+$ T cells require $CD4^+$ T cell help to become activated, it is thought that the presence of the $CD4^+$ T cell compensates for the

inadequate co-stimulation of the naïve $CD8^+$ T cell. The $CD4^+$ T cell induces the APC to increase co-stimulatory activity and thus activates the $CD8^+$ T cell (19).

All T cell subsets develop in the thymus, however, only 3% become mature naïve T cells (20). These naïve T cells constantly recirculate between secondary lymphoid organs, blood and lymphatic systems. Once primed following interaction with an antigen experienced DC, the activated T cells down-regulate L-selectin and increase very late antigen-4 (VLA-4) expression on their cell surface. This change in phenotype results in the loss of lymph node homing, so that they are more likely to enter inflamed or infection sites in response to signals from innate cells such as macrophages (21). Importantly, for the adaptive response, while the vast majority of T cells die by apoptosis as the response resolves, a small subset remain after resolution of an infection. These memory T cells can rapidly mobilise and proliferate should the same antigen be re-encountered. Compared to naïve T cells, memory T cells can be activated by macrophages and generate a faster and more effective response at lower doses of antigen (22).

1.1.2.2 Lymphocyte homing and trafficking

Lymphocytes continuously re-circulate through the blood, lymphatic system and non-lymphoid tissue to ensure continuous surveillance for foreign antigen. It takes approximately 24 hours for a T cell to complete one round of migration through all the body's lymph nodes (23). Their homing and extravasation across endothelium is an important process as it is in the peripheral lymphoid organs where antigen and lymphocytes will eventually meet, triggering the adaptive immune response. The site where a lymphocyte extravasates is determined by the active cell surface receptor on

the lymphocyte interacting with its corresponding ligand on the endothelial cell. Many endothelial adhesion molecules are upregulated under inflammatory conditions. Transendothelial migration takes place in four stages: lymphocyte rolling, activation of integrins, tight adhesion and diapedesis (figure 1.2).

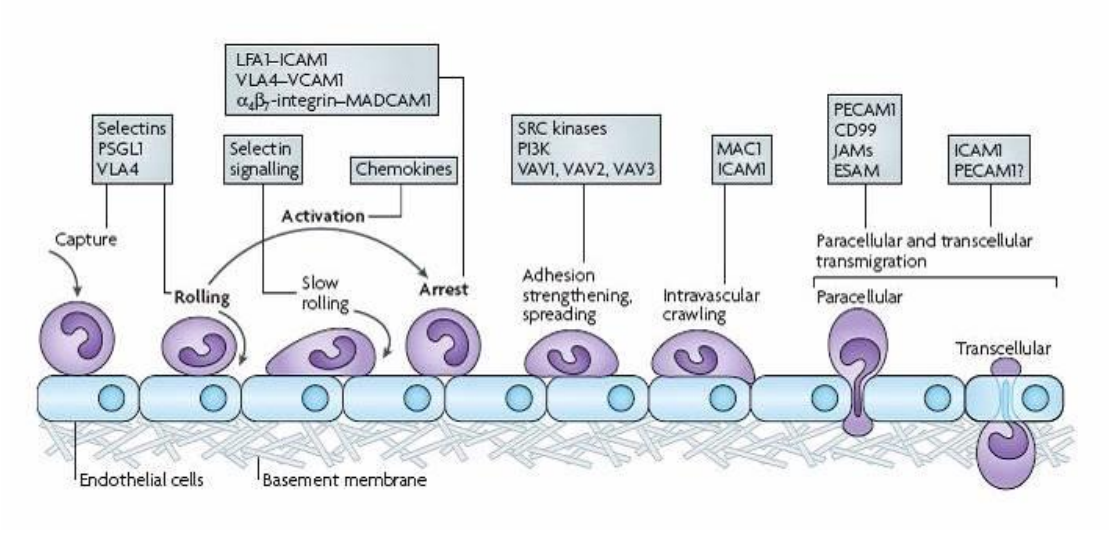

Figure 1.2 Transendothelial migration
Neutrophil recruitment, lymphocyte recirculation and monocyte trafficking all require adhesion and transmigration through blood-vessel walls. The traditional three steps of rolling, activation and firm adhesion, have recently been augmented and refined. Slow rolling, adhesion strengthening, intraluminal crawling and paracellular and transcellular migration are now recognized as separate, additional steps. [Taken from Ley *et al*, 2007 (24)].

Lymphocyte rolling is a reversible attachment of the cell to the endothelium; this slows down the cell in the bloodstream so that it may detect signals from the endothelium. L-selectin is expressed by most lymphocytes, this binds to receptors such as glycosylation-dependent cell adhesion molecule-1 (GlyCAM-1), CD34 and mucosal addressin cell adhesion molecule (MAdCAM) on the endothelium in the rolling process (25). Next the lymphocyte is activated by chemokines produced by the endothelial cells, this leads to increased integrin expression on the lymphocyte and the cells arrest. Tight adhesion of the lymphocyte to the endothelial cell is then induced

by members of the immunoglobulin superfamily present on the endothelial cell surface binding to these integrins (26). The lymphocyte then induces the opening of the junction between two endothelial cells by disrupting cell-cell interactions. This step is believed to involve an immunoglobulin type molecule called platelet/endothelial cell adhesion molecule one (PECAM-1) or CD31; enabling the lymphocyte to 'crawl' along the cell to the basement membrane (24). Finally the lymphocyte secretes enzymes to breakdown the basement membrane and enter the subendothelial tissue (24-26).

1.2 The Lymphoid System

The specialised structure in the human body for the distribution of immune cells is the lymphoid system. The lymphoid system consists of primary lymphoid organs, secondary lymphoid organs, and lymphatic vessels (figure 1.3). Primary lymphoid organs such as the bone marrow and the thymus are where the B and T cells respectively mature (1). After maturation, both B cells and T cells circulate through and accumulate in secondary lymphoid organs. Secondary lymphoid organs consist of the highly organised lymph nodes and spleen as well as the less organised appendix, Peyer's patches and tonsils. Secondary lymphoid organs are the predominant site of lymphoid sensitisation to novel antigens (27). The lymphatic vasculature forms a secondary circulatory system which connects the blood and lymphoid organs (28). Blood plasma constantly leaks out of the capillaries to deliver oxygen and nutrients to the tissues. Whilst most of the fluid re-enters capillaries and is returned to the bloodstream, some enters the lymph vessels. This lymph fluid flows through regional lymph nodes and eventually enters the circulatory system at the heart to maintain the fluid volume of the circulation (1,27).

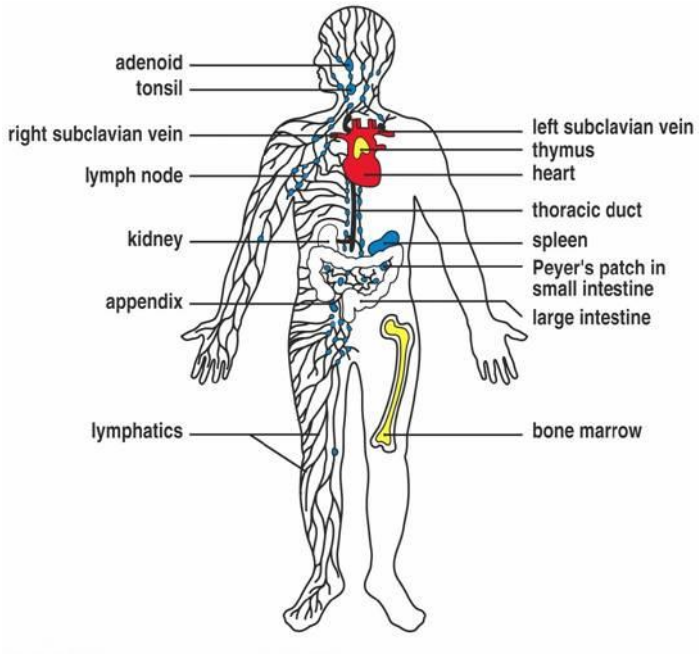

Figure 1.3 The human lymphoid system
Lymphocytes arise from stem cells in the bone marrow and differentiate in the primary lymphoid organs (yellow). They then migrate to secondary lymphoid organs (blue) and recirculate between these and the blood until they encounter their specific antigen. [Taken from Janeway *et al*, 2005 (1)].

1.2.1 Lymph node development

Development of secondary lymphoid tissue has primarily been investigated in the murine system. Lymph node development begins during embryogenesis and is thought to continue several weeks after birth (29). The precise signals that induce lymph node development has yet to be established, however Sabin hypothesised in 1902 that lymphatic vessels arise by sprouting from venous endothelial cells after an appropriate signal (30). More recent work in mice has shown the earliest lymph sacs to develop at embryonic day (E) 10.5 and that the homeobox gene Prox1 is essential for the normal development of the lymphatic system. In Prox1 null mice initial budding from the veins occurred but could not be maintained causing arrest of the lymphatic development. However, the loss of Prox1 did not affect vascular development suggesting it is specifically required for the development of the

lymphatic system (31). As the lymph sacs are forming, mesenchymal cells differentiate into specialised cells that initiate the formation of lymph nodes. This differentiation requires the presence of growth factors such as platelet-derived growth factor (PDGF) (32), fibroblast growth factors (FGF) (33) and transforming growth factor (TGF)-β superfamily (34). After development the lymph sac is colonised by lymphoid tissue inducer cells (LTi), which are haematopoietic cells that express the IL-7Rα chain and CD4 but lack CD3 (figure 1.4, left panel). LTi cells were first discovered by Kelly and Scollay in 1992. These bone marrow-derived cells form small clusters with resident stromal organiser cells, which express vascular cell adhesion molecule-1 (VCAM-1), inter-cellular adhesion molecule-1 (ICAM-1) and lymphotoxin β receptor (LTβR) (figure 4, right panel). This interaction is believed to initiate the maturation of the lymph node. The cross talk between these two cell types has been shown to be critical to lymph node organogenesis (35) and involves the ligands and receptors of the tumour necrosis family (TNF) (36). Lymphotoxin (LT) α, LTβ and TNF are structurally homologous cytokines grouped within the TNF ligand family (37). TNF and LTα can bind to TNF receptors TNFRI and TNFRII. However, LTβ forms a functional heterotrimeric complex, $LT\alpha_1\beta_2$ to bind to its receptor, LTβR (38,39).

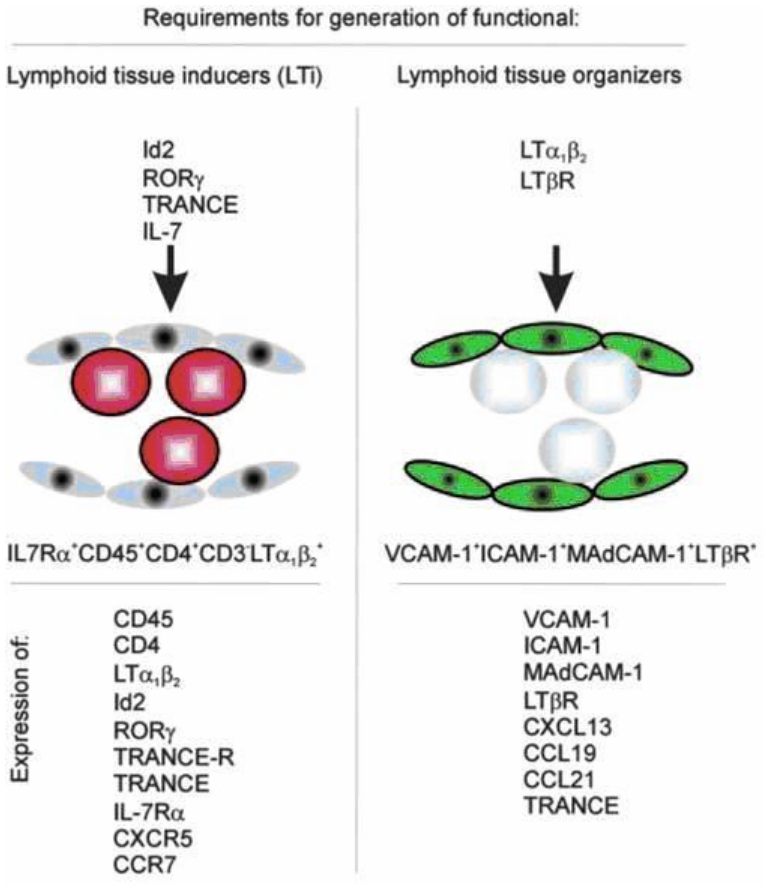

Figure 1.4 Requirements for the generation of functional lymphoid tissue inducers and organisers
Within the lymph node anlagen, LTi cells, expressing the markers shown (left panel), trigger the LTβR on the lymphoid tissue organiser cells. This upregulates the expression of the markers shown on the organiser cell (right panel), which in turn mediates the clustering of the LTi cells [Taken from Cupedo *et al*, 2005, (35)].

1.2.1.1 Lymphotoxin signalling

Studies have shown that LTα and LTβ have essential, non-redundant functions in lymphoid organ development. Mice deficient in LTα have a phenotype which consists mainly of defects in the secondary lymphoid system, with the absence of all lymph nodes and Peyer's patches, and the architecture of the spleen and nasal associated lymphoid tissue (NALT) being highly disorganised (40). This phenotype can be partially restored with transgenic expression of LTα under the rat insulin promoter, although it did not restore Peyer's patches or splenic architecture. The ability of the

spleen to form germinal centres and follicular dendritic cell (FDC) networks was however restored (41). LTβ knockout (KO) mice lack all peripheral lymph nodes and Peyer's patches but retain mucosal, cervical and sacral lymph nodes. The defects seen in the spleen and NALTs are decreased compared with the LTα KO mice (36,42-44). It has been reasoned that mesenteric and cervical lymph node formation in the LTβ KO mice, when other lymph nodes do not form, is due to the differential expression of LTβR by the corresponding stromal cells. Signalling through this receptor initiates a cascade of events during lymph node formation which may not be present in other lymph nodes (45) (section 1.2.1.3). LTβR KO mice lack all lymph nodes, Peyer's patches and colon-associated lymphoid tissue. The architecture of the spleen, germinal centre formation, FDC networks and immunoglobulin responses are also impaired. Interestingly the LTβR KO mice exhibit distinct defects not seen in the LTα or LTβ KOs, which suggests that the LTβR also integrates signals from other TNF family members (46). Taken together, these data using KO mice demonstrate the crucial and non-redundant functions of LTα and LTβ in lymphoid organ development.

1.2.1.2 TNF signalling

TNF binds to TNFRI and TNFRII. TNFRI is expressed in most tissues and can be activated by membrane bound and soluble trimeric forms of TNF, whereas TNFRII is found mainly in cells involved in the immune system and responds to membrane bound TNF. Upon TNFR ligation the adaptor protein TRADD binds to the death domain upon the receptor and acts as a platform for further protein binding. Three signalling cascades are then initiated, activation of NF-kB and MAP kinase pathways and also the induction of cell death pathways. These pathways have conflicting effects with the activation of NF-kB considered anti-apoptotic and the activation of MAP

kinase and cell death pathways pro-apoptotic. This diverse signalling provides a mechanism by which varied responses can occur under different conditions (37).

Tumour necrosis factor-related activation-induced cytokine (TRANCE), a TNF family member, is found on LTi cells and stromal cells within developing lymph nodes, and acts locally by attracting or differentiating LTi. Signalling via the TRANCE-R or the IL-7R initiates surface LT expression (47) and defects in these pathways affect the development of lymph nodes, with mice deficient for each receptor having unique phenotypes (48). Mice deficient in IL-7R signalling lack all Peyer's patches and only develop mesenteric and brachial lymph nodes (49). Whereas in mice lacking TRANCE-R, Peyer's patches are present with most lymph nodes missing (47). Interestingly TRANCE-R KO newborn mice still have LTi cells at sites where the mesenteric lymph nodes should have developed, but their numbers are severely reduced. This leads to a failure of most lymph nodes to develop, which suggests that there is a minimum number of LTi's required to initiate lymph node formation (47). The notion that there is a threshold number of LTi's is supported by, White *et al*, 2007, where a critical number of both LTi and stromal organiser cells was needed for normal inguinal lymph node development. Upon grafting E17 inguinal lymph nodes under the kidney capsule of adult mice, organisation of host T and B cells was observed, however inguinal lymph nodes grafted at E15 had no such organisation. This was thought to be due to the low numbers of LTi and mature stromal organiser cells at E15, as when a purified IL-7 cultured LTi population was added to a to the E15 inguinal lymph node cell suspension, lymphoid tissue formed upon kidney capsule grafting (50).

1.2.1.3 Lymphoid tissue organiser cells

The stromal organiser cells of a lymph node express the LTβR. In mice, when this receptor is ligated, two sequential signalling pathways are initiated. The first signals via RelA, p50 and IκBα and initiates the expression of adhesion molecules such as VCAM-1 (51). Increased expression of VCAM-1 aids the interaction of the stromal organisers with the LTi cells. LTi cells in turn continue activation of the LTβR and trigger a second NF-κB pathway via the NF-κB-inducing kinase, IκB kinase α and RelB (51). This second pathway leads to production of chemokines such as CXCL13, CCL21 and CCL19 which mediate the clustering of LTi cells into specific areas within the lymph node anlagen (50,51). Stromal organiser cells are believed to develop from mesenchymal cells (section 1.2.1). It has been suggested that this mesenchymal specification of a lymph node organiser cell occurs independently from LTβR signalling. Specifically, LTβR-expressing stromal cells were shown to be present in normal numbers in rudimentary mesenteric lymph nodes from LTα KO mice at the day of birth, although they lacked VCAM-1 expression (52). A model incorporating these findings includes two separate lineage determination steps (figure 1.5). First the mesenchymal cells differentiate towards stromal cells that produce TRANCE and then they are induced to express LTβR. Secondly the triggering of the LTβR by cells expressing LT (e.g. LTi) leads to up-regulation of adhesion molecules such as VCAM-1 and the production of chemokines. These cells can then attract and retain haematopoietic cells, allowing the lymphoid tissue to become colonised (45).

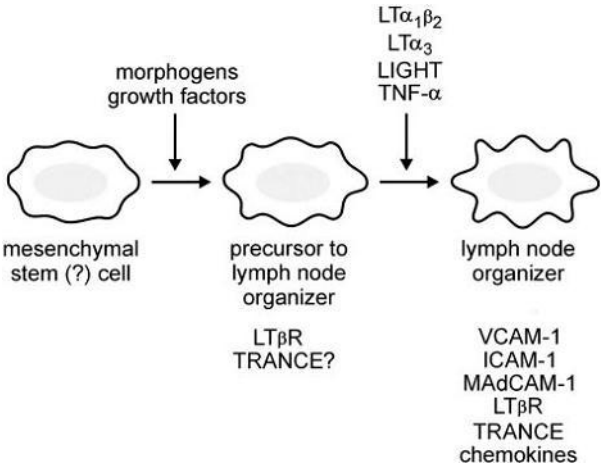

Figure 1.5 Differentiation of stromal organiser cells
A model for the differentiation of the lymph node stromal organiser cell. An intermediate precursor arises from a mesenchymal stem cell which then differentiates into a lymph node organiser cell by the ligation of the LTβR. [Taken from Cupedo *et al*, 2005 (35)].

1.2.1.4 Lymph node developmental progression

Lymph nodes have been demonstrated to develop in a certain order based on *in vivo* blocking experiments with LTαR-Fc. They begin at E10.5 with the mesenteric lymph nodes, next are the cervical at E11.5 and then the brachial and axillary after E12.5. The inguinal and Peyer's patches development begins at E16 but the Peyer's patches continue development until after birth. Finally after birth, the NALT develops (36,42,53). Each lymph node has their own set of developmental cues and signalling, as when different elements are blocked in the signalling pathway varying lymph nodes are affected. One explanation for the differences seen is a variation in the stromal cell compartment of each lymph node. It has been shown that, at least in the mesenteric and peripheral lymph nodes two populations of stromal cells exist; ICAM-1, VCAM-1 and MadCAM high expressing cells (IVM^{high}) and those expressing the same adhesion molecules at an intermediate level (IVM^{int}) (45). The intermediate expressing cells were the larger population and these represented the previously described organiser cells. Both of these populations express LTβR, with the IVM^{int}

population expressing a higher number of LTβRs. They also produced mRNA for homeostatic chemokines CXCL13, CCL19 and CCL21, with the IVM^{int} population expressing lower amounts. The expression profile of these populations identifies these cells as lymphoid tissue organisers. When comparing mesenteric lymph nodes to peripheral lymph nodes it was found that the IVM^{int} population was approximately 10 fold reduced in the peripheral lymph nodes while the IVM^{high} was only slightly reduced. This finding may explain why these lymph nodes have different signalling requirements during embryonic development (45).

1.2.1.5 Adult LTi

It is clear that LTi – stromal cell crosstalk is required in the developing lymph node, however, whether this continues in adult secondary lymphoid organs is a key question. Cells equivalent to LTi have been found in adult mice, a key difference in the adult LTi is their expression of OX40 and CD30 (54). These adult LTi have been described as having a role in the generation of memory T cells (55) as well as having a role in the maintenance in secondary lymphoid tissue structure (56). Recent work has shown that LTi – stromal cell interactions persist in the adult and provide a significant mechanism for restoring secondary lymphoid organ integrity after infection (57). In a mouse model using infection with lymphocytic choriomeningitis virus (LCMV), the T zone stroma is destroyed, rendering the host particularly vulnerable to secondary infection. A study using this model demonstrated T zone stroma restoration through the proliferation of resident LTi cells and their interaction with lymphoid stromal cells. In addition, accumulation of LTi cells was seen in the spleen and lymph nodes coinciding with the peak of immunopathological damage. This accumulation was also shown to be as a result of LTi proliferation during the

infection. When LTi cells were removed from this system however, the restoration of normal splenic architecture post infection was delayed. This delay was also seen when LTβR signalling was blocked, suggesting that following infection, LTi – stromal cell cross talk is reactivated similar to that observed during embryonic development. Of importance, however, this study also showed that under normal conditions LTi cells were not required to maintain secondary lymphoid structure. Therefore it is possible that LTi cells present in the adult tissue are required only when considerable damage is sustained within the secondary lymphoid organs (57). More recently, in adult mice and humans, a population of IL-22 producing mucosal cells in mucosa-associated lymphoid tissues (MALT) have been described that share features of both LTi and NK cells, termed NK22 cells (58). In contrast to LTi cells, they express NKp46, a natural cytotoxicity receptor (59), but compared to NK cells express little or no classical NK markers such as NK1.1 and perforin (60). It has been suggested that LTi cells and NK cells come from a common precursor, with factors such as IL-15 and IL-7 influencing the differentiation into NK or LTi cells and signals from the commensal microflora subsequently inducing the differentiation of NK22 cells from LTi cells (61). These cells are thought to be involved in immunity and homeostasis in mucosal tissues.

1.2.2 Lymph node structure

Two important vascular systems are found in the lymph node; lymphatic vessels and high endothelial venules (HEVs) (62,63). Immediately after birth, all HEVs express MAdCAM-1, the ligand for the integrin $\alpha_4\beta_7$. This is rapidly replaced by peripheral lymph node addressin (PNAd) in mouse peripheral lymph nodes, functioning as the main L-selectin ligand that contributes to the mature peripheral lymph node HEV

phenotype. Conversely, in mucosal lymph nodes HEVs maintain their expression of MAdCAM-1 in addition to PNAd (64).

The mature lymph node can be separated into three distinct regions: cortex, paracortex and medulla (figure 1.6). The cortex contains lymphoid nodules called primary follicles; these are composed of B cells and follicular dendritic cells (FDCs). It is here that the B cells undergo proliferation after antigen stimulation, forming secondary follicles termed germinal centres (65). Inside the cortex is the paracortex which is composed of T cells and DCs. The medulla consists of strings of macrophages and antibody secreting plasma cells known as the medullary cords. Lymphocytes enter the lymph node by extravasation across the HEV. Soluble antigen and DCs enter by afferent lymphatic vessels at multiple sites on the outer capsule (62,66).

There are many types of stromal cell within the lymph node. Fibroblastic reticular cells (FRCs) in the T zone (67) and FDCs (68) and marginal reticular cells (MRCs) (69) in B cell zones. Also present in the CD45 negative cells of the lymph node are blood endothelial cells which express CD31 but not gp38 and lymphatic endothelial cells which express both gp38 and CD31 (67).

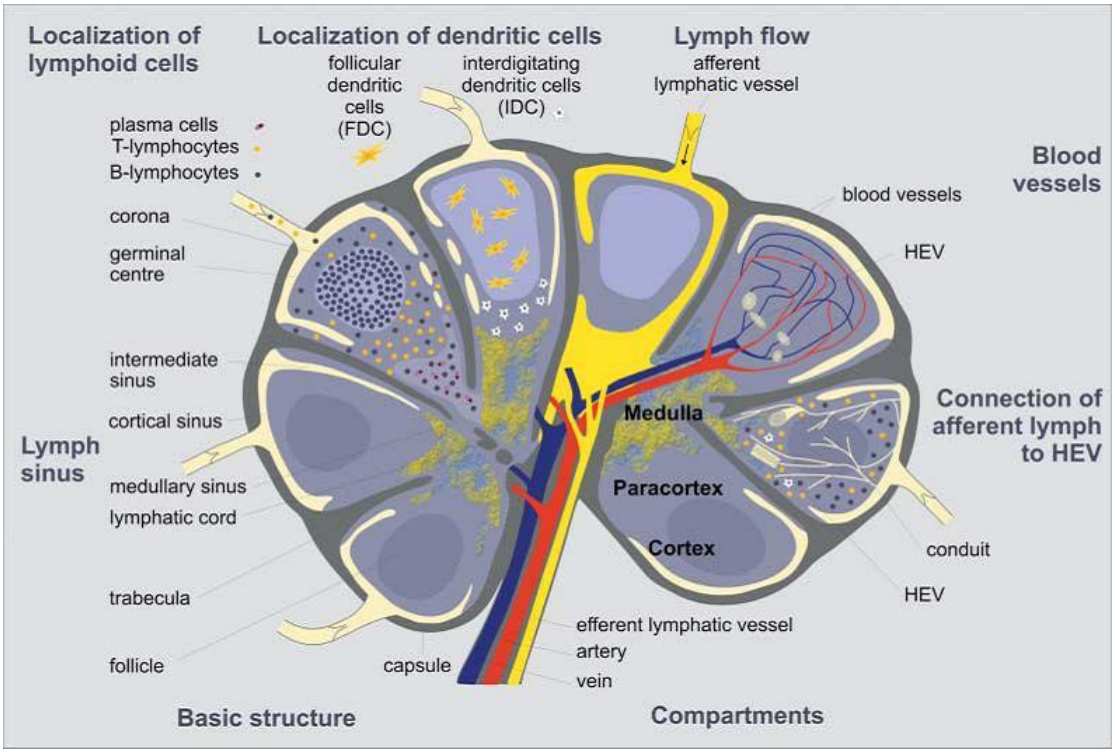

Figure 1.6 Lymph node structure
The lymph node consists of three main regions; the cortex, paracortex and medulla. The cortex consists mainly of B cells organised as primary or secondary follicles. The migration of these cells towards the follicles is mediated by follicular dendritic cells (FDC). T cells migrate to the paracortical region, neighbouring the cortex, they interact with the interdigitating dendritic cells (IDC). The central region, the medulla, mostly contains plasma cells and B cells. The lymphocytes enter the lymph node via the afferent lymphatic vessel or through transmigration of the high endothelial venules (HEV). Both systems, the lymph vasculature and the blood vasculature, are connected via a conduit system. [Taken from Blum *et al*, 2006, (65)].

1.2.2.1 Lymph node T zone stroma

Stromal cells support the distribution and migration of lymphocytes as well as acting as a structural backbone within the lymph node. T zone stromal cells, termed FRCs, produce constitutive chemokines and support migrating T cells and DCs. FRCs are more plentiful than other stromal populations within the lymph node and have been shown to express glycoprotein 38 (gp38 or podoplanin) (section 1.2.2.1.1) (70). They produce extracellular matrix (ECM) components which are crucial to the structural

stability of the lymph nodes and express CCL21 and CCL19 which attract the CCR7 expressing T cells and DCs to the T zone. They also enhance the survival of T cells by producing IL-7 (71).

1.2.2.1.1 Glycoprotein 38 (Podoplanin)

A novel glycoprotein, gp38, was characterised by Farr *et al*, 1992, (72) and was later named podoplanin due to its low level expression in kidney podocytes (73). gp38 is a mucin type transmembrane protein of 43kDa first found to be expressed by stromal cells of peripheral lymphoid tissue, in particular the FRCs of the T cell dependant area (72). In addition, gp38 is also expressed in other cells including lymphatic endothelial cells (74) and thymic epithelial cells (75). The gp38 KO mouse model shows increased embryonic and foetal death; in homozygote embryos, 40% die between stages E10-E16 and in the neonatal homozygotes, 50% die within the first weeks of life. This is in contrast to the heterozygous mice, which have been shown to reach sexual maturity. The causes of embryonic death have been linked to heart defects whereas the cause of neonatal death is still unknown (72,76). In other studies $LT\alpha_1\beta_2$, produced by B cells, was shown to be required for gp38 expression. B cell deficient spleens had a three to five fold reduction in the area stained by CD3 and the T zone stroma marker gp38 (77). This indicates a role for B cells in the development of T zones in the spleen. In addition, impaired B and T cell segregation within the white pulp of the spleen correlates with a lack of gp38 expression on the T zone stroma, suggesting a role for gp38 in the separation of lymphocytes (78). Taken together, these findings suggest that gp38 is important in lymphatic patterning during development (74).

1.2.2.2 Lymph node B zone stroma

The B zone consists of stromal cells and B cells, the main stromal cell being the FDC. FDCs produce CXCL13 which attract and retain CXCR5 expressing B cells to the B zone (68). The fibroblastic morphology of FDCs and their expression of vimentin and desmin suggests a mesenchymal origin (79). FDC development at sites of chronic inflammation indicates their differentiation from local mesenchymal cells (80). The ligands and receptors necessary for B cell growth and survival have been identified as TNF family members (81). B lymphocyte stimulator (BLyS), also known B cell activating factor (BAFF) or TNF13B, is produced by FDCs and plays a role in B cell survival and activation (82).

More recently, a stromal cell population, termed MRCs was found in the outer follicular region immediately underneath the subcapsular sinus of lymph nodes in adult mice (69). These cells expressed VCAM-1, ICAM-1, MadCAM-1, CXCL13, TRANCE, BP-3 and gp38 and have been described as specialised reticular fibroblasts. These cells are thought to be the adult equivalent of embryonic LTo cells with a role in organising the structure of adult secondary lymphoid organs (69).

1.2.2.3 The conduit system

During infection lymph-borne antigens are first found in the subcapsular sinus of the lymph node. From here they are transported either directly into the medullary sinuses or into a reticular conduit system (figure 1.6). The conduit system has been described as the infrastructure of the lymph node, transporting fluid and low molecular weight molecules (<70kDa) (83). It is a network of collagen fibres ensheathed by FRCs, which extends from the subcapsular sinus to the deeper cortex and medullary regions,

suspending blood vessels and sinuses (84). The FRCs produce collagen and basement membrane components that form a highly organised core around which the FRCs are wrapped, they are also connected along the longitudinal axis by junctional complexes. In places where the basement membrane is not covered by FRCs, DCs are positioned, which enables them to gain access to antigens that have entered the conduit (85). This structure means lymphocytes are not in contact with the basement membrane, only the FRC membrane, hence the FRCs have an important role in the guidance of lymphocytes. More recent work has shown that the conduit network does not act as a barrier to lymphocyte migration but rather as an active support and provider of guidance cues underlying T and B cell movement within the T zone of lymph nodes (86). The conduit system is involved in the movement of antigen before it is sampled by APCs, such as DCs, and therefore has a functional role in antigen presentation (87). Small molecules such as chemokines can also be moved through the conduit system, with peripherally produced chemokines able to drain into the conduit system. These can then be presented on the luminal side of HEVs which will ultimately affect leucocyte entry (88). The spleen also contains a conduit system, which is similar to that of the lymph node, with the only major difference being that it is not connected to the lymphatic system but to the blood (84). Further work within the spleen has shown that movement within the conduit system is not just dependent on size but also on the molecule's 3-D configuration or electrostatic charge (83).

1.2.3 Splenic development

Relative to the lymph node, splenic development has been poorly characterised with fewer studies completed. There remains a large gap in the literature to be filled. The spleen is normally situated on the left side of the abdominal cavity, closely associated

with the pancreas and located on the left lateral side of the stomach. During development the leftward expansion of the mesenchyme provides the tissue in which the spleen forms, with the initiation of splenogenesis and leftward pancreatic growth closely linked (89). Splenic development in mice begins at E9.5 with the formation of the splanchnic mesodermal plate (SMP). The SMP, which is derived from mesoderm, is an anlage or organising centre for the formation of the spleen. In conditions where the SMP is defective the spleen does not form, for example mice carrying the dominant hemimelia mutation or a deficiency in bagpipe homeobox homologue 1 (89,90). The first cells to colonise the spleen are the progenitors of the erythroid and myeloid lineages. Later, at E13.5, LTi cells are present in the spleen. These are known to provide the inductive signal for the formation of lymph nodes and may therefore have a role in white pulp formation. Finally at E14.5 the first haematopoietic cells reside in the spleen (91).

1.2.4 Splenic structure

The spleen is the largest single secondary lymphoid organ in mammals. It has a role in both innate and adaptive immunity and also in the removal of senescent red blood cells. The two roles are compartmentalised in two distinct components, the red pulp and the white pulp. The afferent splenic artery branches into central arterioles which are sheathed by white pulp areas. The arterioles end in cords in the red pulp where the blood runs into the venous sinuses and collects in the efferent splenic vein. A capsule surrounds the spleen and contains the connective tissue trabeculae in which the larger arteries and veins run (figure 1.7a) (92).

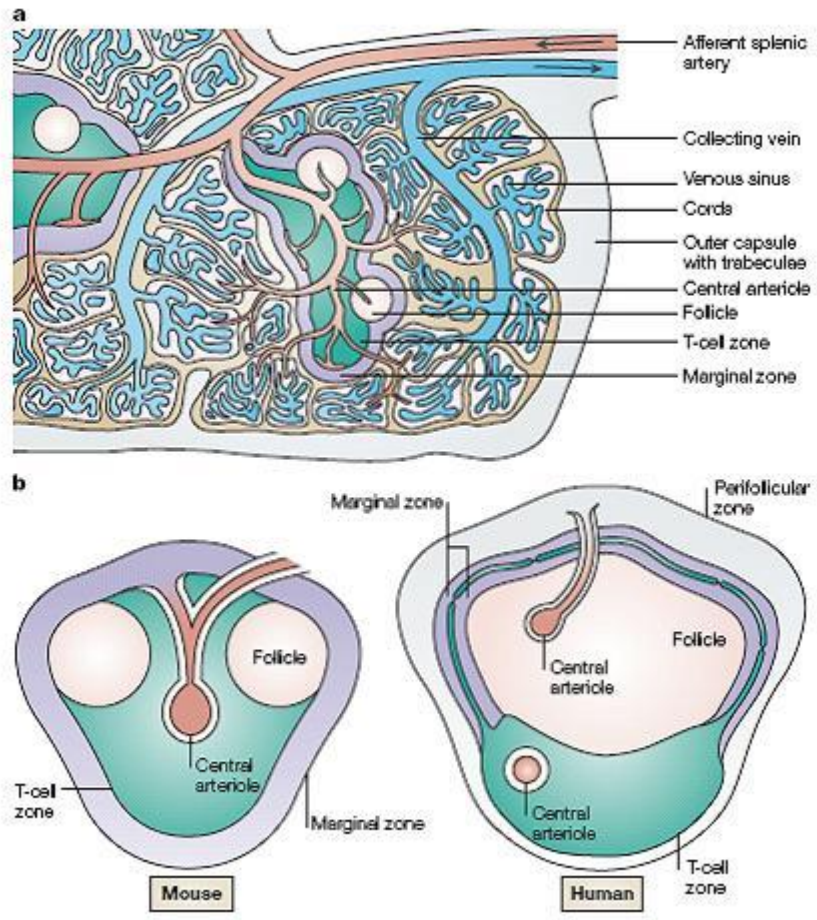

Figure 1.7 Structure of the spleen
a) Cross sectional schematic of the human spleen. b) A comparison of the white pulp in a mouse and human spleen. The main differences are found in the structure of the marginal zone, which surrounds the white pulp. In contrast to mice, humans have an inner and an outer marginal zone, which is surrounded by a large perifollicular zone. [Taken from Mebius *et al*, 2005 (92)].

1.2.4.1 Red pulp

The red pulp consists of large numbers of sinuses and sinusoids filled with blood; its main function is to remove damaged or aging erythrocytes. Arterial blood flows into cords in the red pulp that consist of fibroblasts and reticular fibres with no endothelial lining. The blood then flows into the venous sinuses of the red pulp, which collect into the efferent vena lienalis. These vessels are lined with endothelium but it has a discontinuous structure. Stress fibres run along the long axis of the endothelium and

are most prominent during contraction. This structure forces the blood from the cords into the sinuses through slits formed by the stress fibres. As erythrocytes age, their membranes become rigid, causing slower migration through these stress fibres, thereby enabling phagocytosis by local macrophage (92). In both humans and mice adult erythropoiesis occurs in the bone marrow. However, it is important to note that stress erythropoiesis occurs in the murine splenic red pulp during embryonic development and acute anaemia (93). Splenic erythropoiesis is not a feature of human haematopoiesis, extramedullary erythropoiesis is only seen in certain pathological conditions such as primary myelofibrosis (94).

1.2.4.2 White pulp

The white pulp consists of aggregates of lymphoid tissue and is responsible for the immunological function of the spleen. It is present in the form of a periarteriolar lymphoid sheath (PALS), containing B cell follicles and a T cell zone. At the edge of the T zone is a region known as the marginal zone where larger lymphocytes and antigen presenting DCs are located (figure 1.7b) (92). The white pulp closely resembles the structure of the lymph node, one major difference being that lymph nodes collect antigen from the periphery via afferent lymphatics, whereas the spleen receives antigen directly from the blood (62,95). The splenic organisation is maintained by specific chemokines that attract the T and B cells to their respective zones. Like in the lymph node, CXCL13 here produced by $CD35^{+}$FDCs and their adjacent stromal cells, induce B cells to migrate to the B cell zones via interaction with CXCR5 (96). Signalling through CXCR5 on the B cell induces expression of $LT\alpha_1\beta_1$. This then induces differentiation of neighbouring FDCs and their expression of CXCL13 creating a positive feedback loop (97). The B cells expression of $LT\alpha_1\beta_1$

also induces CCL21 expression by stromal cells which is vital in the recruitment and retention of T cells in the T cell zones. Along with CCL21, CCL19 is also involved in attracting T cells and DCs to the T zones via interaction with CCR7 (98).

LTα has also been found to have a role upstream of these chemokines. LTα deficient mice do not have the normal segregation of B and T cell zones and the average size of the white pulp is decreased. The formation of FDC clusters and germinal centres within the white pulp of the spleen does not occur within these mice, which also lack lymph nodes and Peyer's patches. In addition LTα KO mice do not have the marginal zone of monoclonal antibody (MOMA-1) staining, which highlights metallophilic macrophages. This is in contrast to the TNFR-1 deficient mice, suggesting that LTα can regulate certain aspects of the splenic white pulp through other receptors (99). Interestingly, when BM transplantation was utilised, the LTα deficient mouse demonstrated that although LTα is vital for the initial segregation of B and T zones, it is not crucial for maintaining the structure (100,101). This was in contrast to the generation and continuance of FDC clusters within the spleen, which was shown to be LTα dependent (102).

In the spleen both innate and adaptive immune responses can occur, the white pulp is involved in adaptive immunity whereas the marginal zone is involved in both innate and adaptive immunity (92). An important property of the spleen is that most of the blood flow passes through the marginal zone and then along the white pulp, making the spleen a very efficient monitor of the blood. A critical role of the spleen is protection against blood-borne pathogens, splenectomy due to infection, inflammation or trauma, leads to a lifelong requirement for antibiotics (103).

1.3 Inflammation

Inflammation is a basic mechanism of our immune system. It is an attempt by the body to restore and maintain homeostasis after injury and is an integral part of body defences. Most defence elements are transported in the blood and inflammation is the means by which these elements leave the blood and enter the tissue around the injured or infected site. Inflammation plays three important roles in combating an infection, it delivers additional effector molecules, provides a physical barrier to prevent spreading and promotes the repair of injured tissue (6). The signs of inflammation were first described by Celsus over 2000 years ago as calor, dolor, rubor and tumor (2). Acute inflammation is essentially beneficial; however, excess or prolonged inflammation can cause harm. Chronic inflammation is an inflammatory response characterised by the infiltration of mononuclear cells, tissue destruction, angiogenesis and fibrosis. Persistent inflammatory diseases lead to the development of long-lasting or frequently recurring inflammation, for example rheumatoid arthritis (RA) (section 1.4.4.1), lupus, and inflammatory bowel disease (2).

1.3.1 Acute Inflammation

An acute inflammatory response is a normal process in response to injury or infection. It is characterised by local dilation of blood vessels and increased vessel permeability to improve blood flow to the area. Acute inflammation is primarily mediated by neutrophils, which are the first leucocytes to enter the injured site (2).

Normally after a pathogen has been eliminated the immune response ceases and so the inflammation subsides and is cleared. Clearance of the acute inflammatory response involves apoptosis of the vast majority of the infiltrating leucocytes with subsequent

phagocytosis and tissue structure and function returning to normal (2,104). Acute inflammation is also under strict endogenous control involving anti-inflammatory mediators which reverse vascular changes and inhibit leucocyte migration and activation. Examples of anti-inflammatory mediators include cytokines IL-1, IL-4, IL-10 and TGF-β (6). In addition, there are also pro-resolution agonists that do not just inhibit the inflammatory cascade, as anti-inflammatory mediators do, but actively dismantle it. Pro-resolution agonists include lipoxins, resolvins and protectins (105). Lipoxins have been described as early braking signals for inflammation, increasing apoptotic neutrophil phagocytosis, decreasing adhesion molecule activation and decreasing migration of neutrophils and eosinophils (106,107). Cyclopentenone prostoglandins have also been shown to play a role in the resolution of inflammation through repression of pro-inflammatory macrophage function (108).

1.3.2 Chronic Inflammation

Prolonged inflammation ceases to be beneficial and can contribute to the pathogenesis of many diseases. Chronic inflammation is primarily mediated by monocytes and long-lived macrophages. Later stages involve the persistent accumulation of lymphocytes suggesting a distorted balance between mechanisms that increase cell number, recruitment, retention and proliferation and those that decrease cell number, emigration and death (figure 1.8) (10). For example, clearance of the inflammatory infiltrate by apoptosis can be inhibited by anti-apoptotic factors present in the local microenvironment, such as joints of patients with RA. Interaction with synovial fibroblasts upregulated Bcl-xL but not Bcl-2 and thereby prevented T cell apoptosis (109). Type 1 interferons, which are produced by synovial fibroblasts and macrophages in RA, have also been demonstrated as a survival factor for T cells.

Thereby increasing the number of T cells in the joint (110). As well as increased survival, inappropriate retention of T cells has also been observed. Upregulation of CXCR4 on T cells and it's ligand CXCL12 on stromal cells within the RA joint caused the T cells to be retained within the chronic inflammatory site rather than emigrating (111). Lymphocyte egress requires sphingosine 1-phosphate receptor-1 ($S1P_1$) (112), IFNα and β have been found to inhibit lymphocytes responsiveness to sphingosine 1-phosphate by inducing cell surface activation marker CD69. $S1P_1$ forms a complex with CD69, promoting downmodulation and inhibiting lymphocyte egress (112).

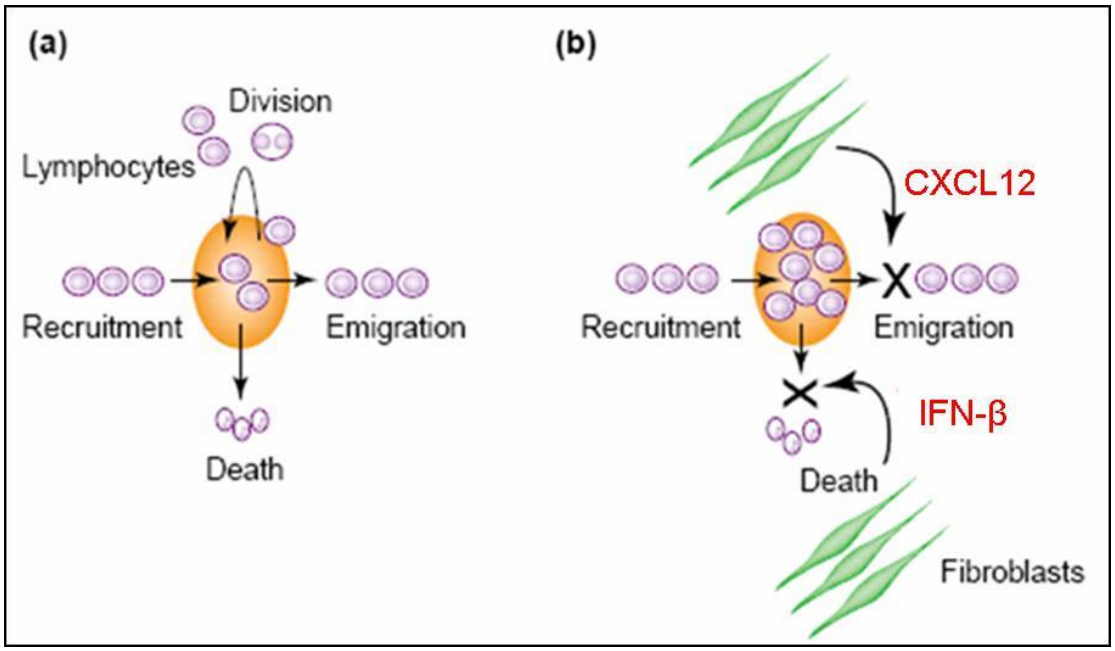

Figure 1.8 Dynamic balance of cell accumulation
(a) During a normal inflammatory response homeostasis is maintained and inflammation resolved (b) In chronic persistent inflammation inappropriate retention of leucocytes occurs as fibroblasts and other resident stromal cells produce pro-retentive (CXCL12) and pro-survival (IFN-β) factors. [Taken from Buckley *et al*, 2001, (113)].

1.3.2.1 Lymphoid neogenesis in inflammation

During chronic inflammation a specialised type of lymphogenesis can occur, which results in tertiary lymphoid neogenesis. Kratz *et al* (1996), demonstrated a unified model for lymphoid organ structure development during chronic inflammation based on LTα expression (104). Tertiary lymphoid organs arise under environmental influences and are the ectopic accumulations of lymphoid cells. It is important to note that these structures have many similarities to secondary lymphoid organs especially lymph nodes (figure 1.9). They arise randomly in adult peripheral tissue often in non-lymphoid locations and have been found in immune diseases (114), microbial infection (115) and chronic allograft rejection (116). In addition, transgenic mouse models of chronic inflammation that over express inflammatory cytokines, for example TNF and LTα have been shown to develop these structures (117). In diseases such as RA, where chronic inflammation occurs, cytokine and chemokine expression is constitutive. It is under these conditions that tertiary lymphoid organs are found in the joints of a RA patients but why they form and the molecular basis for their persistence is unknown (35,118). Stromal cells, in particular fibroblasts, contribute to the microenvironment in chronic inflammation, by providing pro-survival and retention signals via production of factors such as TGF-β and CXCL12. As such they have been implicated in the formation of tertiary lymphoid tissues (110,111).

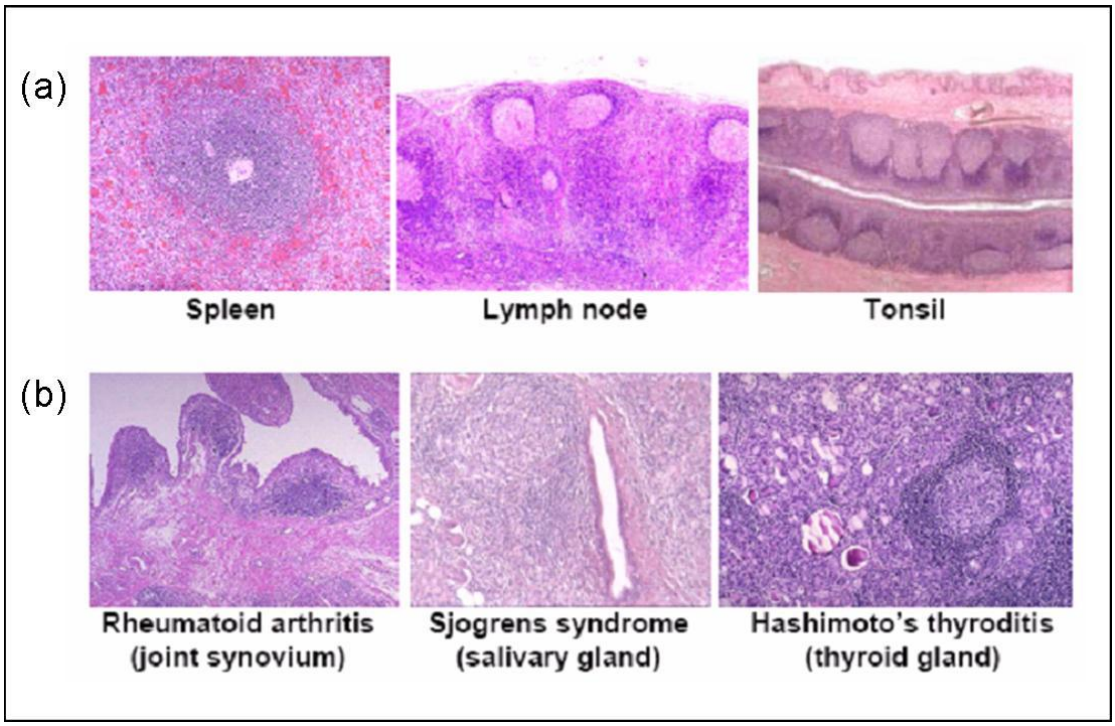

Figure 1.9 Secondary and tertiary lymphoid tissues
(a) Secondary lymphoid tissues; hematoxylin and eosin stain of normal spleen, lymph node and tonsil architecture (b) Tertiary lymphoid tissues; hematoxylin and eosin stain of inflamed synovium in Rheumatoid arthritis, salivary gland in Sjogrens syndrome and thyroid gland in Hashimoto's thyroditis. [Pictures courtesy of Dr Debbie Hardie and Dr Karim Raza, Division of Immunity and Infection, University of Birmingham].

1.4 The Fibroblast

Stroma is an important structural component of vertebrate animals. It consists of ECM, mesenchymal cells and a scaffold consisting of blood and lymphatic vessels, nerves and inflammatory cells (119). The most abundant cell type of tissue stroma is the fibroblast (120) (figure 1.10). Fibroblasts are traditionally identified by their spindle shaped morphology and their ability to adhere to plastic *in vitro* (121). Fibroblasts are ubiquitous cells that provide mechanical strength to tissues by producing ECM components which form a supporting framework. These components include type I, III and V collagen and fibronectin (122). They also produce factors that are involved in the formation of basement membranes such as type IV collagen and laminin (123). Fibroblasts have a role in ECM homeostasis as they not only

produce the ECM components but also the proteases that degrade it and regulate its turnover, such as metalloproteinases (MMPs) (124).

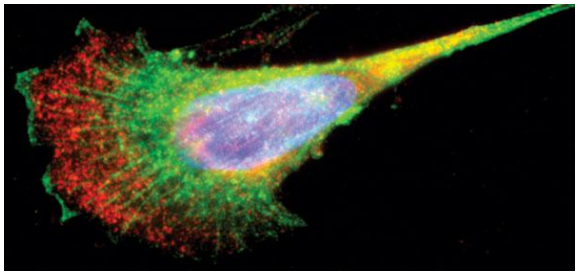

Figure 1.10 A migrating fibroblast
Red = β-actin mRNA, Green = β-actin protein and Blue = nuclear staining. [Taken from Dahm *et al*, 2005, (125)].

1.4.1 Fibroblast origin

Fibroblasts are believed to arise from three distinct cellular origins: primary mesenchyme, local epithelial-mesenchymal transition (EMT) or bone marrow derived precursors.

It is widely accepted that the majority of fibroblasts originate from primary mesenchymal cells and that upon the appropriate stimulation these fibroblasts can proliferate to generate new fibroblasts (126). Local EMT is a central mechanism for diversifying cells in the formation of complex tissues (figure 1.11) (127). Fibroblasts can be derived by this process in adult tissue following epithelial stress such as inflammation or tissue injury. Essentially EMT disaggregates epithelial cells and reshapes epithelia for movement. The epithelium loses polarity, adherens junctions, tight junctions, desmosomes and cytokeratin intermediate filaments. They also rearrange their F-actin stress fibres producing filopodia and lamellopodia (127). A combination of cytokines associated with digestion of the basement membrane is believed to instigate EMT, as well as MMPs (128) and TGF-β (129). However, the

order of importance of the cytokines involved during inflammation is still unclear as many are present in significant amounts at the site. EMT also contributes to the growing premise that fibroblasts are not a homogeneous population and are a much more active and heterogeneous cell population than first appreciated (130-132).

Generation of fibroblasts has also been reported from precursor cells called fibrocytes. These cells represent ~0.05% of circulating blood cells that are believed to arise from $CD14^+$ peripheral blood monocytes (133). They express both haematopoietic and stromal cell markers and are thought to differentiate into fibroblasts at inflammatory or wound sites (134,135). All three of these processes appear to contribute to the pathological accumulation of fibroblasts (126,127,136,137).

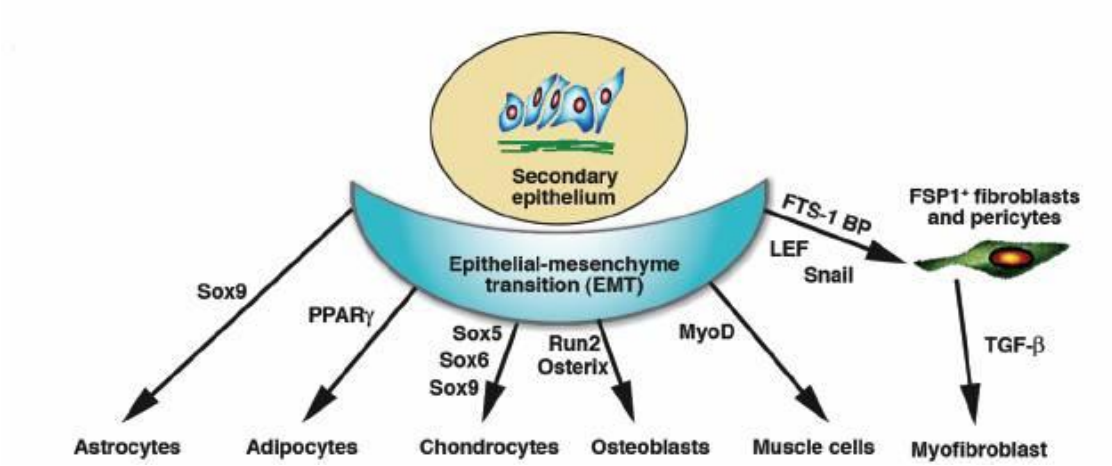

Figure 1.11 The cellular variation arising from EMT
Epithelia undergo EMT to form the cells of connective tissue, including astrocytes, adipocytes chondrocytes, osteoblasts, muscle cells, and fibroblasts. These processes are regulated by morphogenic cues and a variety of transcription factors. [Adapted from Kalluri *et al*, 2003, (138)]

1.4.2 Identifying fibroblasts

Research into fibroblasts has lagged behind that of other cell types, partly due to their phenotypic and functional heterogeneity but also their plasticity in differentiation capacity (section 1.4.3). Moreover, a lack of selective markers for isolating and

discriminating between fibroblast subtypes has hampered previous studies. Therefore, the lack of markers for other cell lineages is used to indicate the presence of a fibroblast i.e. non-lymphoid, non-endothelial and non-epithelial. Currently a panel of markers are used to identify fibroblasts but as none are exclusive to fibroblasts they can provide only an indication. This panel includes intermediate filament associated protein Vimentin, the relatively newly isolated cell surface protein CD248 (section 1.4.2.1), α-smooth muscle actin (SMA) and VCAM-1. A comprehensive list can be found in table 1.1 (138).

Marker	**Function**	**Fibroblast types in which it is found**	**Other cell types in which it is found**
Vimentin	Intermediate filament associated protein	Miscellaneous	Endothelial cells, myoepothelial cells, neurons
α-SMA	Intermediate filament associated protein	Myofibroblasts	Vascular smooth muscle cells, pericytes, myoepithelial cells
Desmin	Intermediate filament associated protein	Skin fibroblasts	Muscle cells, vascular smooth muscle cells
FSP1	Intermediate filament associated protein	Miscellaneous	Invasive carcinoma cells
Discoidin-domain receptor 2	Collagen receptor	Cardiac fibroblasts	Endothelial cells
FAP	Serine protease	Activated fibroblasts	Activated melanocytes
$\alpha_1\beta_1$ integrin	Collagen receptor	Miscellaneous	Monocytes, endothelial cells
Prolyl 4-hydroxylase	Collagen biosynthesis	Miscellaneous	Endothelial cells, cancer cells, epithelial cells
Pro-collagen 1α2	Collagen-1 biosysnthesis	Miscellaneous	Osteoblasts, chondroblasts
CD248	Unknown	Miscellaneous	Pericytes
VCAM-1	Cell adhesion	Miscellaneous	Activated endothelial cells

Table 1.1 Fibroblast indicators
Markers used to identify fibroblast cells [adapted from Kaluri *et al*, 2006, (138)].

1.4.2.1 CD248

CD248, also known as endosialin or tumour endothelial marker-1 (TEM-1) has been described as a marker of interstitial fibroblasts in human (139) and mouse (140) tissues. It was identified after screening for monoclonal antibodies (mAbs) that recognise proteins with a fibroblast-restricted distribution. CD248 is found in its immature form within the Golgi network, it is then modified by approximately 95kDa of highly sialylated O-linked oligosaccharides to form the 175kDa mature protein (139). In addition, CD248 is expressed on a subset of pericytes, a relatively undifferentiated cell associated with the walls of small blood vessels (141). Expression of CD248 on pericytes as well as interstitial fibroblasts, suggests that they may have been recruited from a stromal fibroblast population or that they are undergoing fibroblast differentiation (139).

CD248 is part of a family of molecules implicated in tissue remodelling and repair, including CD93 and CD141 (142,143). It has been demonstrated to be involved in development, showing high expression in the embryo which decreases postnatally (140,144). Although this pattern of expression has been observed in many tissues, variations in expression were noted between different lymphoid tissues, suggesting site specific expression (140,145). Interestingly, a role for CD248 in remodelling has been suggested. When challenging a mouse with Salmonella infection, induced splenomegaly occurs, which is associated with complete remodelling of the splenic architecture. Upon remodelling of the spleen CD248 expression is significantly increased which then decreases upon resolution of the infection (140). These findings suggest that populations of CD248 expressing fibroblasts are involved in embryonic development and the remodelling of tissues in the adult. Loss of CD248 expression

due to siRNA-mediated silencing showed a decrease in fibroblast proliferation and migration (146). Studies in the CD248 KO mouse confirmed these effects on migration and proliferation as tumour growth, invasiveness and metastasis was reduced in abdominal sites (147). However normal tumour growth was seen in tumours implanted in subcutaneous sites, again indicating site specific expression. In addition, CD248 expression has been observed on mesenchymal stromal cells (MSCs) (section 1.4.4.3) and it has been postulated that CD248 can be used as a marker for MSCs (146,148).

1.4.3 Fibroblast heterogeneity

The difficulty of finding specific fibroblast markers is further complicated as fibroblasts isolated from different anatomical sites exhibit different functional properties, such as altered migratory capacity, ECM production, degradation and contractility (149). Previous work in our group, identified two groups of human fibroblasts based on their gene and protein expression. These were termed typical (peripheral) and atypical (lymphoid) fibroblasts (figure 1.12) (150). It was shown that upon stimulation with inflammatory mediators such as TNFα, IL-4 and IFNγ the gene expression of the typical fibroblast could be modified such that they adopt features of atypical fibroblasts. This finding strongly suggests that inflammation can, at least transiently, alter fibroblast gene expression profiles (150).

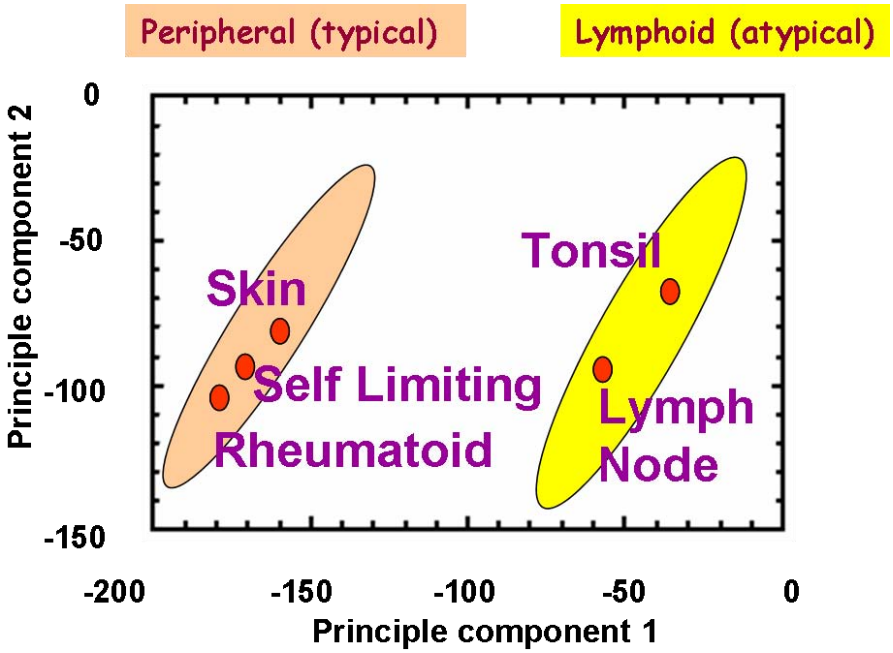

Figure 1.12 Principle component analysis of peripheral and lymphoid fibroblasts Using whole genome microarrays, fibroblasts can be grouped based on their gene expression into typical and atypical fibroblasts. [Adapted from Parsonage *et al*, 2003, (136)].

Moreover, gene expression profiles of primary human fibroblasts have shown large scale differences related to three broad anatomical divisions; anterior-posterior, proximal-distal and dermal-nondermal (151). A set of 337 genes was found to vary according to these divisions. This set included genes involved in pattern formation, cell-cell signalling and matrix remodelling. Interestingly, HOX gene expression was differentially expressed according to the location where the fibroblasts were isolated. Specifically HOXA13 was found to maintain the distal specific transcriptional programme in adult fibroblasts (figure 1.13). More recently Rinn *et al*, (2008) demonstrated that in serially passaged fibroblasts HOX gene expression levels were stable for at least 35 passages *in vitro*. Within the same study they also found that addition of cultured medium from one fibroblast culture to another from a different site did not affect the clustering of these genes and a clear separation between sites was still observed. In addition, co-culturing different fibroblasts together did not alter

their gene expression. This suggests that secreted factors from adult fibroblasts are unable to reprogramme the site-specific gene expression of other fibroblasts, implying that the majority of site-specific gene expression in fibroblasts is controlled by a cell-autonomous epigenetic mechanism (152).

Taken together, these data suggest that the gene expression profile of adult human fibroblasts may play a significant role in assigning positional identity within an organism (151,152) and has led to the proposal of a stromal address code, analogous to that of an endothelial address code (153). In this hypothesis, the fibroblasts posses a gene expression profile specific for their anatomical position. This gene expression profile could be an important source of molecular landmarks for site specific differentiation, by constructing an identifiable ECM expressing structure and cell surface proteins that provide site specific signalling for a given anatomic origin (151). The stromal address code hypothesis therefore provides an attractive mechanism for the switch from resolving to chronic inflammation, as an altered code could cause inappropriate recruitment, retention or proliferation of leucocytes.

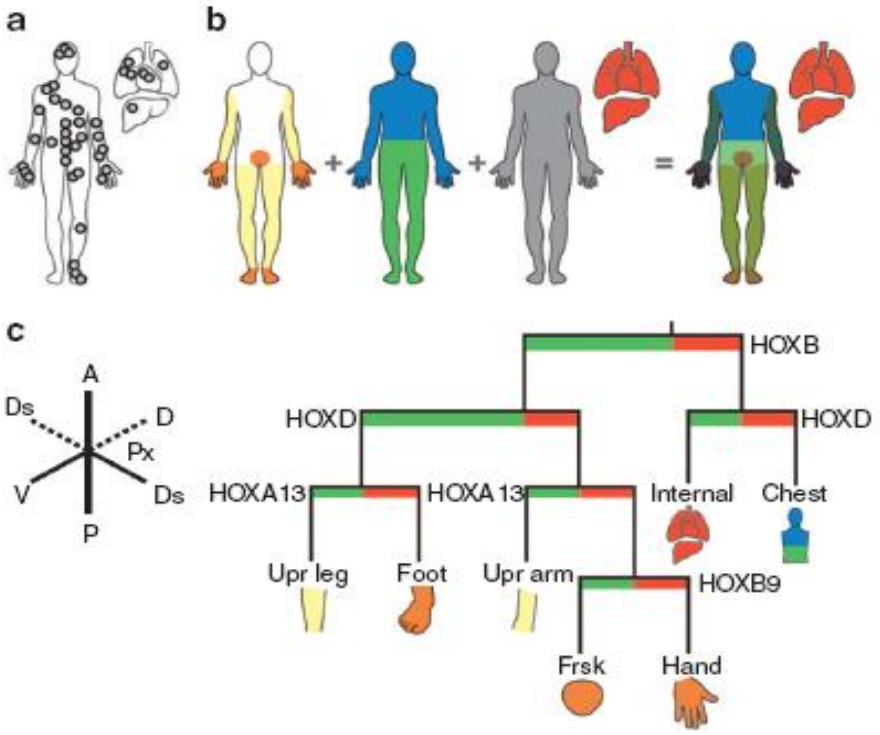

Figure 1.13 Human fibroblast gene expression patterns
(a) A total of 47 primary cultures representing 43 unique anatomic sites (grey circles) that map the human body were profiled by gene expression microarrays. (b) Model of fibroblast differentiation by overlapping positional patterns of gene expression: proximal (yellow), distal (orange), anterior (blue), posterior (green) and internal organs (red). (c) A decision tree of HOX expression that distinguish unique anatomic positions. Right: red indicates higher-than-average and green lower-than-average expression of a given HOX gene, relative to the average expression level across 47 cultures. Each anatomic site can be correctly identified by monitoring the expression level of three HOX genes or less. Left: the developmental axes that demarcate site-specific gene expression of fibroblasts: anterior–posterior, proximal–distal and dermal–non-dermal. A third developmental axis, dorsal–ventral, did not correlate with large-scale site-specific gene expression in fibroblasts. [Taken from Rinn *et al*, 2008, (154)].

1.4.4 The function of fibroblasts

It is becoming clear that fibroblasts play not only an active role in defining the structure of tissue microenvironments but also modulating immune cell behaviour by conditioning the local cellular content and cytokine production, specifically tailoring the response to the cause of the damage (113).

Fibroblast activation leads to the production of appropriate cytokines, chemokines and prostanoids such as PGE_2 (138). Fibroblasts can also regulate the behaviour of haematopoietic cells present in damaged tissue, CD40-CD40 ligand interaction lead to activation of the NF-κB family of receptors, causing fibroblasts to synthesise high levels of IL-6, IL-8, cyclooxygenase-2 and the polysaccharide hyaluronan (155). This mechanism is analagous to the cross talk that occurs between lymphocytes and APCs, suggesting a role for fibroblast and leucocyte crosstalk during an immune response. Therefore as fibroblasts are relatively long lived it is important that their activation is tightly regulated (156-158). Fibroblasts have been shown to contribute to the pathology of many diseases, either directly for example by overproduction of matrix components during fibrosis and/or indirectly by influencing the behaviour of neighbouring cell types (159-161).

1.4.4.1 The role of fibroblasts in rheumatoid arthritis

Rheumatoid arthritis is the most common chronic inflammatory disease affecting approximately 1% of the population worldwide (162). The main feature of RA is persistent joint inflammation. The disease is characterised by inflammation and hyperplasia of the synovial membranes of diarthrodial joints in a symmetrical fashion (163). This causes pain and joint failure and can eventually lead to disfiguration and disability (164,165). Over 20 years ago fibroblasts isolated from diseased tissues were shown to be phenotypically different from those taken from normal tissue. Fassbender, (1983) described subpopulations of fibroblasts within the synovial membrane which showed morphological and biological differences (166). In RA, specifically, fibroblasts are thought to play a key role in the pathogenesis of the disease, as synovial fibroblasts are not only different between healthy and RA patients

but also between the layers of the rheumatoid synovium (155). Fibroblasts from the lining layer have features of cell activation and are believed to result in aggressive, invasive behaviour. This has been demonstrated *in vivo* using co-implantation of fibroblasts and cartilage under the kidney capsule. Fibroblasts from RA synovium invade cartilage when implanted together whereas fibroblasts from osteoarthritis or healthy patients do not (167). In addition, these fibroblasts also appear to differ morphologically, with a more rounded shape, a larger pale nucleus and prominent nucleoli. Differences in shape were further reported in RA patients, where a reorganisation of the actin cytoskeleton and disregulation of ECM adhesion was observed (155). As well as the phenotypic changes, synovial fibroblasts from RA patients have also been shown functionally to affect the accumulation and survival of lymphocytes in the joint by increasing survival and recruitment of T cells (109). The properties of these fibroblasts suggest a transformed cell phenotype and lead to the hypothesis that the rheumatoid synovium is a locally invasive tumour (168,169).

1.4.4.2 The role of fibroblasts in cancer

The microenvironment surrounding malignant cells is named the tumour stroma, this consists of non-malignant cells, ECM and growth factors embedded in the ECM (170). Fibroblasts are a component of the tumour stroma and have also been shown to have a role in cancer at all stages including progression (171), growth (172) and metastasis (173). Specifically, at the site of a tumour the surrounding fibroblasts remain continuously activated and have a modified phenotype. It is believed that they may facilitate angiogenesis and cancer progression, such fibroblasts have been named cancer-associated fibroblasts (CAFs) (138). In breast carcinomas, approximately 80% of stromal fibroblasts are thought to have this activated phenotype, expressing α-SMA

and have been termed myofibroblasts. Myofibroblasts and CAFs produce increased amounts of MMPs, affecting ECM turnover and altering the ECM composition (174). A source of CAFs may be EMT (section 1.4.1) from cancer cells and also normal epithelial cells, this process has been recognised as an important factor in cancer progression and may also modulate the progression by providing fibroblasts-like cells with an altered genome (175). The stromal elements of a tumour have, in recent studies, shown significant prognostic value. The stromal gene signature found could be used alone or in combination with existing techniques to improve molecular classification and outcome prediction, such as patients who would respond better to aggressive treatment (176).

1.4.4.3 Fibroblasts and their relationship to MSC

Mesenchymal stem cells (MSCs) are typically found in the bone marrow but can also be expanded from a wide variety of adult and fetal tissues (177,178). MSCs are multipotent stem cells that can differentiate into a variety of cell types including osteoblasts, chondrocytes and adipocytes (179). In recent literature, it is important to note that the terms mesenchymal stem cell and mesenchymal stromal cell have been used interchangeably. Whether they describe an identical cell type remains controversial. Of relevance to this thesis, it has been found that MSCs can suppress virtually all immune cell responses. For example they can suppress T cell proliferation, induce T cell anergy and apoptosis and modulate cytokine production through the production of soluble factors (180). A role for IFN-γ in the immunosuppression mediated by stromal cells has been suggested. IFN-γ induces indoleamine 2,3-dioxygenase (IDO) which accelerates tryptophan degradation, thereby suppressing T cells (181). However, to distinguish fibroblasts from MSCs is

difficult as cell surface antigens used to define MSCs are also expressed on fibroblasts (182). Fibroblasts have also been found to have the potential to differentiate into other cell types such as adipocytes, osteocytes and chondrocytes and effect proliferation and survival of lymphocytes (120). Despite this it may be that all stromal or fibroblast-like cells have immunosuppressive potential. A study by Jones *et al* (2007) supports this theory as they conclude that immunosuppressive effect is a fundamental characteristic of all stroma (183).

MSCs have been described as a heterogeneous population and it is quite plausible that fibroblasts such as those described previously by our group and Rinn *et al*, 2008 may be termed mesenchymal stromal cells (183).

1.5 Hypothesis

Previous work by our group has proposed that in addition to the well described endothelial area code fibroblasts help define a stromal postcode that regulates leucocyte survival, retention, proliferation and differentiation within tissues (136). Inappropriate expression of all or parts of the code may be involved in the switch from resolving to persistent inflammation.

The hypothesis is that fibroblasts derived from different murine lymphoid sites have site specific gene and protein expression and that this results in functional differences during interactions with other cell types and products.

1.6 Aims of thesis

The main aims of this thesis were to:

a) **identify whether mouse fibroblasts from lymphoid and peripheral organs have site specific gene expression as reported in the human studies (151) and if so what genes are site defining.**
b) **determine whether LTα stimulation affects this pattern of gene expression, for example inducing a more lymphoid like profile in peripheral fibroblasts.**
c) **consider the functional relevance of these differing fibroblast gene expression profiles in the mouse by using *in vivo* models of organ grafting under the kidney capsule and assessing leucocyte accumulation in differing fibroblast microenvironments.**

Chapter Two

Materials and Methods

CHAPTER TWO

Materials and Methods

2.1 Media, solutions and other reagents

All reagents were purchased from Sigma Aldrich (Poole, UK) unless otherwise stated.

2.1.1 Complete fibroblast medium
Dulbecco's Modified Eagles Medium
10% Fetal Calf Serum
2mM glutamine
100U/ml penicillin
100µg/ml streptomycin

2.1.2 Washing medium
RPMI 1640
10% Fetal Calf Serum

2.1.3 Phosphate buffered saline (PBS)
Dissolve 1 tablet in 100ml distilled water -autoclave at 115°C for 10 minutes.

2.1.4 Tissue digestion buffer
RPMI 1640
10% Fetal Calf Serum
1mg/ml Collagenase/Dispase (Roche Diagnostics, Germany)
20µg/ml DNase

2.1.5 Red blood cell lysis buffer (pH 7.2)
1 litre dH_20
8.29g NH_4Cl (0.17M)
1g $KHCO_3$ (1µM)
37.2mg EDTA (1mM)

2.1.6 10x Annexin V staining buffer
100ml dH_20
0.1M HEPES
1.4M NaCl
25mM $CaCl_2$

2.1.7 Freezing medium
Fetal Calf Serum
10% Dimethyl sulfoxide

2.1.8 TBE buffer
89nM Tris HCL
89nM Boric Acid
3mM EDTA

2.1.9 1% Agarose gel

4g Agarose (1%)
400mls TBE Buffer
40µl ethidium bromide (10mg/ml)

2.1.10 Hoechst nuclear counterstain

1µl Hoechst bisBenzimide 332382 (10mg/ml)
1ml PBS 0.05% azide

2.1.11 1, 4-diazabicyclo[2.2.2]octane (DABCO)

2.4g DABCO
10mls PBS

2.2 Antibodies

2.2.1 Isotype controls

Isotype	Format	Source
Rat IgG1	PE	SouthernBiotech 0116-09
Rat IgG2a	Fitc	eBioscience 11-4321-82
Rat IgG2b	APC	BD Pharmingen 556924
Rat IgG2b	PE	BD Pharmingen 553989
Rat IgG2b	Biotin	eBioscience 13-4031-82
Rat IgG2b	Fitc	eBioscience 11-4032-82
Rabbit IgG	uncongugated	Dako x0903
Armenian Hamster IgG	Fitc	SeroTec MCA2356F
Armenian Hamster IgG1	uncongugated	eBioscience 14-4888-81
Mouse IgG1	uncongugated	Dako x0931

Table 2.1 Isotype control antibodies

2.2.2 Anti-mouse primary antibodies

Antigen	Isotype	Format	Source	Working Dilution (confocal)	Working dilution (FACS)
α-SMA	Mouse IgG2a, κ	Purified	Lab Vision UK	1/50	-
B220	Rat IgG2a, κ	Fitc	eBio 11-0452-85	1/200	1/200
Caspase-3	Rabbit IgG	Purified	BD Pharmingen 559565	1/50	-
CD3	Hamster IgG	Fitc	eBio 11-0031-85	1/50	1/100
CD11c	Hamster IgG	Fitc	eBio 11-0114-82	1/50	1/50
CD31	Rat IgG2a	Fitc	eBio 11-0311-81	1/50	1/100
CD45	Rat IgG2b, κ	PE	BD Pharmingen 553081	-	1/200
CD45	Rat IgG2b	APC	BD Pharmingen 550864	-	1/300
CD54	Rat IgG2b, κ	PE	eBio 12-0541-81	-	1/1500
CD248	Polyclonal Rabbit IgG	Purified pre-absorbed	JRM	1/50	1/50
F4/80	Rat IgG2b	Fitc	SeroTec MCA497F	1/50	1/50
gp38	Hamster IgG	Uncongugated	Kind gift from Andy Farr (72)	1/5	1/50
PDGF-Rα	Rat IgG2a, κ	Biotin	eBio 13-1401-82	1/100	-
VCAM-1	Rat IgG1, κ	Biotin	SouthernBiotech 1510-08	1/50	1/100
Vimentin	Mouse IgG1, κ	Uncongugated	Lab Vision	1/50	1/50

Table 2.2 Primary antibodies

2.2.3 Secondary antibodies

Antigen	Source	Working Dilution (confocal)	Working Dilution (FACS)
Donkey anti Goat Alexa 546	Molecular Probes A11056	1/100	-
Donkey anti Goat Cy5	Jackson Immunoresearch 705-176-147	1/100	-
Donkey anti Goat Cy2	Jackson Immunoresearch 705-226-147	1/100	-
Donkey anti Goat Fitc	Jackson Immunoresearch 705-096-147	1/200	-
Donkey anti Sheep	Jackson Immunoresearch 713-176-147	1/200	-
Goat anti Rat Alexa 546	Molecular Probes A11081	1/100	-
Goat anti Rabbit Alexa 633	Molecular Probes A21072	1/100	-
Goat anti Mouse Alexa 488	Molecular Probes A21121	1/100	-
Goat anti Mouse IgG2a Tritc	Southern Biotech 1080-03	1/50	-
Goat anti Hamster Cy5	Jackson Immunoresearch 107-176-142	1/100	-
Goat anti Fitc 488	Molecular Probes A11096	1/100	-
Goat anti Rabbit PE	Southern Biotech 4050-09	-	1/100
Goat anti mouse IgG1 Fitc	Southern Biotech 6061-02	-	1/100
Goat anti hamster Fitc	Southern Biotech 1072-02	-	1/75
Rabbit anti Rat Biotin	Dako E0468	1/100	-
Streptavidin Alexa 546	Molecular Probes S-11225	1/50	
Streptavidin Alexa 633	Molecular Probes S21375	1/100	-

Table 2.3 Secondary antibodies

2.3 Mice

All experiments were performed in accordance with UK laws and with the approval of the University of Birmingham ethics committee. All mice were bred and maintained in the Biomedical Services Unit (BMSU) at the University of Birmingham.

2.4 Cell culture

Required tissues were isolated from mice by dissection under sterile conditions; routinely spleen, liver, thymus, skin, lung and inguinal, axillary and cervical lymph nodes were taken. The tissues were stored in 2mls of RPMI/10%FCS on ice. These were then either non-enzymatically (section 2.4.1.) or enzymatically (section 2.4.2) digested for culture. All cells were cultured in complete fibroblast medium (section 2.1.1) and maintained at 37°C, 5% CO_2, with media changed every 3-4 days.

2.4.1 Non-enzymatic digestion

Tissues were mashed directly on a sterile 50µm-nylon filter gauze in a Petri dish with approximately 200µl of complete fibroblast medium (section 2.1.1) using a 5ml syringe plunger. The gauze was then washed with a further 2ml complete fibroblast medium and the cell suspension transferred to a 6 or 24 well plate; 6 well plates were routinely used with 24 well plates used for those organs where a small cell suspension was obtained e.g. lymph nodes. Complete fibroblast medium was then added to the well to a total volume of 4mls per well in a 6 well plate and 2mls per well in a 24 well plate. Cell cultures were washed in PBS (section 2.1.3) after 7 days to remove cell debris and all non-adherent cells.

2.4.2 Enzymatic digestion

Bone marrow flushes were collected, centrifuged at 300g for 5 minutes at 4°C and resuspended in 2mls tissue digestion buffer (TDB) (section 2.1.4). All solid organs were cut into small pieces and incubated at 37°C in 2ml TDB for a maximum of 40 minutes, resuspending the cells every 5 minutes by pipetting. The quality of the cell suspension was checked every 10 minutes microscopically. Once a single cell suspension was obtained 1ml of washing medium (section 2.1.2) was added and the cells centrifuged at 300g for 4 minutes at 4°C. Cells were resuspended in 1ml complete fibroblast medium (section 2.1.1) and transferred into 6 or 24 well plates as in section 2.4.1. Cell cultures were washed in PBS (section 2.1.3) after 7 days to remove cell debris and all non-adherent cells.

2.4.3 Passaging

Once 90-100% confluence was reached cultures were washed with PBS and passaged using a 2X trypsin-ethylene-diamine-tetra-acetic acid (EDTA) solution (Sigma). Once cells had detached, as assessed microscopically, fresh complete fibroblast medium (section 2.1.1) was added to neutralise the trypsin and the resulting cell suspension centrifuged at 300g for 4 minutes at 4°C. The cells were then either resuspended in 33% conditioned fibroblast medium diluted with fresh complete fibroblast medium for continued culture or in 1 ml of culture medium ready for long term storage (section 2.4.4).

2.4.4 Freezing of cell cultures for long term storage

Cells resuspended in 1ml of culture medium as described in section 2.4.3 were counted using trypan blue (Sigma) and then centrifuged at 300g for 4 minutes at 4°C.

Cells were resuspended in freezing medium (section 2.1.7) and stored at -80°C for 24 hours after which they were then transferred to liquid N_2 for long term storage. The number of cells frozen was then used to compare with the number of live cells obtained post-recovery from storage as described in section 2.4.5.

2.4.5 Cell recovery from long term storage

Cells were defrosted at 37°C, reconstituted in 12ml of complete fibroblast medium (section 2.1.1) and centrifuged at 300g for 4 minutes at 4°C. The cell pellet was then resuspended in 1ml complete fibroblast medium and the number of live cells were counted using trypan blue. The number of live cells being brought up per vial was recorded for comparison with number frozen down. The cells were then maintained at 37°C in a 5% CO_2 atmosphere.

2.4.6 Cell imaging

During their time in culture, cells were imaged in 6 well plates at x10 magnification using the Axiover 200 microscope (Zeiss, Germany). Images were processed using capture (AIC) software (Digital Pixel, UK).

2.4.7 Cell sorting

Cells were sorted into two populations based on their CD45 expression using the MoFlow Cell Sorter (Coulter). Briefly, cells were lifted from the plate using a non-enzymatic cell dissociation buffer (Gibco). The cells were centrifuged at 300g at 4°C for 8 minutes and resuspended in tissue digestion buffer (section 2.1.4) for 10 minutes at 37°C to negate cell clumping. The cells were washed, pelleted as above, re-suspended in 500µl RPMI 10% FCS containing anti-mouse CD16/32 (1:50) to block

Fc receptors on the cells and incubated on ice for 20 minutes. The cells were then centrifuged at 300g for 8 minutes at 4°C and resuspended with 220µl of RPMI 10%FCS. Two 10µl aliquots of cells were then added to 190µl of RPMI 10%FCS for the unstained and irrelevant controls, with the remaining to be stained with the antibody of interest. Antibodies (section 2.2.1 and 2.2.2) were added to the respective tubes and incubated on ice for 30 minutes after which, the cells were washed with RPMI 10% FCS and pelleted before being filtered through a 50µM filter to remove any clumped cells or debris. The cells were then sorted based on their CD45 expression using the MoFlow Cell Sorter (Coulter). Sorted cells were resuspended in complete fibroblast medium (section 2.1.1) and transferred into 6 or 24 well plates for culture.

2.5 RNA extraction

Using the RNeasy mini kit (QIAgen, 74965) RNA extraction was performed as per the manufactures instructions. Briefly, pelleted, trypsinised cells (section 2.4.3) were lysed by 600µl of a highly denaturing guanidine-thiocynate-containing buffer, containing 1% β-mercaptoethanol, which immediately inactivates RNases to ensure purification of intact RNA. The lysate was then homogenised using a QIAshredder spin column (QIAgen, 79654). Genomic DNA was removed from each sample using the RNase-free DNase kit (QIAgen, 79254) according to the manufactures instructions. Purified total RNA was eluted with 30µl of RNase-free water, the concentration determined using a spectrophotometer (BioPhotometer, Eppendorf) and stored at -80°C.

2.5.1 cDNA preparation

Complementary DNA (cDNA) was synthesised using the smart PCR cDNA synthesis kit (BD Biosciences, K1052-1) as per the manufacturer's instructions. Briefly, 5µg of total RNA was incubated with 3µg of oligo-dN_6 to prime for cDNA synthesis for 10 minutes at 70°C, after which the reaction was stopped by placing it on ice. Reverse transcription (RT) was performed for 1 hr at 41°C with the enzyme deactivated by incubating the mixture at 90°C for 10 minutes; using the following master mix;

1.25µl H_2O
6µl 5X first strand buffer
3µl 0.1M DTT
1.5µl dNTP (10mM)
0.75µl RNAse Inhibitor (RNAguard, Pharmacia, ~40 U/µl)
1.5µl M-MLV (Gibco) (1 µl/µg RNA, stock 200 U/µl)

The cDNA was stored at 4°C for up to a week and -20°C for longer periods.

2.5.2 Polymerase chain reaction (PCR)

Using cDNA as the template (section 2.5.1), PCR was performed using ReddyMix manufactured by ABIgene (AB-0575-LDb), along with primers for the gene of interest. Reactions were carried out using a PCR Sprint Thermal Cycler (Hybaid systems, Waltham, MA). The general programme used was: 92°C for 2 minutes, 30 cycles of 92°C for 15s, 65°C for 30s and 70°C for 45s. Then finally 72°C for 5 minutes. Cycle number and the annealing temperature were dependent on the primers being used (table 2.4). The PCR products obtained were then analysed by running on a 1% (w/v) agarose gel containing EtBr (section 2.1.9) in a TBE running buffer (section 2.1.8). One microgram of one hundred base pair molecular weight markers were also run on each gel (Roche Diagnostics, Germany). The DNA bands were

visualised using a Syngene ultraviolet (UV) transilluminator (Cambridge, UK) and identified by product size.

Gene	Primer sequences 5' – 3'	Annealing temperature (°C)	Number of cycles	Product size (base pairs)
β-actin	**F:**ATCTACGAGGGCTATGCTCTCC	55	30	148
	R:CTTTGATGTCACGCACGATTTCC			
BP-3	**F:** AGGGACAAGTCACTGTTCTGG	55	34	105
	R: AACTTTGCCATACAGCACGTC			
CCL7	**F:** TCTGTGCCTGCTGCTCATAG	55	34	81
	R: TTGACATAGCAGCATGTGGAT			
CCL11	**F:** CACGGTCACTTCCTTCACC	55	34	76
	R: GGTCATGATAAAGCAGCAGGA			
CCL19	**F:**ACTCACATCGACTCTCTAGG	60	30	370
	R:ACTCACATCGACTCTCTAGG			
CCL21	**F:** TCCCGGCAATCCTGTTCTC	60	30	249
	R:TTCTGCACCCAGCCTTCCT			
CD3	**F:** TGCCTCAGAAGCATGATAAGC	60	35	200
	R: GCCCAGAGTGATACAGATGTCAA			
CD19	**F:** GGAGGCAATGTTGTGCTGC	60	35	164
	R: ACAATCACTAGCAAGATGCCC			
CD31	**F:**CATGATGCCAAGTCTGAGA	55	35	165
	R:GTGGGCTTATCTGTGAATGT			
CD248	**F:**TTCCCACTCCCAAATCAGTG	56	30	480
	R:GAGTCCTGGTGTGCCTTTG			
CXCL1	**F:** CTGGGATTCACCTCAAGAACATC	55	34	117
	R: CAGGGTCAAGGCAAGCCTC			
CXCL12	**F:** GCTCTGCATCAGTGACGG TA	55	34	163
	R: TGTCTGTTGTTGTTCTTCAGC			
CXCL13	**F:** TGAGGCTCAGCACAGCAA	55	34	77
	R: ATGGGCTTCCAGAATACCG			
EpCAM	**F:** GCGGCTCAGAGAGACTGTG	60	34	139
	R: CCAAGCATTTAGACGCCAGTTT			
F4/80	**F:**CTTTGGCTATGGGCTTCCAGTC	56	30	165
	R:GCAAGGAGGACAGAGTTTATCGTG			
FOXN1	**F:**CTCGTCGTTTGTGCCTGAC	55	34	243
	R:TGCCTCTTGTAGGGGTGGAAA			
gp38	**F:**ACCGTGCCAGTGTTGTTCTG	56	30	159
	R:AGCACCTGTGGTTGTTATTTTGT			
ICAM-1	**F:** GTGATGCTCAGGTATCCATCCA	55	34	213
	R: CACAGTTCTCAAAGCACAGCG			
Lhx8	**F:** GAGCTCGGACCAGCTTCA	55	34	67
	R: TTGTTGTCCTGAGCGAACTG			
IL-6	**F:** GCTACCAAACTGGATATAATCAGGA	55	34	78
	R: CCAGGTAGCTATGGTACTCCAGAA			
IL-7	**F:**TTCCTCCACTGATCCTTGTTCT	55	34	200
	R:AGCAGCTTCCTTTGTATCATCAC			
IL-15	**F:**TCTCCCTAAAACAGAGGCCAA	55	34	125
	R:TGCAACTGGGATGAAAGT			
IL-17RA	**F:** AGTGTTTCCTCTACCCAGCAC	55	34	194
	R: GAAAACCGCCACCGCTTAC			
IL-17RF	**F:** TGCCATTCTGAGGGAGGTAG	55	34	205
	R: GGGGTCTCGAGTGATGTTGT			
IL-22R	**F:**CATTGCCTTCTAGGTCTCCTC	55	34	134
	R:CCTGCTTGCCAGTGCAAAAT			

LTα	**F:**GATGCCATGGGTCAAGTGCT **R:**GCTTGGCACCCCTCCTGTC	55	34	136
LTβR	**F:**GAGCAGAACCGGACACTAGC **R:**GAAGGTAGGGATGAGCACC	55	34	255
Lyve-1	**F:**CGCCCATGATTCTGCATGTAGA **R:**CAGCACACTAGCCTGGTGTTA	55	34	112
Meox2	**F:** AATCTAGACCTCACTGAAAGACAGG **R:** CTTTGACCCGCTTCCACTT	55	34	73
PDGFRα	**F:** TGGCATGATGGTCGATTCTA **R:** CGCTGAGGTGGTAGAAGGAG	55	34	152
PDGFRβ	**F:** TTCCAGGAGTGATACCAGCTT **R:**AGGGGGCGTGATGACTAGG	55	34	104
Prox-1	**F:**GGCATTGAAAAACTCCCGTA **R:**CGGACGTGAAGTTCAACAGA	55	34	279
Prrx1	**F:** AGTCACCGGGACTGACCA **R:** TCTTCTCCTCAGAGTTCAACTGG	55	34	72
TNFR1	**F:**ATGTACACCAAGTTGGTAGC **R:**AATATCCTCGAGGCTCTGAGA	55	34	213
TRANCE	**F:**TGCTAATGTTCCACGAAATG **R:**ATTCAGGTGTCCAACCCTTCC	55	34	102
TSLP	**F:**ACGGATGGGGCTAACTTACAA **R:**AGTCCTCGATTTGCTCGAACT	55	34	128
VCAM-1	**F:**GACCTGTTCCAGCGAGGGTCTA **R:**CTTCCATCCTCATAGCAATTAAGGTG	56	30	122
VEGFa	**F:** GCAGCTTGAGTTAAACGAACG **R:** GGTTCCCGAAACCCTGAG	55	35	94
VEGFc	**F:** CAGACAAGTTCATTCAATTATTAGACG **R:** TGTCTTGTTAGCTGCCTGACAC	55	35	73

Table 2.4 Primer sequences and conditions

2.6 Real time PCR (Q-PCR)

Gene expression profiles of purified total RNA from cell cultures were analysed using the Quantitech Probe one-step Q-PCR kit (QIAgen, 204443) in combination with TaqMan Low Density Arrays (www.appliedbiosystems.com). A working solution of 50% Quantitech buffer, 1% Quantitect RT-PCR enzyme mix and 49% total RNA was prepared per sample; typically 100µl buffer, 2µl enzyme and total RNA sample diluted to 98µl in RNase-free water. Approximately 95µl of each sample's working solution was then pipetted into two ports of the card. The cards were then centrifuged twice at 300g for 1 minute to allow adequate distribution of the sample over the probes. The plate was then sealed and the ports cut off. The Applied Biosystems

7900HT Fast Real-Time PCR System was used to perform the real time-PCR with the following cycle conditions: 50°C for 30 minutes, 94.5°C for 15 minutes and the 40 cycles of 96°C for 30 seconds and 59.7°C for 1 minute.

Data was analysed using SDS 2.2 (Applied Biosystems). Relative quantification of signal per cell was achieved by setting thresholds within the logarithmic phase of the PCR for the control gene and the target gene. The cycle number (C_t) at which the threshold was reached was then determined. The C_t for the target gene was subtracted from the C_t for the control gene and the relative quantity was calculated as $2^{-\Delta CT}$. RT-PCRs using identical primers and probes run in separate plates were analysed together with the same threshold and baseline settings so that they could be compared.

2.7 Microarrays

Whole mouse genome arrays of 37,632 genes (AROS version 4.0, Operon, USA) were printed by Liverpool Microarray Facility (Liverpool University, England).

2.7.1 cDNA amplification

For use with microarrays first strand cDNA was synthesised and amplified from approximately 0.05-1ug of total RNA. The protocol supplied for the SMART cDNA synthesis kit (BD biosciences, K1052-1) was utilised with the following adaptations: 3'SMART CDS Primer II A (sequence 5'-AAGCAGTGGTATCAACGCAGAGTACT$_{(30)}$N$_{-1}$N-3' (Invitrogen); SMART II A oligonucleotide (sequence 5'-AAGCAGTGGTATCAACGCAGAGTACGCGGG-3', (Invitrogen); 5' PCR primer II A (sequence 5'-AAGCAGTGGTATCAACGCAGAGT-3' (Invitrogen); superscript II reverse

transcriptase (Invitrogen) and its accompanying 1st strand buffer used in place of Powerscript reverse transcriptase.

After amplification the cDNA was purified using NucleoSpin Extract II (Macherey Nagel, 740609.250) following the kit instructions, with cDNA eluted in 50µl H_2O. The eluted cDNA was then quantified by measuring absorbance at 260nm with a spectrophotometer (BioPhotometer, Eppendorf) and purity assessed visually by β-actin PCR on an electrophoresis gel. All cDNA was stored at -20°C.

2.7.2 CyDye labelling of cDNA

Cy3-dCTP and Cy5-dCTP labelling was performed using 10µl of sample cDNA. To do this 20µl of random primer mix (Bioprime Labelling Kit, Invitrogen, 18094-011) and 13µl deionised H_2O was added. The mix was heated to 94°C for 5 minutes and then cooled on ice for the addition of other reagents.

The following was then added: 1.2µl 10mM dATP; 1.2µl dTTP; 1.2µl dGTP; 0.72µl dCTP (100mM dNTP Set PCR Grade, Invitrogen 10297-018); 0.68µl H_2O; 1µl of either Cy3 dCTP (sample) (Amersham Biosciences, PA53021) or Cy5 dCTP (reference) (Amersham Biosciences, PA55021); 1µl 40U/µl Klenow enzyme (Bioprime Labelling Kit, Invitrogen, 18094-011). The reaction was then incubated at 37°C for 8 hours.

The labelled cDNA was purified by means of NucleoSpin Extract II (Macherey Nagel, 740609.250) as per the instructions eluting in 70µl H_2O. The quantity of labelled cDNA was then assessed using a spectrophotometer by calculating

absorbance at 550nm (Cy3-dCTP) or 650nm (Cy5-dCTP). The yield in pmol was calculated by the following:

For Cy3 = Abs550 x 50µl/0.15

For Cy5 = Abs 650 x 50µl/0.25

The labelled cDNA was then stored in the dark at 4°C before hybridisation.

2.7.3 Array hybridisation and analysis

GAPS II coated slide arrays (Corning, 40006) were pre-hybridised as per the instructions using formamide (Sigma, F-9037) with the pre-hybridisation solution for 2 hours at 42°C. The pre-hybridised slide was dipped in H_2O, and spun to dry. It was then placed into a corning hybridisation chamber (Corning, 2551) and the preparation instructions for the chamber followed.

Labelled cDNA (100pmols) from test and reference samples was taken, mixed and concentrated using Microcon YM-30 concentration columns, as per the instructions, (Millipore, 42410) eluting in a final volume of 30µl H_2O. 50µl of cDNA mix containing 5µg PolyA DNA and 8µg Cot1 DNA as nucleic acid-blockers and formamide was added to the 30µl labelled probe and the mix denatured at 95°C for 5 minutes. The probe mix was then applied to the surface of the slide and a Lifter Slip (VWR International, 7370042) applied. The hybridisation chamber was then closed, wrapped in a damp paper towel and foil and hybridised at 42°C for 16-20 hours. After hybridisation the slides were immersed in 2x saline-sodium citrate (SSC) buffer + 0.1% SDS at 42°C to remove the coverslip. The slide was then subsequently washed for 5 minutes at 42°C in 2 x SSC + 0.1% SDS, followed by 5 minutes room

temperature in 0.2 x SSC and four 5 minutes room temperature washes in 0.05 x SSC. Finally, slides were dipped into H_2O and centrifuged at 500g for 15 minutes at room temperature to dry.

The arrays were then scanned using Scan Array GX Plus (Perkin Elmer) and software Scan Array Express (Perkin Elmer) and aligned manually. MultiExperiment Viewer version 4.0 (TM4 Software Suite) was used to analyse the data obtained. Hierarchical clustering was performed to group samples together based on the similarity of their gene expression profiles. Significance analysis of microarrays (SAM) was used to find the genes significantly different between the samples. This is based largely upon the student T-test with the addition of a false discovery rate (FDR). The relative difference (d(i)) was compared to the distribution of d(i) following random permutation of the sample categories. For each d(i), a certain proportion of all genes in the permutation set (control set) will be found to be 'significant' by chance and this parameter was then used to calculate a FDR. The FDR was set to 10% when SAM analysis was completed.

2.8 Indirect-immunofluorescent staining

Cells to be used for immunofluorescence analysis were grown in 8-well chamber slides (BD Biosciences, 354108). Once confluent, the media and chambers were removed, slides washed in PBS for 5 minutes at room temperature and left to air dry for 1 hour. The cells were fixed in 100% acetone at 4°C for 20 minutes, allowed to dry at room temperature for 10 minutes and stored at -80°C for future use.

When staining, the slide was removed from the freezer and defrosted at room temperature. Each cell area was drawn round with a hydrophobic pen to prevent

leakage and placed in PBS for 10 minutes to re-hydrate the cells. Cells were blocked with 10% goat serum diluted in PBS/2%BSA for 10 minutes at room temperature to prevent non-specific binding. Cells were then incubated with primary or irrelevant control antibodies in PBS/2%BSA (sections 2.2.1 and 2.2.2, respectively). Subsequently, the slides were washed in PBS for 10 minutes and cells incubated with secondary antibody in PBS/2%BSA (section 2.2.3). All incubations were at room temperature, for 1 hour in a humidity chamber, with fluorophores protected from light. Finally, the slides were washed in PBS for 10 minutes and incubated with the nuclear counterstain Hoechst (section 2.1.10) for 2 minutes to visualise cell nuclei. The sections were then mounted with glycerol containing anti-fade reagent, DABCO (section 2.1.11), a coverslip was added and slides stored at -20°C. Cell staining was visualised using a LSM510 confocal microscope (Zeiss, Germany) at x10 or x40 magnification. Images were captured and processed using Zeiss LSM image software (Zeiss, Germany).

2.9 Flow cytometry

All flow cytometry on stromal cells was performed using an EPICS XL Flow Cytometer (Beckman Coulter). The Dako Cyan-ADP high performance flow cytometer (Colorado, US) was used with all other cells.

The analysis of specific surface molecules from freshly isolated cells was achieved using standard flow cytometry techniques. Briefly, cells were resuspended at $1x10^6$/ml in PBS/2%BSA. Approximately $1x10^5$ cells were transferred into a fetal calf serum (FCS) coated well of a 96 well round-bottomed plate to reduce adherence of the cells to the plate. These were washed, pelleted by centrifuging at 300g for 4

minutes, and then re-suspended in PBS/2%BSA containing anti-mouse CD16/32 (1:20) to block Fc receptors on the cells. The plate was then incubated on ice for 20 minutes after which cells were pelleted and resupended in primary antibody (section 2.2.2) and incubated on ice for a further 20 minutes. The cells were then washed twice with 150µl PBS/2%BSA and resuspended in secondary antibody (section 2.2.3) or PBS 2%BSA (depending on whether immunofluorescence was direct or indirect) and incubated on ice for 20 minutes. Finally the cells were washed as above and transferred to FCS-coated FACS tubes in a total volume of 400µl. For each antibody irrelevant controls (section 2.2.1) were also performed using the same working concentration. The cells were then run through the EPICS XL Flow Cytometer (Beckman Coulter) or the Dako Cyan-ADP high performance flow cytometer (Colorado, USA). Flow cytometry data was analysed using WinMDI software (version 2.8, Scripps Research Institute, La Jolla, CA) or Summit software (version 4.3, Dako, Colorado, USA).

2.10 Lymphotoxin α treatment

CD45 negative stromal cells were seeded at $5x10^4$ in a 24-well plate in 500µl of complete fibroblast medium (section 2.1.1). After 24 hours the medium was replaced with 500µl of fresh complete fibroblast medium containing 1µg/ml lymphotoxin (LT) α. Control wells with no LTα were also carried out. After 24 hours the stromal cells were washed in PBS and removed from the plate by incubating with 1ml cell dissociation buffer (Gibco) for 20 minutes at 37°C, 5%CO_2. The cells were then stained for VCAM-1 and ICAM-1 expression using flow cytometry (section 2.9).

2.11 Cellular co-culture

CD45 negative stromal cells were seeded at $3x10^5$ in a 6-well plate in 3mls of complete fibroblast medium (section 2.1.1). After 24 hours 1.5mls of conditioned medium from the cultures was added to a fresh well and a further 1.5mls of fresh complete fibroblast medium was added to every well. 3mls fresh complete fibroblast medium was also used as a control. A spleen, taken from a C57BL6 mouse was mashed through a 0.22µm filter, the cells washed and resuspended in red blood cell lysis buffer (section 2.1.6) for 10 minutes on ice. The lymphocytes were then counted and resuspended in complete fibroblast medium. $1x10^6$ lymphocytes isolated from the spleen were added to each well. The plate was then incubated at 37°C, 5% CO_2. After 4 days the wells were washed vigorously and the splenocytes stained for flow cytometry (section 2.9). The percentage of viable cells was also determined by flow cytometry with Annexin V. Post antibody incubations, cells were washed in cold PBS, followed by a single wash in Annexin V staining buffer (section 2.1.6). The cells were then pelleted as above, resuspended in 100µl of the staining buffer, containing Annexin V Fitc antibody (5:200) and incubated on ice for 20 minutes. The cells were then analysed by flow cytometry (section 2.9).

2.12 Reaggregates

Reaggregates were formed using $1x10^5$ cells/200µl complete fibroblast media (section 2.1.1) in a well of a V-well plate (Sterilin, UK). The plate was then centrifuged at 900g for 5 minutes at room temperature and again at 225g for 5 minutes at room temperature, to ensure complete formation of the pellet. The plate was then placed at 37°C/5%CO_2 for 24 hours prior to use. For the LTα treated reaggregates, 1µg/ml LTα was added to the media in the V-well plate during the formation of the reaggregate.

When using the collagen sponge for structural support, $1x10^5$ cells in 50µl of complete fibroblast media were added to the sponge (2-3mm^3) (Pfizer, UK) and incubated at 37°C/5%CO_2 for 2 hours prior to use.

2.12.1 Grafting under the kidney capsule

Cell reaggregates (section 2.12) were grafted under the kidney capsule of a 6-8 week old C57BL6 mouse (figure 2.1). Mice were anaesthetised using 4% Isofluorane (May and Baker, Dagenham, UK) carried in oxygen. Pre-operative Buprenorphine (Temgesic, AnimalCare, York, UK) was administered sub-cutaneously using a syringe fitted with a 25 Gauge needle at a dose of 2mg/kg. The fur was removed from the left lumbar region using clippers and area cleaned with 70% ethanol (figure 2.1A). A small cut was made in the left lower lumbar region approx 0.5-1cm in length depending on the size of the mouse, using surgical blunt ended scissors (F.S.T) (figure 2.1B). Scissors were used to make space between the skin and peritoneum before making a similar size cut in the peritoneum. Blunt forceps were used to locate the kidney, which was then eased out of the body cavity using the fat attached to the lower end, the kidney was kept moist using gauze soaked in PBS (figure 2.1C). Sharp forceps were used to pierce a small hole in the capsule of the kidney, and open up a small space beneath the capsule. The reaggregate was then placed under the capsule with up to three reaggragates placed under each kidney capsule. The edges of the skin and peritoneum were lifted from beneath the kidney to allow it to slip back into the abdominal cavity. The peritoneum was closed with at least two stitches using size 5, round-bodied, vicryl sutures (Johnson and Johnson Intl). The skin was cleaned using a cotton bud dipped in PBS and the wound closed with a clip (VetTech Solutions, UK)

(figure 2.1D). The grafts were removed and analysed by immunofluorescence (section 2.8) after 1-4 weeks.

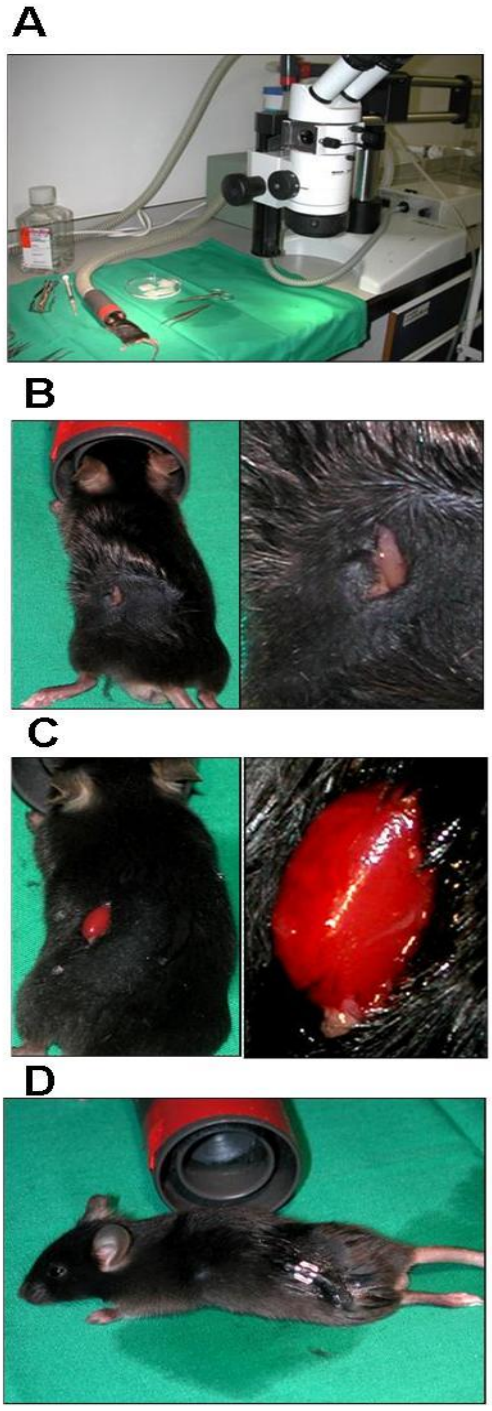

Figure 2.1 Kidney capsule transfer
Reaggregates were inserted under the kidney capsule of adult C57BL6 mice after (A) anaesthetising the mouse, (B) removing the fur from the left flank of the mouse and making a small cut through the skin and peritoneum and (C) manoeuvring the kidney out of the body cavity. Up to three stromal cell reaggregates were grafted under one kidney capsule (C) before the wound was closed with sutures and a clip (D). [Pictures courtesy of Dr Stephanie Glanville, Division of Immunity and Infection, Birmingham UK].

2.13 Statistical analysis

Statistical analysis of flow cytometry data was carried out using GraphPad Prism computer software (GraphPad Software, Inc., San Diego, CA) and performing a paired T-test.

Chapter Three

Characterisation of Fibroblasts from Lymphoid and Peripheral Sites in the Adult Mouse

CHAPTER THREE

Characterisation of Fibroblasts from Lymphoid and Peripheral Sites in the Adult Mouse

3.1 Introduction

Fibroblasts are a heterogeneous population that can arise from at least three different pathways. They differentiate from mesenchyme, arise by epithelial-mesenchymal transition (EMT) or from bone marrow derived precursor cells (127). Their gene expression profile in humans has been found to be site-specific and it is possible to group fibroblast populations based on three anatomical divisions: anterior-posterior, proximal-distal and dermal-nondermal (151). This site specific gene expression is thought to be controlled by a cell-autonomous mechanism, as culturing fibroblasts from one site with conditioned medium from another did not alter the expression of the genes used to group them. Co-culturing fibroblasts from different sites was also unsuccessful at modifying gene expression (152). Previous work from this group has looked at human fibroblast gene expression and the changes in our gene expression in response to certain cytokines which mimic Th_1, Th_2 and inflammatory stimuli. It was reported that inflammation can, at least transiently, alter a fibroblasts gene expression profile (150).

In this chapter fibroblast heterogeneity in several mouse organs was investigated by comparing cell morphology, gene expression and protein expression. By fully characterising these cells the aim was to group fibroblasts by anatomical site of origin based on the criteria previously described in the human studies (151). Stromal cells were successfully cultured from the spleen, thymus, liver, skin, lung and inguinal,

axillary and cervical lymph nodes of 6 week old female C57BL6 mice. Site specific differences were observed between these cultures in cell morphology, protein expression and gene expression.

3.2 Results

3.2.1 Fibroblast characterisation

Stromal cells were isolated from the spleen, liver, thymus and inguinal, axillary and cervical lymph nodes from 6 week old female C57BL6 mice. Female mice were chosen as in human studies a female predominance is found in autoimmune diseases (184) and the age of 6 weeks old was used to ensure the lymphoid system was fully developed after birth (62). To isolate cells from tissues, both mechanical and enzymatic digestion protocols were tested. Enzymatic digestion with collagenase, dispase and DNase (section 2.4.2) proved to be more consistent at obtaining a confluent monolayer than non-enzymatic digestion (section 2.4.1) and thus was used throughout the study (data not shown). Selection for stromal cells was based on their ability to adhere to plastic, with non-adherent cells removed after 7 days, and proliferate.

3.2.1.1 Fibroblast morphology

From the outset it was clear that the enzymatically digested cell cultures derived from different organs were morphologically different from each other (figure 3.1). They demonstrated heterogeneity not only in cell shape but also in size, suggesting that these cultures may also contain different cell types. The digestion was reproducible as three different mice gave similar findings (figure 3.2).

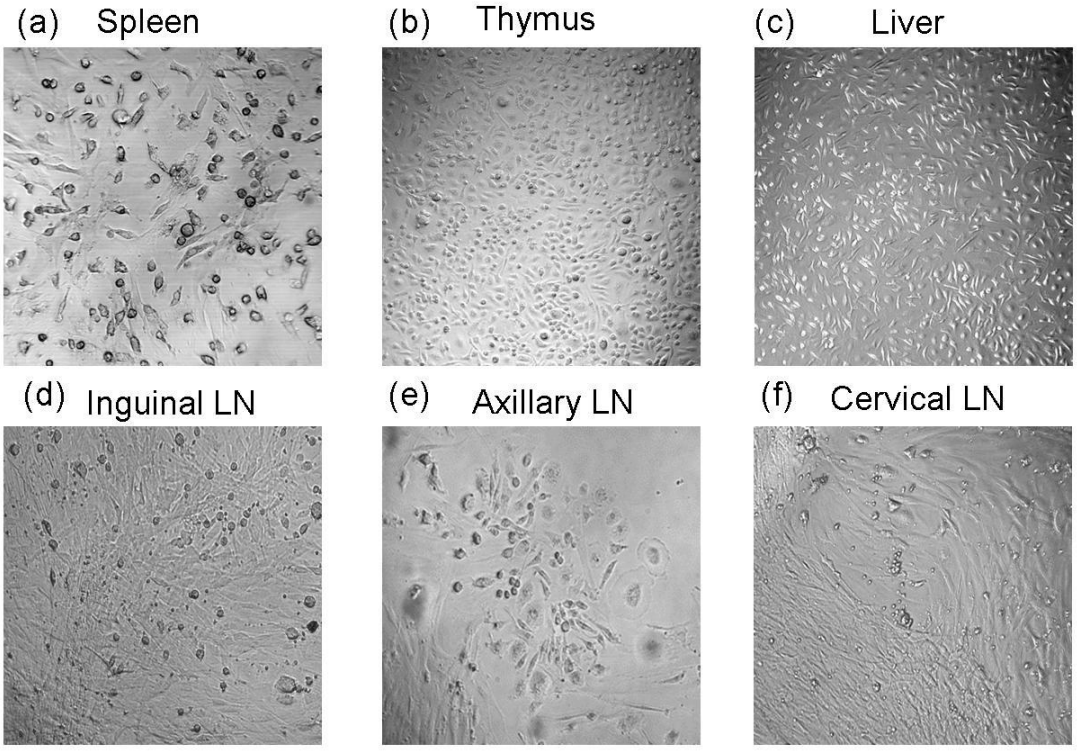

Figure 3.1 Stromal cell culture heterogeneity
Images from cell cultures derived from different organs at passage two after six weeks in culture, (a) spleen (b) thymus (c) liver (d) inguinal lymph node (e) axillary lymph node (f) cervical lymph node. Heterogeneity seen is representative of 3 independent cultures for each organ. Images taken at x10 magnification.

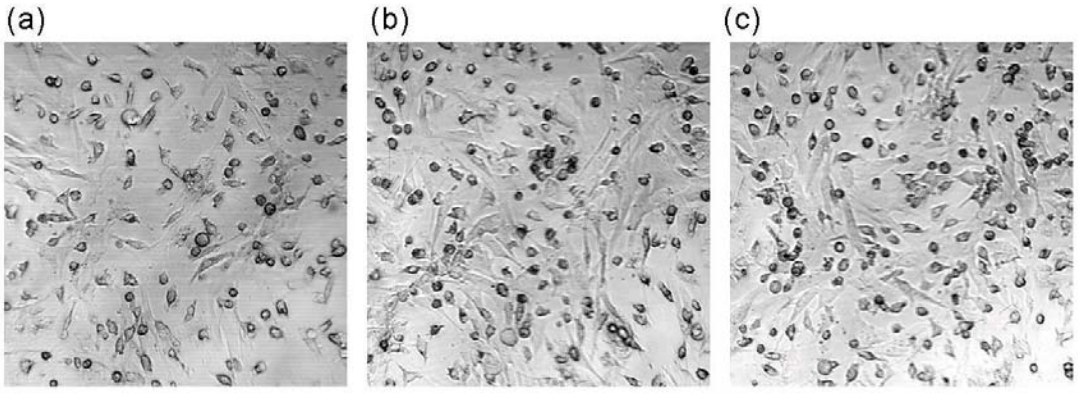

Figure 3.2 Splenic stromal cell culture heterogeneity
Images from splenic stromal cells at passage two after six weeks in culture. Demonstrating the heterogeneity observed within three separate cultures (a-c). Images taken at x10.

3.2.1.2 Fibroblast gene expression

The TaqMan low density array (LDA) is a customisable 384-well micro fluidic card, designed for use with the Applied Biosystems 7900HT Fast Real-Time PCR System, to perform hundreds of real-time PCR reactions simultaneously (section 2.6). To determine the gene expression profiles of the cultured cells described in section 3.2.1.1 a Fibroblast LDA was used containing a variety of genes. This included stromal cell associated genes, for example VCAM-1, vimentin and collagen type 1 and 3 isoforms, TNF family genes which are important in stromal cell interactions with many cell types, genes expressed by other cell lineages for elimination purposes and housekeeping genes such as β-actin as controls (appendix 8.1).

To analyse gene expression data from each of the cell cultures, RNA was extracted at passage four to six and approximately 1µg was hybridised to the Fibroblast LDA. Following real-time PCR all data was normalised to the expression of β-actin (appendix 8.2). Significance analysis of microarrays (SAM) analysis (section 2.7) was used to determine the gene expression that differed significantly between the cultures (figure 3.3a). There were 28 differentially expressed genes (table 3.1), these included TNF family members, interleukins and cytokine receptors. Genes indicative of the presence of other cell types such as CD86 expressed on antigen presenting cells (185) and CD80 expressed on activated B cells and monocytes (186) were observed in lymphoid organ cultures. CD117 which is expressed on haematopoietic stem cells (187) and PECAM-1 (CD31) which is expressed on endothelial cells, monocytes and lymphocytes (188,189) were seen within lymph node cultures. Using principle component analysis (PCA) the samples could cluster based on the expression of these 28 genes (figure 3.3b). The principle component analysis clearly demonstrates that the

liver, spleen and thymus stromal cell cultures cluster together whereas the lymph node stromal cell cultures form a more tightly clustered separate group. This suggests that it is possible to differentiate between stromal cells from the lymph node compared to the liver, spleen and thymus based on their gene expression.

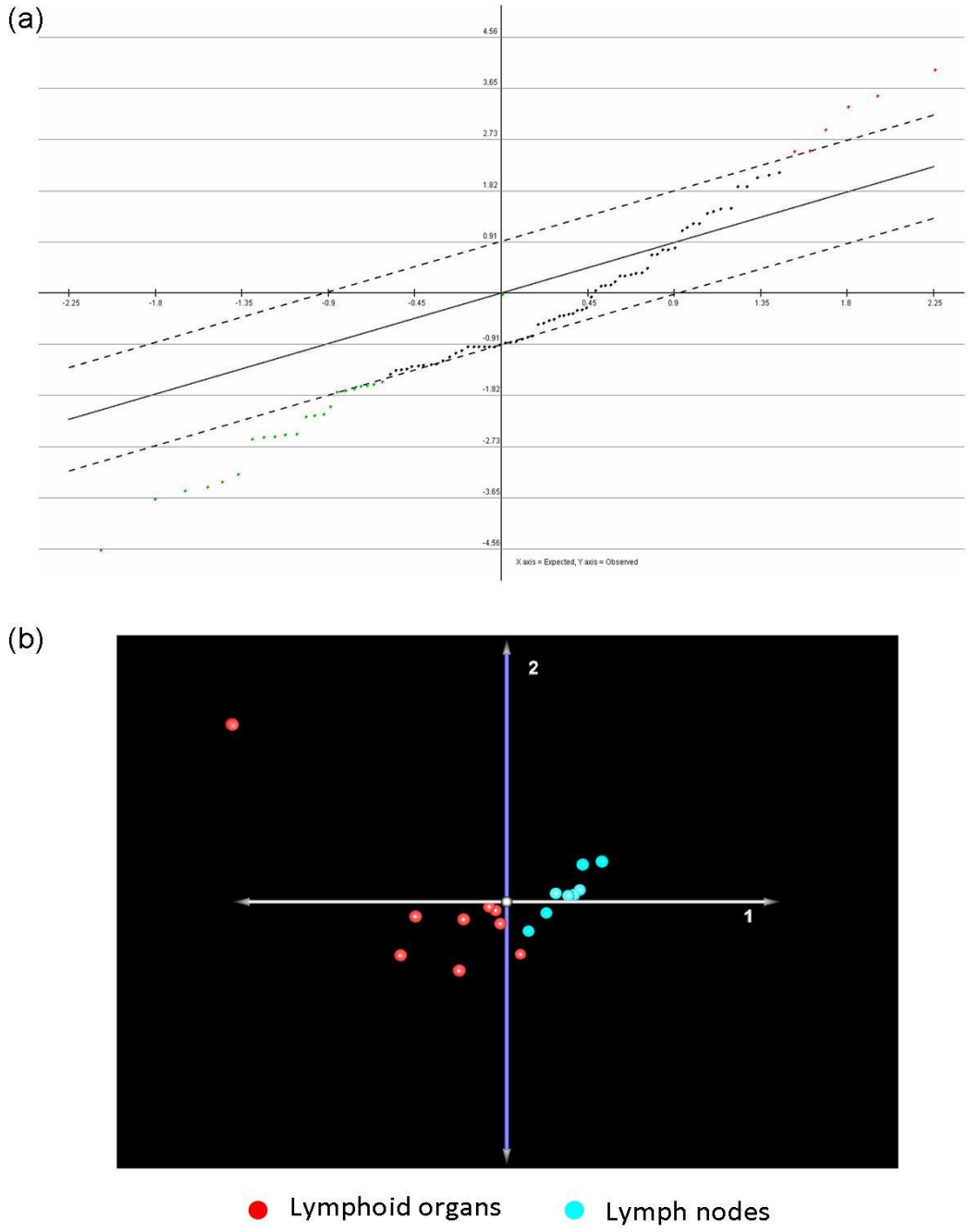

Figure 3.3 Differential gene expression between lymphoid organs and lymph nodes

(a) SAM analysis of Fibroblast LDA, dashed lines indicate the threshold of significantly different expressed genes using a 10% false discovery rate. Red dots = genes significantly upregulated in lymph nodes and green dots = genes significantly upregulated in lymphoid organs (b) PCA analysis based on the 28 significantly different expressed genes from the SAM analysis, red circles = lymphoid organs; spleen, liver and thymus and blue dots = lymph nodes; inguinal, axillary and cervical (n=3 independent stromal cell cultures for each tissue type).

Assay ID	Gene Name	Gene Name
Mm00432086_m1	Blr1	Burkitt lymphoma receptor 1
Mm00839967_g1	Ccl19	chemokine (C-C motif) ligand 19
Mm00438260_s1	Ccr1	chemokine (C-C motif) receptor 1
Mm00515543_s1	Ccr3	chemokine (C-C motif) receptor 3
Mm00711660_m1	Cd80	CD80 antigen
Mm00444543_m1	Cd86	CD86 antigen
Mm00486906_m1	Cdh1	cadherin 1
Mm00483888_m1	Col1a2	procollagen, type I, alpha 2
Mm00457902_m1	Ctss	cathepsin S
Mm00438259_m1	Cxcr3	chemokine (C-X-C motif) receptor 3
Mm00469294_m1	Ebi3	Epstein-Barr virus induced gene 3
Mm00439616_m1	Il10	interleukin 10
Mm00434151_m1	Il10ra	interleukin 10 receptor, alpha
Mm00434228_m1	Il1b	interleukin 1 beta
Mm00434295_m1	Il7r	interleukin 7 receptor
Mm00802901_m1	Lgals3	lectin, galactose binding, soluble 3
Mm00442991_m1	Mmp9	matrix metalloproteinase 9
Mm00443258_m1	Tnf	tumor necrosis factor
Mm00619239_m1	Tnfrsf14	tumor necrosis factor receptor superfamily, member 14 (herpesvirus entry mediator)
Mm00446361_m1	Tnfrsf21	tumor necrosis factor receptor superfamily, member 21
Mm00444567_m1	Tnfsf14	tumor necrosis factor (ligand) superfamily, member 14
Mm00437154_m1	Tnfsf9	tumor necrosis factor (ligand) superfamily, member 9
Mm00432087_m1	Bmp4	bone morphogenetic protein 4
Mm00445212_m1	Kit	kit oncogene
Mm00476702_m1	Pecam1	platelet/endothelial cell adhesion molecule 1
Mm00443242_m1	Tek	endothelial-specific receptor tyrosine kinase
Mm00446231_m1	Tgfa	transforming growth factor alpha
Mm00457866_m1	Tnfrsf10b	tumor necrosis factor receptor superfamily, member 10b

Table 3.1 Fibroblast LDA differentially expressed genes
Genes highlighted in red = genes significantly upregulated in lymphoid organs. Genes highlighted in turquoise = genes significantly upregulated in lymph nodes.

3.2.1.3 Fibroblast protein expression

To characterise more fully the phenotype of the cells within the stromal cell cultures and establish if the gene expression data was indicative of the proteins expressed on the cell surface flow cytometry was used. Flow cytometry allows simultaneous multiparametric analysis of the physical and/or chemical characteristics of single live cells. VCAM-1 (150), gp38 (72), Vimentin (138) and CD248 (140) were selected as fibroblast markers; CD45 to indicate haematopoietic cells (189), F4/80 to indicate macrophages (190); CD11c to indicate dendritic cells (191) and CD31 for endothelial cells (188). Protein expression heterogeneity was seen within our cultured stromal cells (figure 3.4). Reassuringly, expression of CD248, VCAM-1 and gp38 was seen in all cultures, except in the cervical lymph node culture where VCAM-1 was not detectable. The expression of these fibroblast indicators confirms their presence within the stromal cell cultures. Low expression of F4/80 and CD11c was observed suggesting there are few macrophage and dendritic cells present. CD31 expression was seen only in the inguinal and axillary lymph node cultures suggesting that the predominant cell population could be lymphatic endothelium. Interestingly, CD45 expression was present albeit at differing levels, in the spleen, thymus, liver and cervical lymph node cultures. The CD45 expression observed indicates that there are haematopoietic cells present in all cell cultures except those from inguinal and axillary lymph nodes. The presence of these other contaminating cell types could affect the aim of defining gene and protein expression differences between the stromal cell cultures.

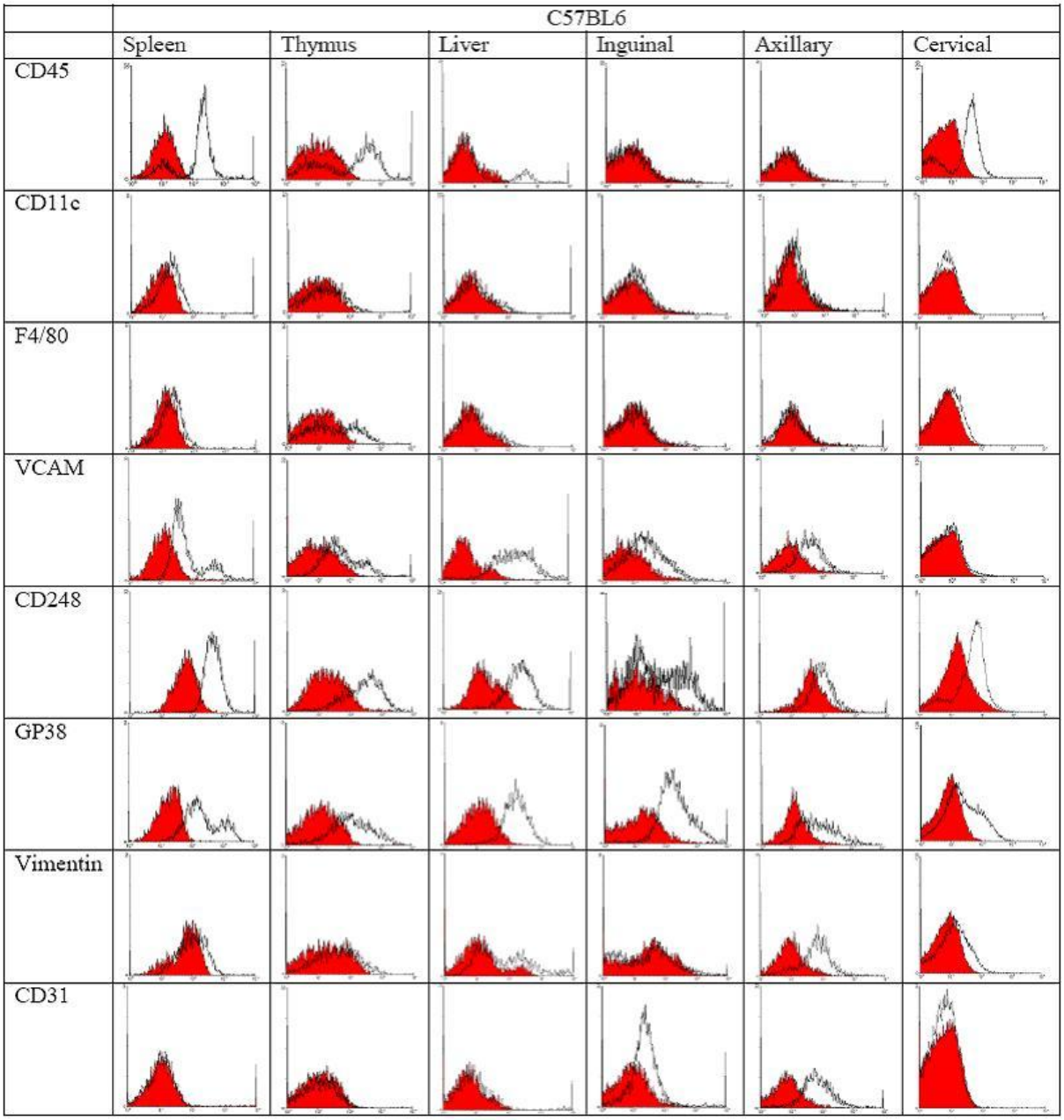

Figure 3.4 Cell surface protein expression of cultured stromal cells from different lymphoid organs

Flow cytometry data of cultured stromal cells at passage four obtained from different lymphoid organs of C57BL6 mice. Red = irrelevant control, black outline = positive protein staining (Plots representative of n=3 independent stromal cell cultures for each tissue type).

3.2.2 Homogeneous stromal cell cultures

Having observed differences in gene and protein expression when comparing the *in vitro* stromal cells, there were concerns that these may be due to, or influenced by, the heterogeneity within the cell cultures. The primary concern being, the contaminating CD45 positive cells, which are not classically thought to be stromal. Although this population decreased over time, it was still present after twelve passages (data not shown). One solution was to sort the cell cultures based upon their CD45 expression, culturing CD45 negative cells only and therefore leading to a more homogenous cell population.

3.2.2.1 Sorting stromal cell cultures

Sorting of the stromal cell cultures was originally attempted straight *ex vivo*, however the number of CD45 negative cells was very low, typically with poor survival in culture. Therefore, stromal cells were cultured without selection (section 3.2.1) until at least passage five and then sorted based on CD45 expression. Figure 3.5 shows a representative sort where two populations were collected; CD45 negative and positive cells. Both fractions were transferred back into culture to achieve a more homogeneous population. The typical purity for cell sorts was above 98%.

The CD45 negative sorted cells survived well in culture and continued proliferating up to at least 35 passages *in vitro* (data not shown). However, the CD45 positive cells grew poorly and when analysed by flow cytometry it appeared that the contaminating 1-2% of CD45 negative cells out competed the CD45 positive cells (data not shown). Thus, in all subsequent experiments CD45 negative sorted stromal cells were used.

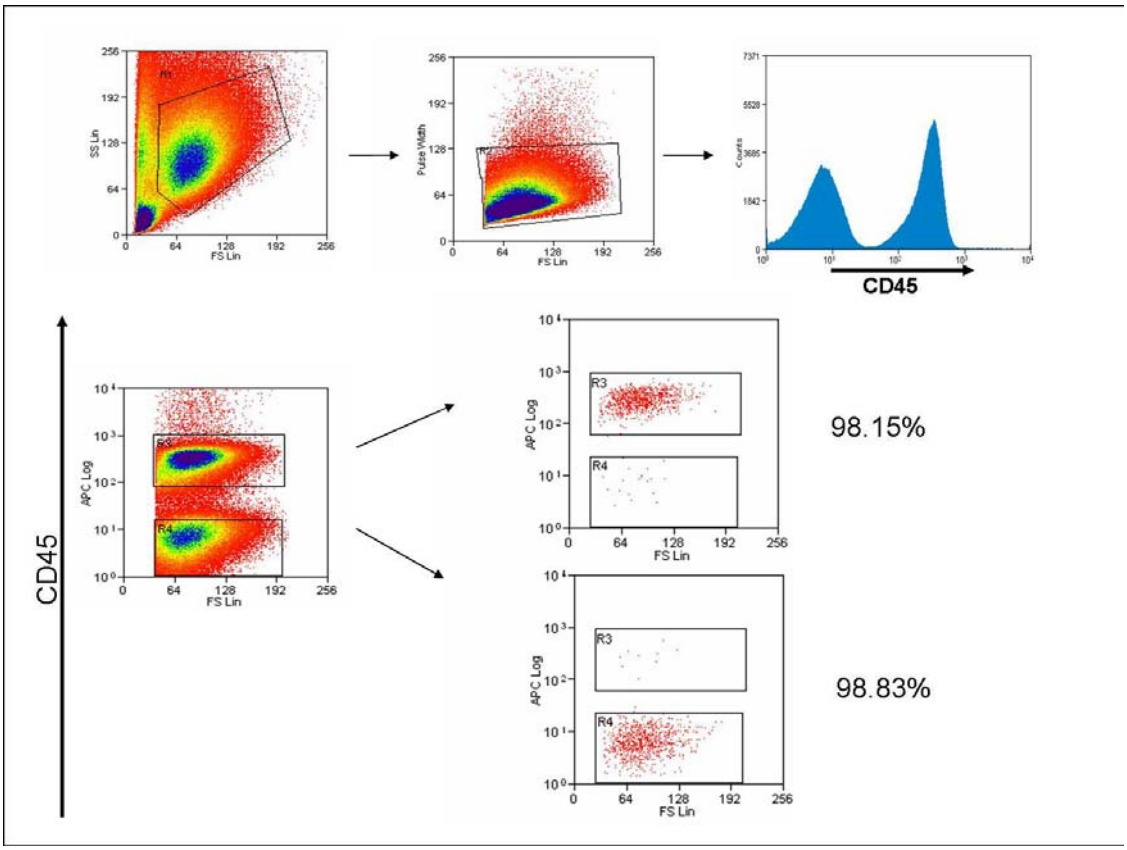

Figure 3.5 Stromal cell sorting based on CD45 expression
A forward scatter (FS) and side scatter (SS) gate was set for cell size, with a FS and pulse width gate set to ensure doublets were excluded. Finally two gates were set to acquire the positive and negative CD45 protein expressing populations. The gates shown are those typically used, with the usual percentage purities obtained.

3.2.2.2 Flow cytometry analysis of sorted stromal cell cultures

To determine the homogeneity of the sorted CD45 negative populations, the panel of surface protein markers used on the unsorted cell cultures (figure 3.4) was repeated on the cultures at passage 4/5 post sorting (figure 3.6).

Importantly, it was observed that the sorted CD45 negative stromal cells maintain their CD45 negative expression phenotype. In addition, in comparison to the unsorted cells there was a more homogeneous phenotype across all stromal cell cultures; there was no F4/80 expression with concomitant high expression of VCAM-1, CD248 and gp38. Interestingly, the low CD31 expression observed only in the inguinal and axillary lymph node stromal cell cultures still remained post sorting. This indicates that these stromal cell cultures have an endothelial-like phenotype. CD11c expression was not assessed as this expression was very low in the unsorted cultures, however inter-cellular adhesion molecule 1 (ICAM-1) was added to the panel as current literature states its importance in stromal cell interactions with other cell types (35). ICAM-1 is differentially expressed amongst the stromal cell cultures, with spleen, liver and inguinal lymph node stromal cell cultures contain ICAM-1 positive cells whereas the thymus, axillary and cervical lymph nodes do not. At this juncture CD45 negative sorted stromal cell cultures from peripheral sites such as lung and skin were also included. This is a significant comparison to include as previous work in humans has shown that fibroblasts from peripheral sites can be grouped separately to those from lymphoid sites using gene expression analysis (150). Whether this is mirrored in the murine system is an important point to clarify. In addition to the lymphoid organ stromal cell cultures, the lung and skin stromal cell cultures also maintained their CD45 negative phenotype. They did not express F4/80 or CD31 and had high

expression of VCAM-1, CD248 and gp38. The lung stromal cell cultures expressed ICAM-1 whereas the skin stromal cells did not.

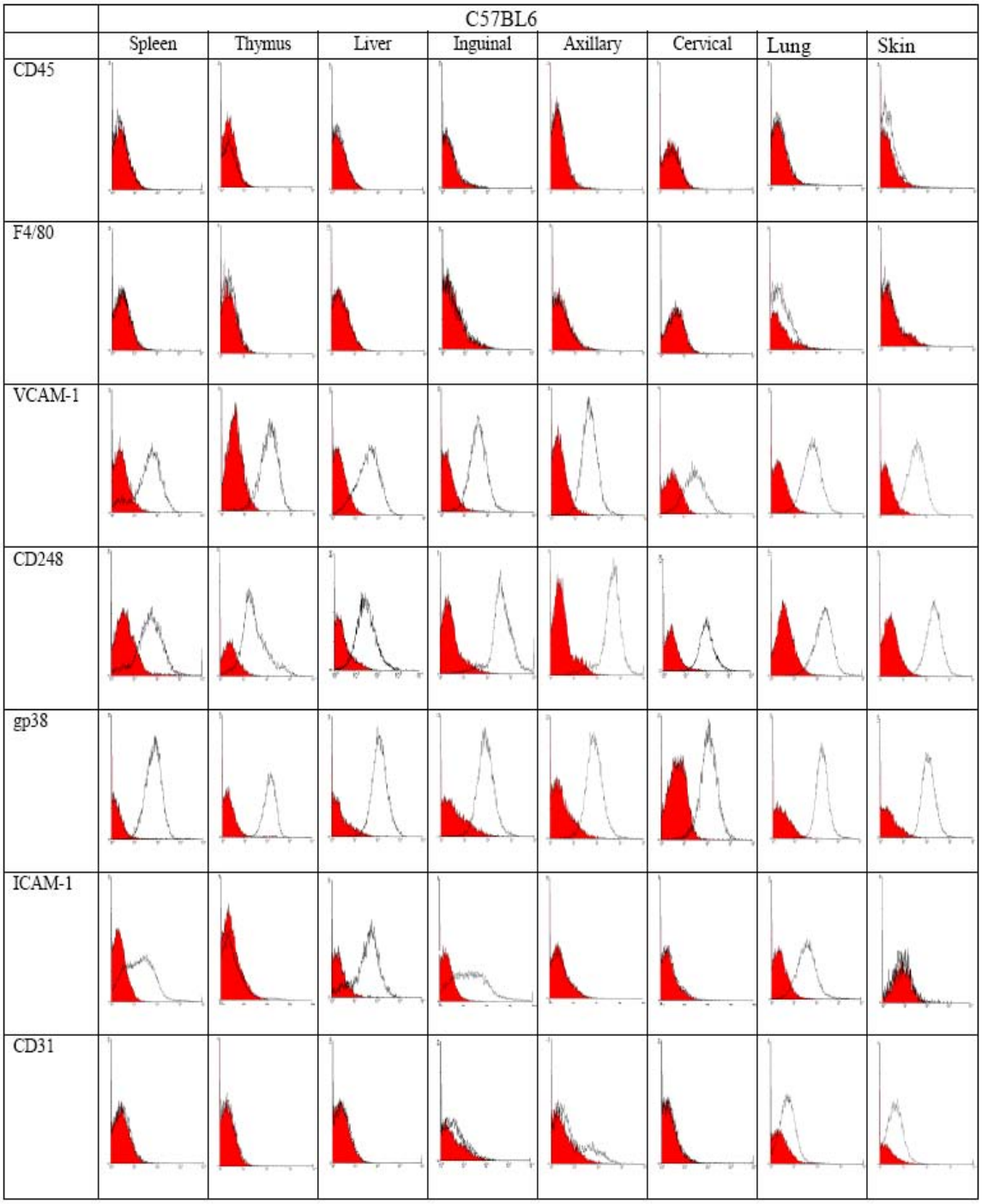

Figure 3.6 Cell surface protein expression of cultured CD45 negative stromal cells from lymphoid and peripheral organs

Flow cytometry data of cultured CD45 negative sorted stromal cells at passage 4/5 post sort, from lymphoid and peripheral organs of C57BL6 mice. Red = irrelevant control, black outline = positive protein staining (Plots representative of n=3 stromal cell cultures for each tissue type).

3.2.2.3 Immunofluorescent analysis of sorted stromal cell cultures

As a complimentary method to flow cytometry, immunofluorescence was used to examine the cell surface proteins present on the cultured stromal cells. As with flow cytometry, it can determine both the presence and relative quantity of a specific protein but also has the added benefit of revealing the location of the protein within a cell population. Protein heterogeneity was observed within cultured CD45 negative stromal cell populations (figure 3.7 – 3.9). Importantly, no CD45, F4/80 or CD11c positive staining was observed (data not shown). This suggests that not only do the sorted stromal cell cultures maintain their CD45 negative phenotype but also that sorting provides a more homogeneous cell culture with no haematopoietic, dendritic or macrophage cell contamination, confirming the flow cytometry data. Again consistent with the flow cytometry data all cultures expressed the stromal markers gp38 and CD248. Interestingly, both single and double positive populations were present in all cultures although to differing extents. In contrast however, VCAM-1 expression differed from that observed by flow cytometry, with only very low levels observed in the liver (figure 3.7c), cervical lymph node (figure 3.8c) and skin (figure 3.9b) stromal cell cultures. Co-expression of gp38 and VCAM-1 was observed in the spleen (figure 3.7a), thymus (figure 3.7b) and inguinal lymph node (figure 3.8a) stromal cell cultures with co-expression of CD248, VCAM-1 and gp38 only observed in spleen (figure 3.7a) and axillary lymph node (figure 3.8b) stromal cell cultures. In all stromal cell cultures, where seen, CD248, gp38 and VCAM-1 protein expression was observed uniformly on the cell surface with no nuclear staining apparent. Taken together these data demonstrate that there are phenotypic differences between stromal cell cultures from distinct sites. Although more homogeneous, immunofluorescence

highlights that the stromal populations present still differ within each culture, even when looking at only three stromal markers.

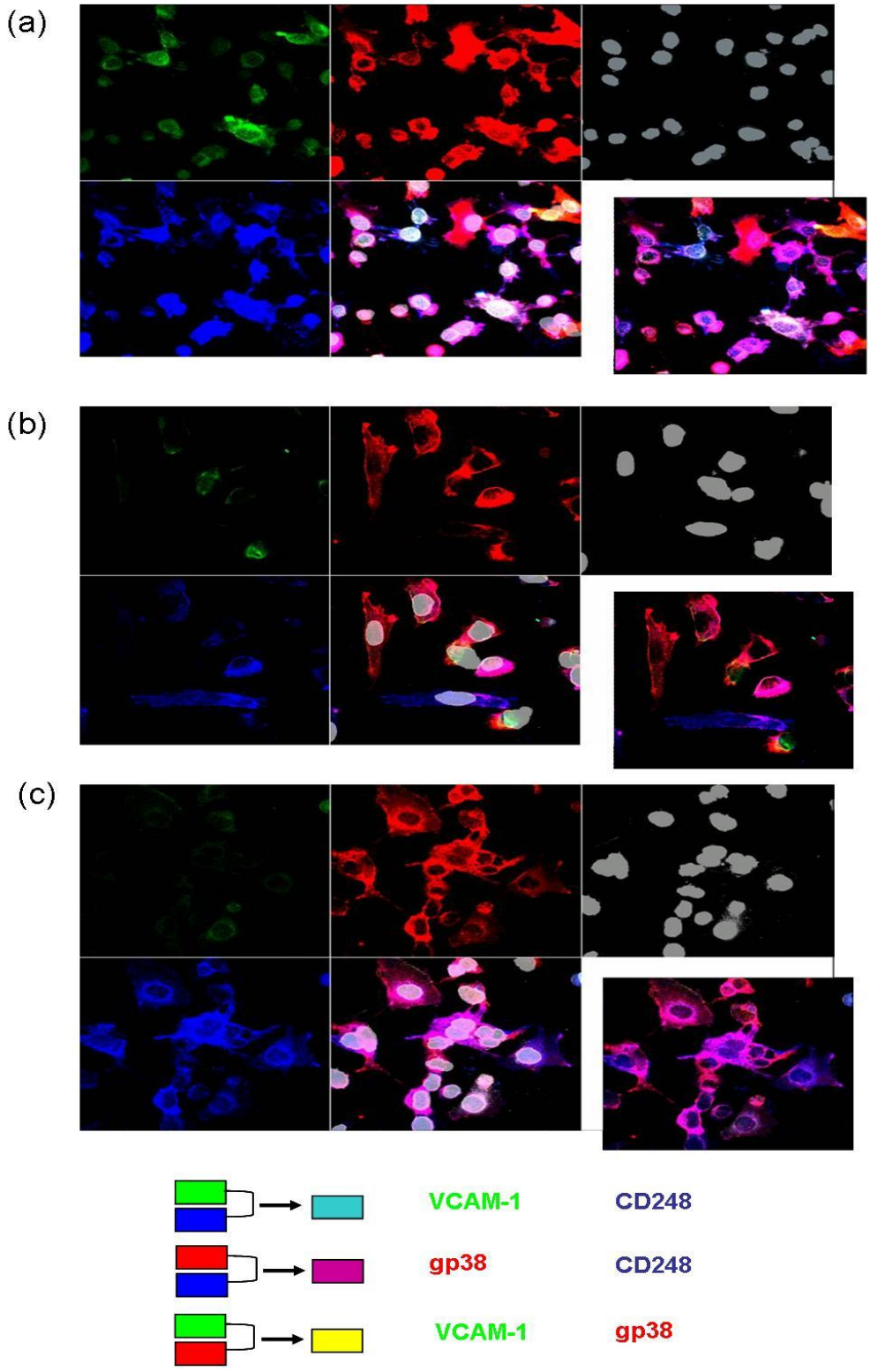

Figure 3.7 Immunofluorescence staining of CD45 negative sorted stromal cells Stromal cells fixed in acetone (passage 10) (a) spleen (b) thymus (c) liver, were co-stained for surface proteins CD248 (blue), gp38 (red) and VCAM-1 (green) and cell nuclei (grey) and viewed at a magnification of x40. Differences between the cell cultures can be observed (n=2).

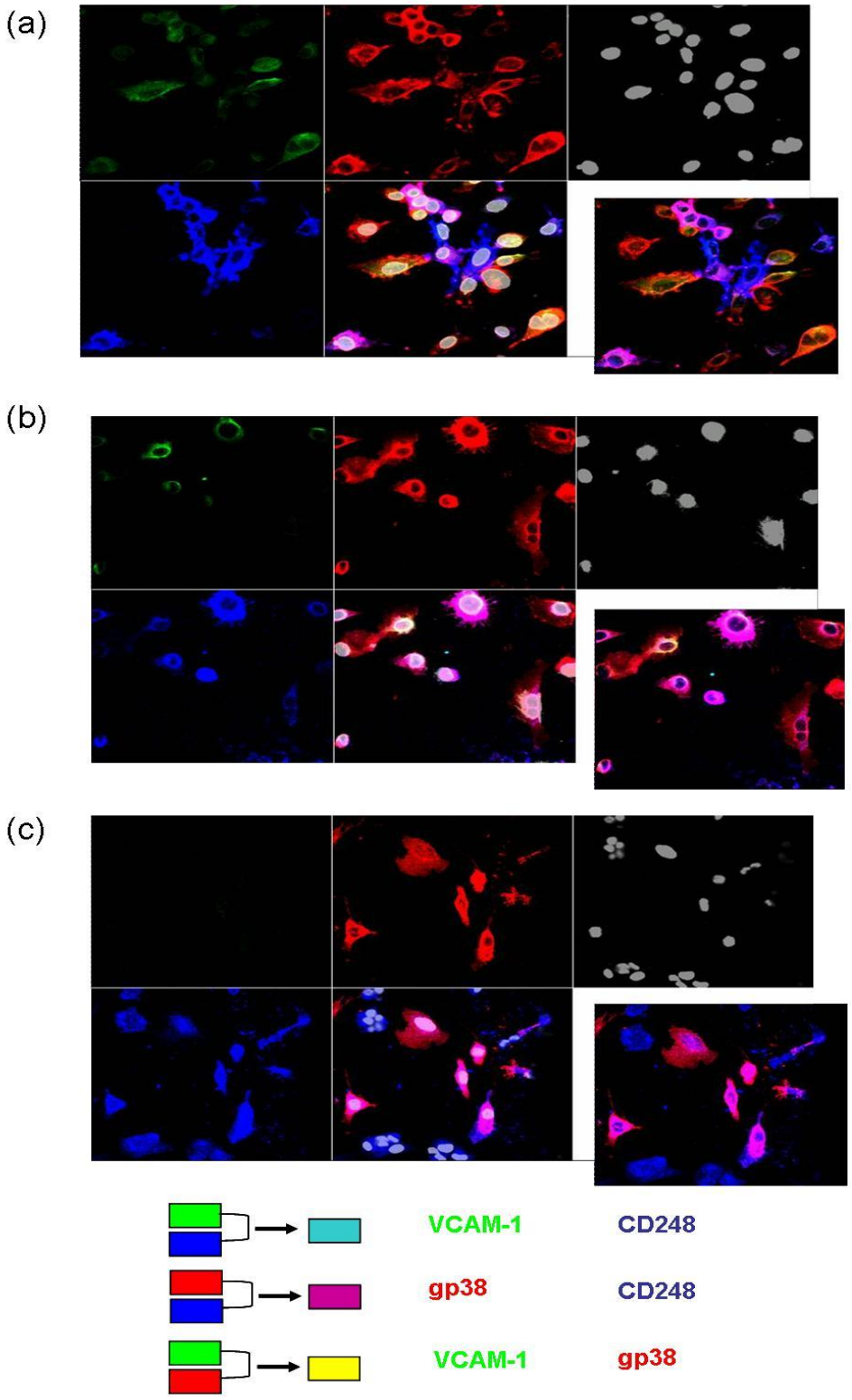

Figure 3.8 Immunofluorescence staining of CD45 negative sorted lymph node stromal cells

Stromal cells fixed in acetone (passage 10) (a) inguinal (b) axillary (c) cervical, were co-stained for surface proteins CD248 (blue), gp38 (red) and VCAM-1 (green) and cell nuclei (grey) and viewed at a magnification of x40. Differences between the cell cultures can be observed (n=2).

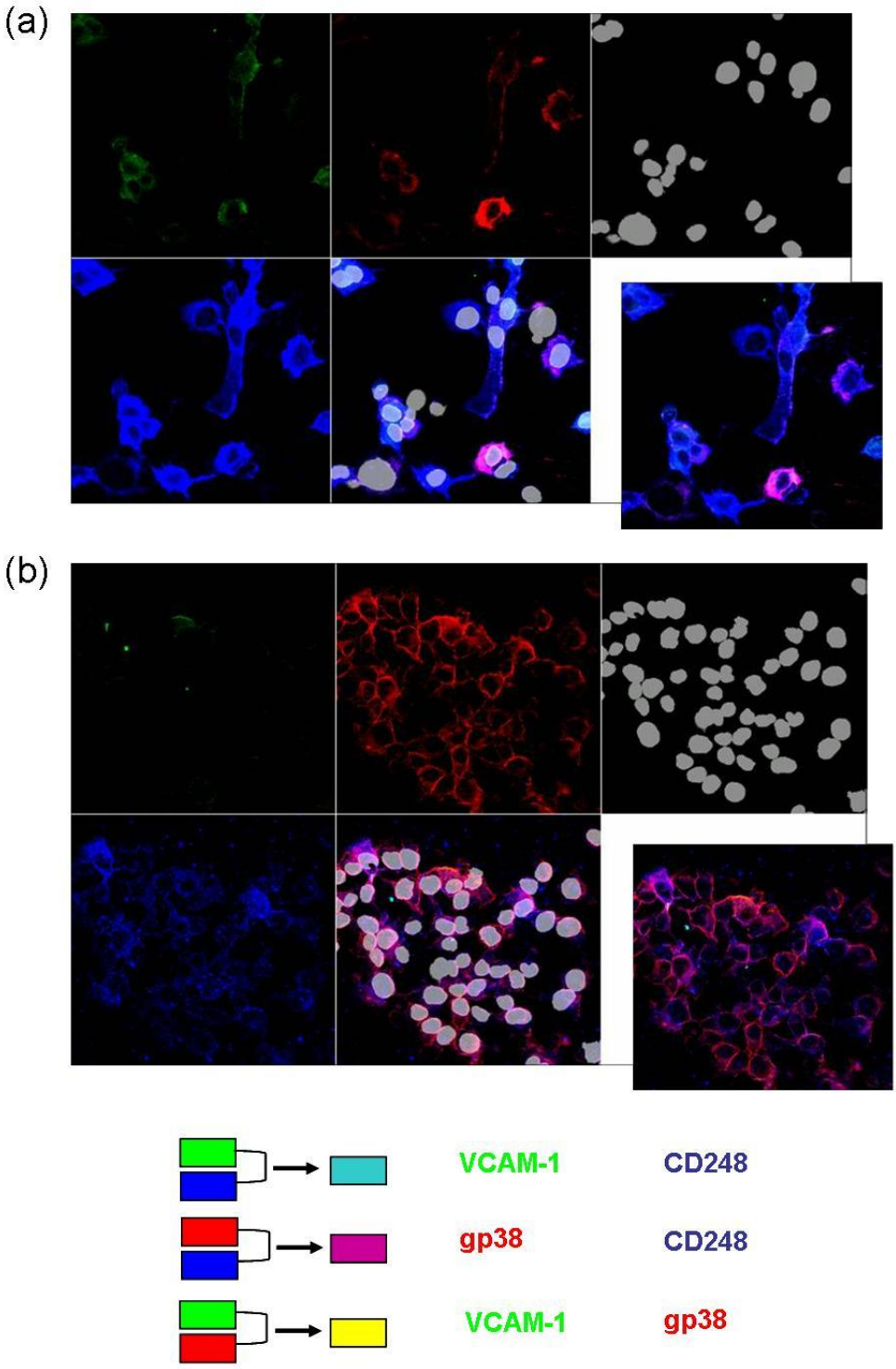

Figure 3.9 Immunofluorescence staining of CD45 negative sorted peripheral stromal cells

Stromal cells fixed in acetone (passage 10) (a) lung (b) skin, were co-stained for surface proteins CD248 (blue), gp38 (red) and VCAM-1 (green) and cell nuclei (grey) and viewed at a magnification of x40. Differences between the cell cultures can be observed (n=2).

3.2.2.4 Whole genome array analysis of sorted stromal cells

Having observed heterogeneity between cultures derived from different sites based on protein expression, the gene expression profiles of each culture were next analysed to determine whether they could be grouped anatomically analogous to the human studies (151). RNA was extracted from all stromal cell lines, reverse transcribed and CyDye labelled with approximately 100pmols of labelled cDNA hybridised onto whole mouse genome arrays (section 2.7). The arrays contained 37,632 genes and were used as an unbiased approach to determine if a specific lymphoid organ fibroblast gene signature could be established (appendix 8.3).

As with the Fibroblast LDAs, SAM analysis was used to determine the gene expression that differed significantly between the cultures (section 2.7.3). Using a 0.03% false discovery rate (FDR), 2935 genes were found to be significantly different between peripheral and lymphoid stromal cell cultures (appendix 8.4). Normally the FDR is set to 10% during SAM analysis, however this gave a gene list that was too large to further analyse and therefore the FDR was decreased to 0.03%, which gave a workable number of genes. A hierarchical cluster, produced by the Institute of Genomic Research multi-experiment viewer (TMEV), of all samples using the 2935 genes, showed peripheral stromal cell cultures, skin and lung, to be more similar to each other than to the lymphoid organ stromal cell cultures (figure 3.10a). PCA was used to cluster the samples based on the expression of the 2935 genes (figure 3.10b). This observation agrees with that found in human studies where whole genome expression grouped peripheral and lymphoid fibroblasts separately (150). When using this approach within the lymphoid stromal cell cultures alone, significant site specific gene expression was unable to group the samples into the lymphoid organ from which

they were obtained. To assess the biological significance of the 2935 genes found to be differentially expressed between peripheral and lymphoid stromal cell cultures, a database for annotation, visualisation and integrated discovery (DAVID) (david.abcc.ncifcrf.gov/tools.jsp) was used to determine pathways in which the genes were involved. Prior to DAVID analysis the 2935 genes were re-clustered in TMEV. This clusters the genes into groups based on similar expression patterns, from which individual clusters can be annotated (figure 3.11a). Each individual gene cluster was then put into DAVID and functional annotation clustering performed. From the list of pathways produced, those with a fold enrichment over two and a FDR of less than 10% were selected, this is an accepted cut off to analyse significant changes (figure 3.11b). These interestingly included a cluster of genes that were upregulated in the peripheral tissues when compared to lymphoid tissues which are involved in the innate immune response (section 3.3).

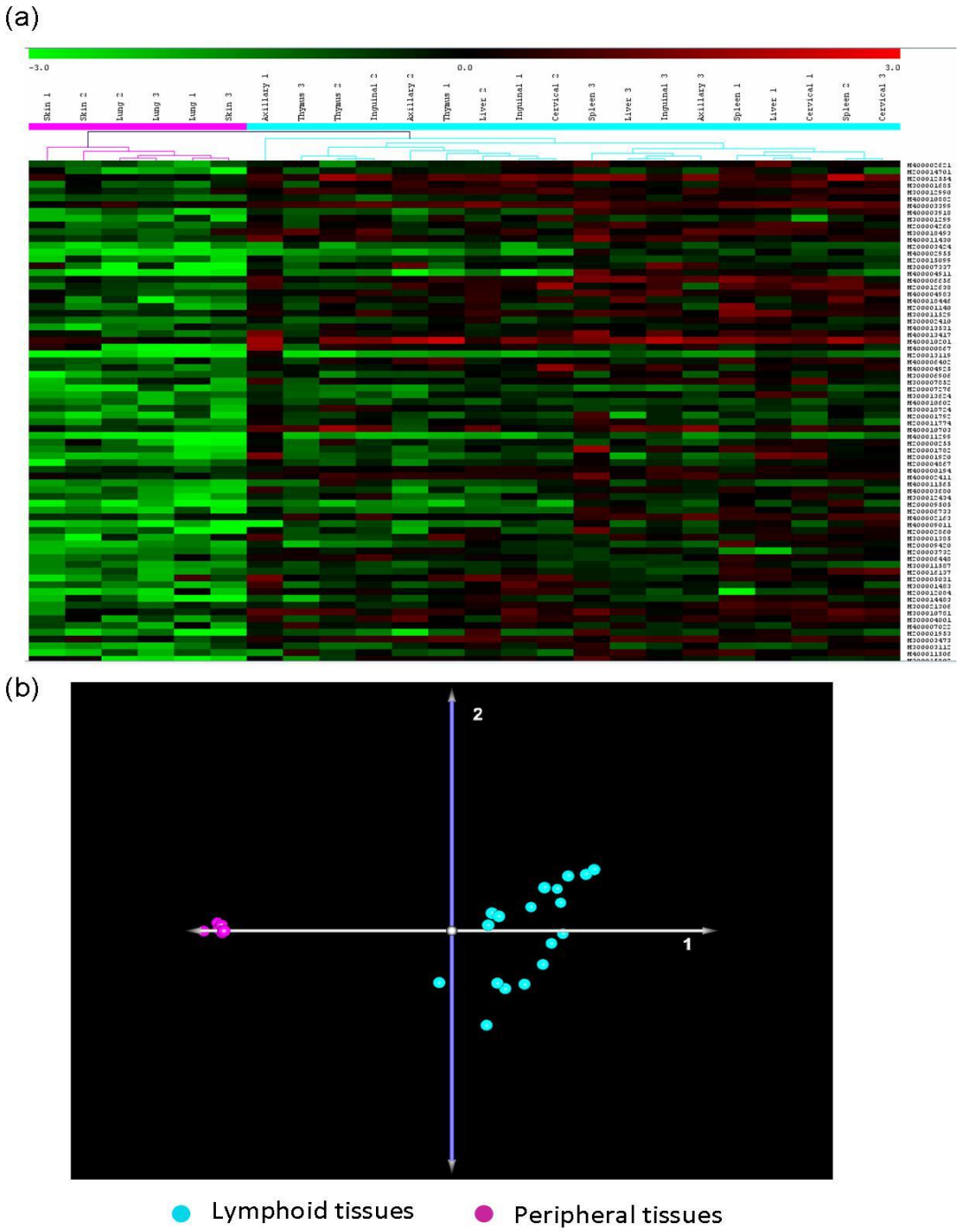

Figure 3.10 Whole mouse genome array analysis of CD45 negative sorted stromal cell gene expression

Total RNA from CD45 negative sorted stromal cells was extracted, reverse transcribed, CyDye labelled and hybridised onto a whole mouse genome microarray of 37,632 genes (a) Hierarchical cluster analysis of samples revealed that peripheral CD45 negative stromal cells were more similar to each other than to the lymphoid CD45 negative stromal cells. Red = low, green = high and black = medium gene expression. (b) PCA of the 2935 genes differentially expressed within the stromal cell cultures. Pink circles = peripheral sites; skin and lung and turquoise circles = lymphoid sites; spleen, thymus, liver and inguinal, axillary and cervical lymph nodes (n=3 independent stromal cell cultures for each tissue type).

(a)

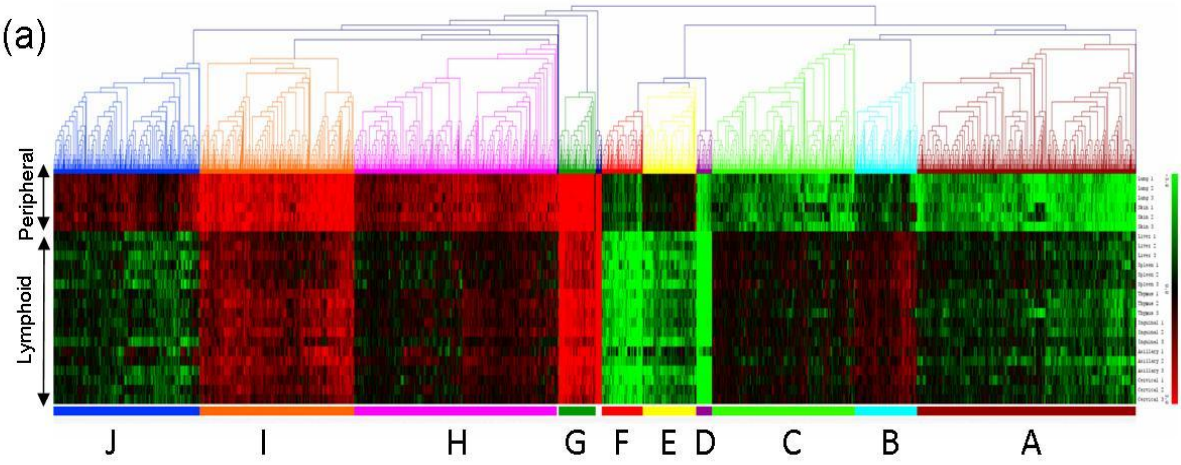

(b)

Cluster	Pathway	Fold Enrichment	FDR (%)
A	GO:0044262~cellular carbohydrate metabolic process	2.83	0.44
	GO:0005975~carbohydrate metabolic process	2.29	1.25
	GO:0019318~hexose metabolic process	3.27	3.77
	GO:0005996~monosaccharide metabolic process	3.21	4.35
	GO:0008610~lipid biosynthetic process	2.60	3.83
C	GO:0031589~cell-substrate adhesion	5.32	9.66
	GO:0045087~innate immune response	4.97	5.26
E	GO:0051301~cell division	5.89	6.00
F	GO:0006396~RNA processing	5.91	0.63
H	GO:0016071~mRNA metabolic process	3.51	0.19
	GO:0006397~mRNA processing	3.46	0.74
	GO:0006396~RNA processing	2.77	0.86
	GO:0008380~RNA splicing	3.73	1.42
I	GO:0006325~establishment and/or maintenance of chromatin architecture	3.82	2.29
	GO:0006323~DNA packaging	3.73	2.72
	GO:0051276~chromosome organization and biogenesis	2.87	9.11

Figure 3.11 DAVID pathway analysis of 2935 genes differentially expressed between peripheral and lymphoid stromal cells

Significant genes from SAM analysis of whole genome microarrays were (a) Hierarchically clustered into groups of similar gene expression patterns A-J. Red = low, green = high and black = medium gene expression. (b) Pathways over two fold enriched with a FDR <10% are shown.

As well as comparing the CD45 negative cultured stromal cells, immortalised spleen, thymus and mesenteric and peripheral lymph node stromal cell lines derived from clones and *ex vivo* splenic stromal cells sorted on gp38 and CD31 expression were also analysed using the whole mouse genome arrays. These were prepared and used with the permission of Dr Tobias Vogt and Dr Mirjam Britchgi, University of Lausanne, Switzerland. The purpose of this comparison was to determine the differential gene expression between *in vivo, in vitro* and immortalised cells. PCA of all 99 samples shows a clear separation of the *ex vivo* sorted cells from the *in vitro* cultured and immortalised cells lines (figure 3.12). Due to the large sample size SAM analysis could not be performed to determine the gene expression that differed significantly between all the samples. Therefore, SAM analysis was performed only on immortalised lymph node cell lines and the *in vitro* CD45 negative cultured lymph node cultures. Following analysis, 261 genes were found to be expressed differentially, with a FDR of 10%, between the five groups (appendix 8.5). Hierarchical clustering using these genes demonstrates that the immortalised cell lines group together, as do the *in vitro* cultured cells (figure 3.13a). PCA of these samples using the 261 genes shows not only a clear separation of immortalised cells lines and *in vitro* cultured cells but also separation within these groups based on the precise lymph node from which the cells were obtained, although the inguinal and axillary lymph node stromal cells were less tightly clustered (figure 3.13b). These genes were then clustered in TMEV and their grouped genes annotated for use in DAVID (figure 3.14a). Pathways with a fold enrichment over two and a FDR of less than 10% were selected (figure 3.14b). Interestingly, five of the eight pathways that were different between the immortalised and the CD45 negative cultured lymph node stromal cells

were related to apoptosis (section 3.3). These were increased in the CD45 negative cultured cells compared with the immortalised cells.

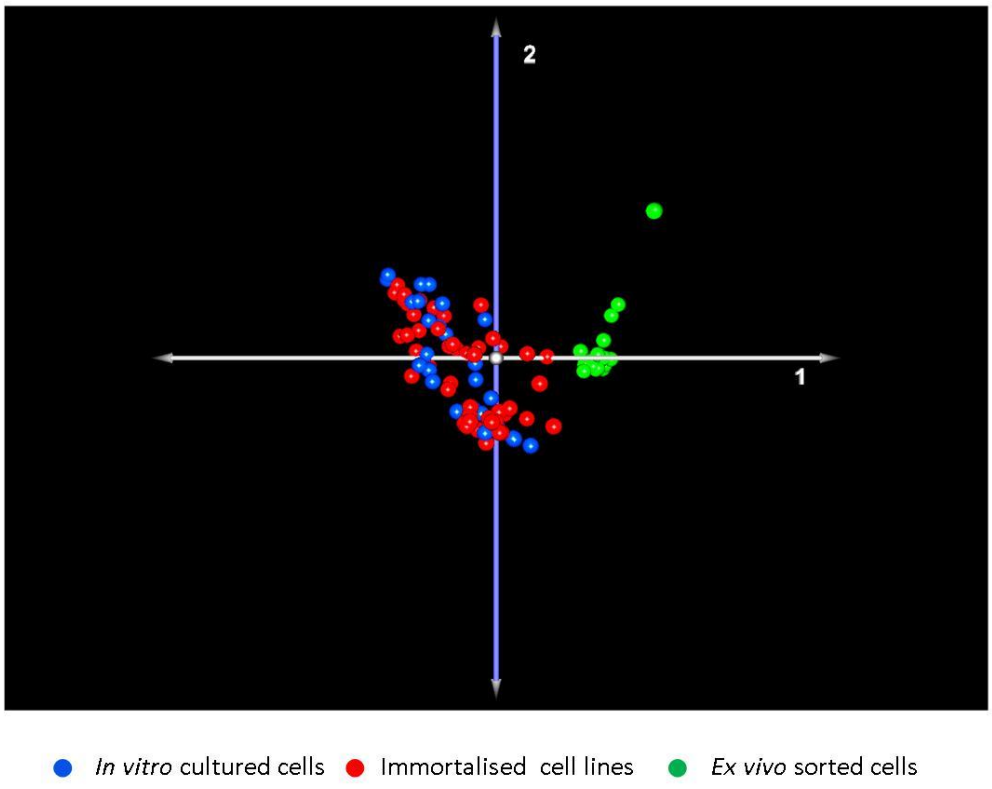

Figure 3.12 PCA of the *in vitro* cultured cells, immortalised cell lines and *ex vivo* sorted cells

Total RNA from all cells was extracted, reverse transcribed, CyDye labelled and hybridised onto a whole mouse genome microarray. PCA grouped immortalised cell lines from $p19^{-/-}$ peripheral lymph nodes and $p53^{-/-}$ spleen, thymus and peripheral and mesenteric lymph nodes (red) with *in vitro* cultured stromal cells from spleen, thymus, liver, skin, lung and inguinal, axillary and cervical lymph nodes (blue), with *ex vivo* $CD45^{-}$ and $CD35^{-}$ stromal cells from peripheral lymph nodes noticeably separate (green).

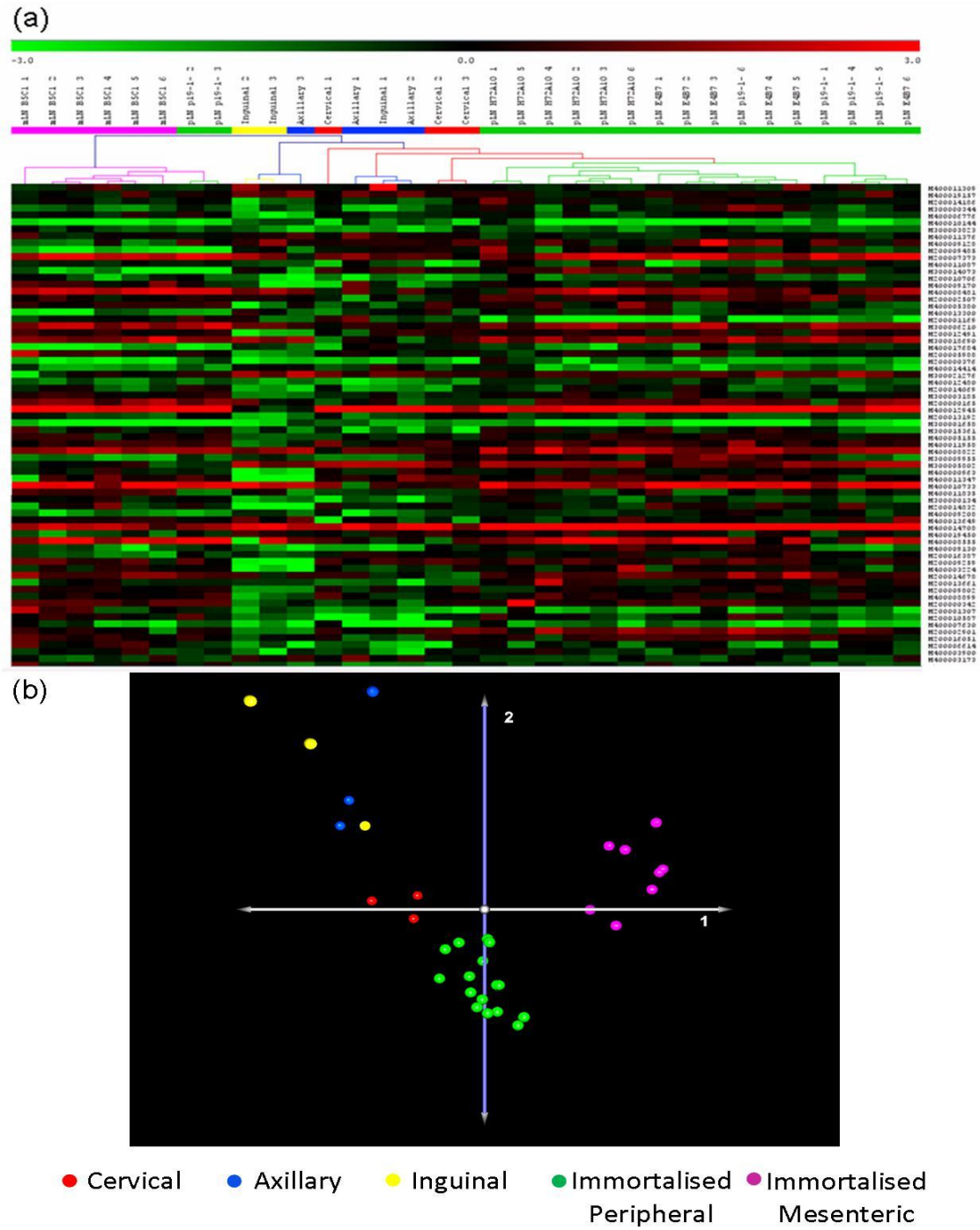

Figure 3.13 Whole mouse genome array analysis of *in vitro* cultured CD45 negative lymph node stromal cell cultures and immortalised lymph node stromal cell lines

Total RNA from *in vitro* cultured CD45 negative lymph node stromal cells and immortalised lymph node stromal cell lines was extracted, reverse transcribed, CyDye labelled and hybridised onto a whole mouse genome microarray. (a) Hierarchical cluster analysis of samples grouped stromal cells from immortalised cell lines separately to those from *in vitro* cultured cells. Red = low, green = high and black = medium gene expression. (b) PCA analysis of the 261 differentially expressed genes. Red = cervical, blue = axillary, yellow = inguinal, green = immortalised peripheral and pink = immortalised mesenteric lymph node stromal cells.

(a)

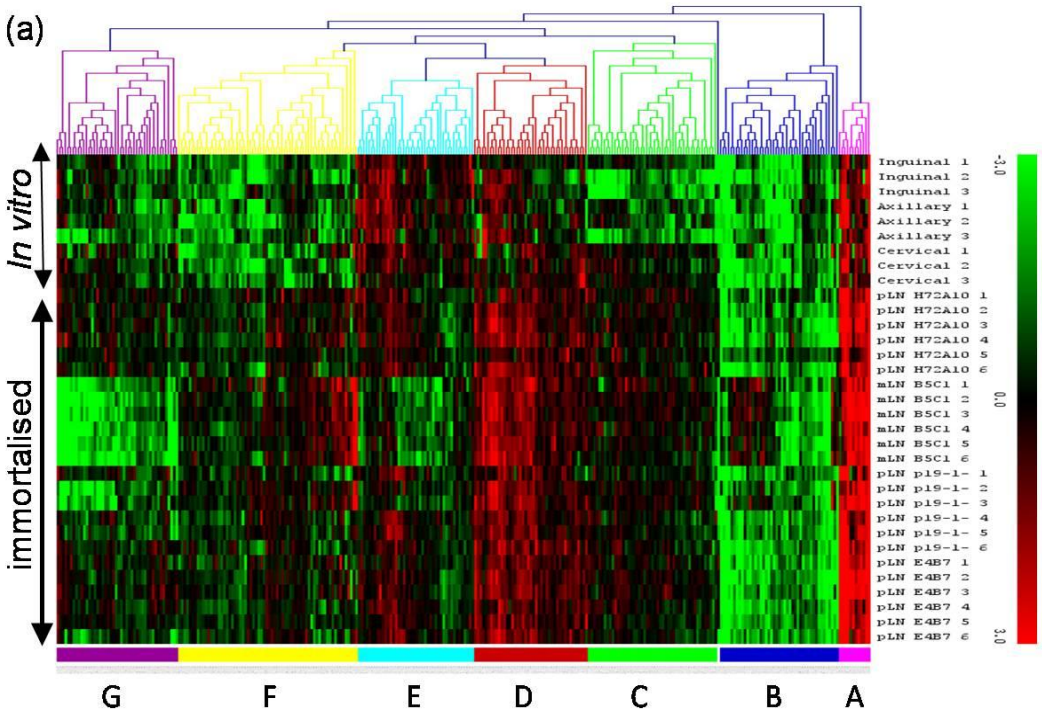

(b)

Cluster	Pathway	Fold Enrichment	FDR (%)
A	GO:0006915~apoptosis	17.44	0.71
	GO:0012501~programmed cell death	17.14	0.74
	GO:0008219~cell death	16.53	0.83
	GO:0016265~death	16.48	0.84
	GO:0048468~cell development	9.72	3.92
B	GO:0007155~cell adhesion	6.18	1.08
	GO:0022610~biological adhesion	6.18	1.08
G	GO:0007218~neuropeptide signaling pathway	30.03	0.50

Figure 3.14 DAVID pathway analysis of 261 genes differentially expressed between *in vitro* cultured and immortalised lymph node stromal cells

Significant genes from SAM analysis of whole genome microarrays were (a) hierarchically clustered into groups of similar gene expression patterns A-G. The top six samples are *in vitro* cultured lymph node stromal cells and the bottom twenty four are immortalised stromal cells from peripheral or mesenteric lymph nodes. Red = low, green = high and black = medium gene expression. (b) Pathways over two fold enriched with a FDR <10% are shown.

3.2.2.5 End point PCR

End point PCR was used to validate microarray results by determining the expression of a number of genes thought to be highly expressed for example CCL7, CCL19. CCL21, CXCL12, IL-7, LTβR, TNFR1, TRANCE. In addition, to validate the presence of fibroblasts expression of genes such as CD248, gp38, ICAM-1 and VCAM-1 were also determined. The end point PCR was analysed by running the products on a 1% agarose gel with molecular weight markers to determine their size (section 2.5.2) (figure 3.15). All stromal cell cultures showed expression of CCL7, CCL19, CCL21, CD248, CXCL1, CXCL12, gp38, ICAM-1, IL-7, IL-17RA, LTβR, PDGFRα, PDGFRβ, TNFR1, TRANCE, VEGFa, VEGFc and VCAM-1, which is consistent with the gene expression observed in the whole genome microarrays. Many of the genes expressed throughout the stromal cell cultures are stromal organiser cell markers, VCAM-1, ICAM-1, LTβR, TRANCE, CCL19 and CCL21 (35). Interestingly CXCL13, which is thought to be produced by stromal organiser cells, was only expressed in stromal cell cultures from the inguinal lymph node, skin and lung. In addition expression of other stromal markers gp38, CD248, PDGFRα, PDGFRβ and TNFR1 was consistently seen. However differential gene expression between the stromal cell cultures was also observed, the lymphatic endothelial markers CD31 and Lyve-1 were expressed in the cervical and axillary lymph node and the skin and lung stromal cell cultures but not in the others. EpCAM was not expressed in any of the cell cultures. The differential expression observed between stromal cell cultures was not mirrored by the pattern of expression seen using the microarrays. However, expression of EpCAM was very low in all stromal cell cultures using microarray analysis. The gene expression observed by end point PCR of CD248, gp38 and VCAM-1 correlated with protein expression observed by flow

cytometry in the stromal cell lines (section 3.2.2.2). However, ICAM-1 gene expression was seen in all stromal cell cultures by end point PCR whereas ICAM-1 protein expression was only seen in the spleen, liver, inguinal lymph node and lung stromal cells. This differential expression between transcript and protein may be due to the lack of translation of that gene in particular cell lines.

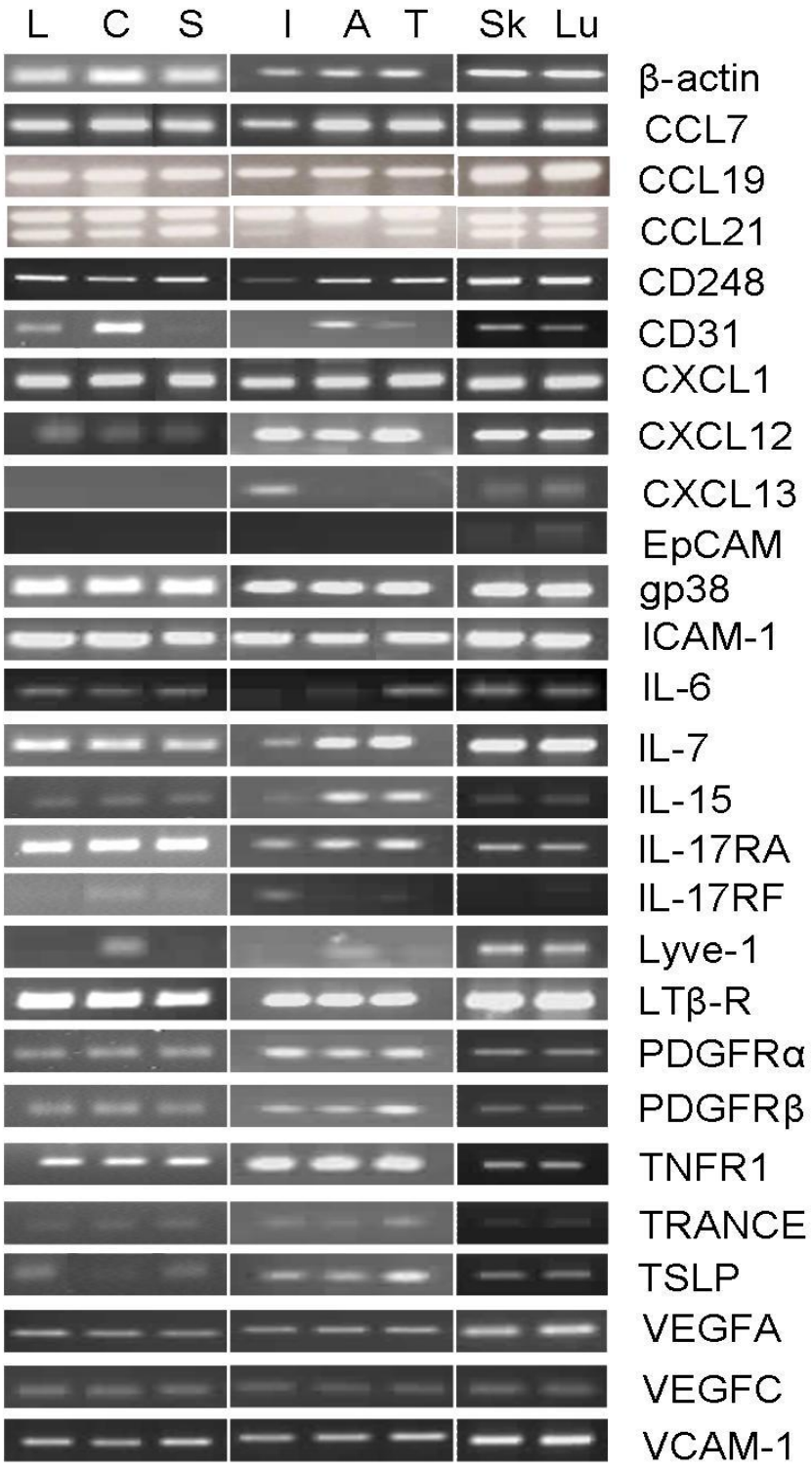

Figure 3.15 End point PCR results of selected genes from CD45 negative sorted stromal cells

RNA from CD45 negative sorted stromal cell cultures, was reverse transcribed and end point PCR performed S=Spleen, T=Thymus, L=Liver, I=Inguinal lymph node, A=Axillary lymph node, C=Cervical lymph node, Sk=Skin and Lu=Lung. (n=2).

3.2.2.6 Site Specific TaqMan LDA

The whole mouse genome microarrays were used as an unbiased approach to determine if a specific lymphoid organ fibroblast gene signature could be established. From these it was possible to separate cultured stromal cells from peripheral and lymphoid tissues but not those within the lymphoid tissue group. Therefore, a TaqMan LDA was designed based on the 337 genes found to be human fibroblast site specific as previously described by Rinn *et al*, 2006. The site specific LDA contained 47 of the genes found to important in defining human fibroblast site specificity, covering a broad range of families (appendix 8.6). To analyse gene expression data from each of the stromal cell cultures, RNA was extracted and approximately 1µg was hybridised to the LDA. Following real-time PCR all data was normalised to the expression of housekeeping gene 18S (appendix 8.7). Hox gene expression was analysed first given their reported importance in the literature (151,152) (figure 3.16a). Similar high gene expression levels were seen of Hoxa5 with very low gene expression of Hoxa13 across all stromal cell cultures. Hoxb2 expression was decreased in the skin stromal cell cultures with Hoxa11 noticeably decreased in lung stromal cells and to a lesser extent in the thymus. Hoxd8 showed the greatest variation between the stromal cell cultures, very high expression was seen in all lymph node stromal cell cultures, with a decrease in spleen, thymus and liver and to a greater extent in the skin and lung stromal cell cultures. From the 47 genes on the low density array 15 non-Hox genes were observed to have differential expression between the stromal cell cultures (figure 3.16b). CD31 and Lyve-1 were highly expressed in the inguinal, axillary and cervical lymph node stromal cell cultures compared to all other stromal cell cultures, mirroring that seen in the whole mouse genome arrays (section 3.2.2.4). In addition, CD248, Wisp2, Fxf1a, Gulp, Fn, Adam9, Col11a1, Plat and

Bmp4 gene expression was lower in the skin and lung stromal cell cultures than the lymphoid stromal cell cultures. A decrease in expression of Wisp2 was also observed in the liver stromal cell cultures and a decrease in Plat expression in the splenic stromal cell cultures. In addition, CXCL1 was increased in the cervical lymph node stromal cell cultures alone and Grem2 expression was increased in the cervical lymph node, skin and lung stromal cell cultures. Grem2 is thought to play a role in regulating organogenesis, body patterning, and tissue differentiation (192). Moreover, this low density array also demonstrated some differences in gene expression between all the stromal cell cultures with Cdh1 and Mmp3 having variable expression. Cdh1 is the gene for the cell adhesion protein epithelial-cadherin (193) and Mmp3 is an enzyme involved in the breakdown of extracellular matrix (194). The site specific LDA highlights again the gene expression differences between lymphoid and peripheral stromal cell cultures. In addition, it reveals genes, Grem2, Cdh1 and Mmp3, that are differentially expressed between all the stromal cells cultures.

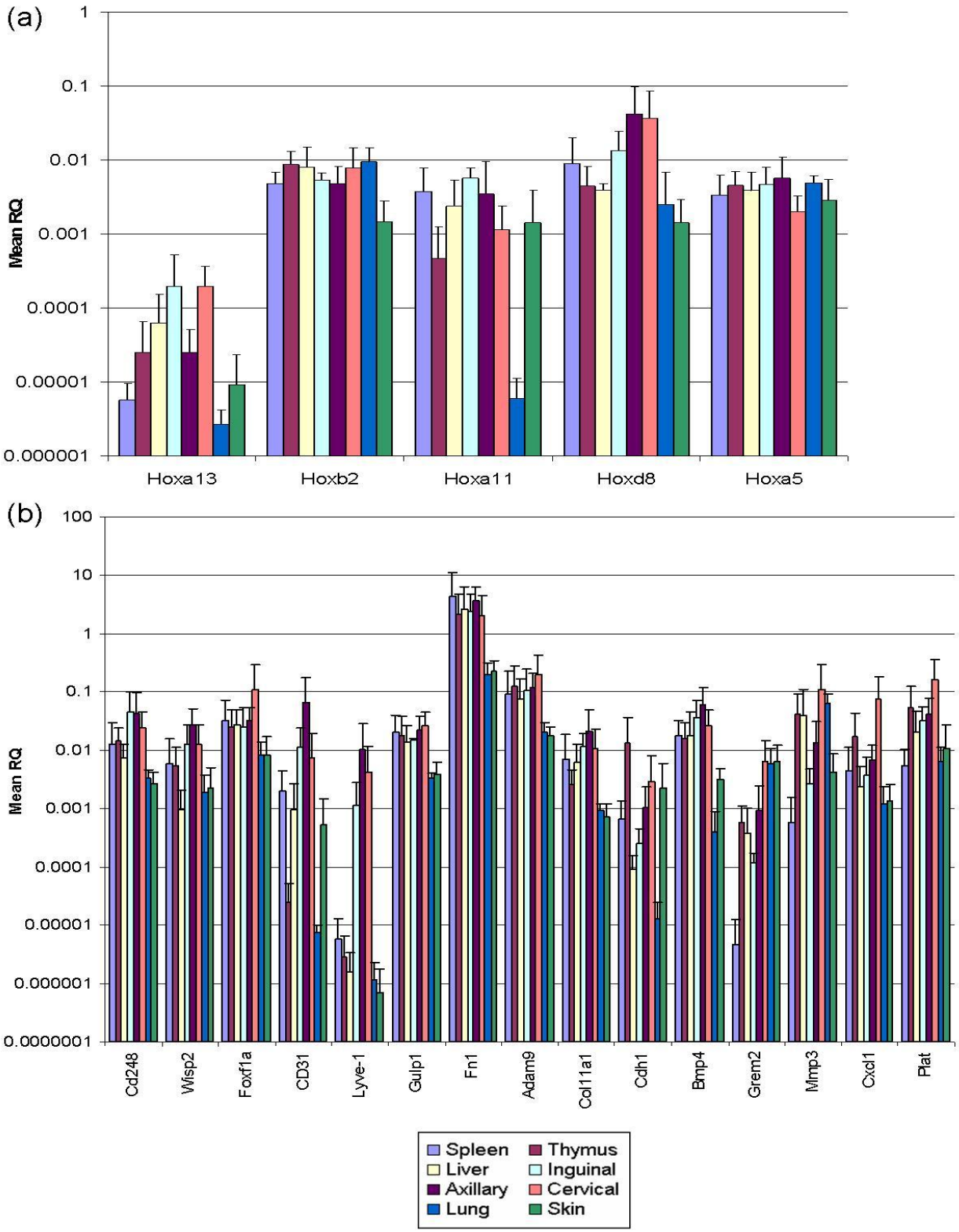

Figure 3.16 Gene expression of CD45 negative stromal cells on site specific LDA Gene expression from stromal cell cultures was determined using a site specific designed TaqMan LDA (a) Hox gene expression (b) differentially expressed genes (n=3 independent stromal cell cultures for each tissue type).

3.3 Discussion

The aim of this chapter was to characterise fibroblasts from different sites within the mouse; gene and protein expression was assessed to achieve this.

Importantly from this chapter an efficient protocol for the growth of stromal cells from mouse lymphoid tissues, which can be reliably used for future functional studies, has been derived. In the literature the most favourable culture conditions for growing human and mouse fibroblasts are stated as 10% FCS in Dulbecco's Modified Eagles Medium (167,195,196). This method is now part of our standard operating procedure (SOP) for mouse fibroblast cell culture. For experimental work, fibroblasts have previously been described to be used at between passage five (151) and passage ten (119). We found that above passage five was an optimum passage number for use with the cell sorter and after sorting cells have maintained their phenotype above passage 35 so far.

Although a specific marker has not yet been found for fibroblasts, there are several markers that can be used, however none are exclusive (138,197). For these reasons a panel of fibroblast indicators were used on the stromal cell populations acquired by enzymatic digestion from the spleen, thymus, liver, skin, lung and inguinal, axillary and cervical lymph nodes. This included VCAM-1 (150), CD248 (140) and gp38 (72) along with classic markers of other cell types, including haematopoietic cells (CD45) (189), macrophages (F4/80) (190), dendritic cells (CD11c) (191) and endothelial cells (CD31) (188), to exclude non-fibroblast-like cells. Parsonage *et al* (2003), observed morphological, mRNA and protein expression differences when growing human fibroblasts in culture (150). This correlates with the differential gene and protein

expression seen in cultured stromal cells (section 3.2); following FACS analysis CD248, gp38 and VCAM-1 protein expression was observed in all cultures. Moreover, genes such as vimentin and the pro-collagens were shown to be highly transcribed in the Fibroblast LDA (figure 3.3). Taken together these data suggest that fibroblasts are present in the cultures. However, protein expression of markers for other cell types including haematopoietic cells (CD45), dendritic cells (CD11c), endothelial cells (CD31) and macrophages (F4/80) was also seen. From the Fibroblast LDA, it became clear that other cell populations were present in the cell cultures. SAM analysis gave gene expression that differed significantly between cultures. For example CD80 and CD86 were increased in spleen, liver and thymus stromal cultures, suggesting the presence of antigen presenting cells. CD80 is expressed on activated B cells and monocytes (185). CD86 provides co-stimulatory signals for T cell activation and survival (186). CD117 (KIT), a molecule expressed on the surface of haematopoietic stem cells showed high expression on lymph node stromal cell populations (187). Furthermore high CD31 expression was observed in lymph node stromal cell populations, which indicates the presence of endothelial cells (188). The conclusion from the flow cytometry and Fibroblast LDA data was that the *in vitro* cultures were heterogeneous and included cell types other than the fibroblast.

To address the concerns about the heterogeneity of the cultures, the stromal cells were sorted on CD45 expression (section 3.2.2.1), with CD45 negative stromal cells grown successfully to obtain a more homogenous population. Upon analysis of gene and protein expression of these CD45 negative sorted cells (section 3.2.2.4 and 3.2.2.2/3.2.2.3 respectively) differences in gene and protein expression between the cell cultures was still observed, which was not due to contaminating CD45 positive

cells. It was at this stage that peripheral sites, lung and skin, were included. It has been shown previously within humans that fibroblasts can be grouped into peripheral and lymphoid sites using whole genome microarray analysis (150). This is an important finding to address within the murine studies and was intended to be used as a positive control in addition to the groupings within the lymphoid tissues. The protein expression of the CD45 negative sorted cells (section 3.2.2.2) assessed by flow cytometry showed a more homogeneous population, with no F4/80 expression and high levels of VCAM-1, CD248 and gp38 in all stromal cell cultures. High expression of CD248 and gp38 was also seen by immunofluorescence (section 3.2.2.3), along with an elongated, spindle shaped morphology which is associated with fibroblasts. The single positive CD248 or gp38 stromal cells observed may due to their stage in the cell cycle, as by flow cytometry all cells expressed both markers. Interestingly, VCAM-1 expression was variable when analysed by immunofluorescence where it was highest in spleen, with lower expression detected in all but the cervical lymph node stromal cell cultures where none was detected. However, VCAM-1 gene expression was found to be high in gene arrays and end point PCR so there may have been technical issues with the immunofluorescent staining. This could be due to the treatment of the cells prior to staining, cells are fixed before immunofluorescent staining, which could have affected the VCAM-1 protein expression or available epitope required. Whereas, for flow cytometry, cell dissociation buffer is used, which may preferentially release VCAM-1 high populations of stromal cells. Finally, when immunofluorescence was performed triple staining of CD248/gp38/VCAM-1 was used whereas for flow cytometry single colour staining was performed for each marker. It is possible that the fluorescence of the other antibodies affected that of the VCAM-1. Ultimately the sensitivity of the

techniques could explain the differences seen, if there is only a small amount of VCAM-1 present a more sensitive technique would highlight it. The dysregulation between mRNA and protein expression is often seen and probably due to the high sensitivity of PCR and post-transcriptional control. In the inguinal and axillary lymph node stromal cell cultures there was a very low amount of CD31 expression observed by flow cytometry, indicating these cells may have a more endothelial-like phenotype. This was confirmed by the whole genome microarrays and the site specific LDA where expression of CD31 and lymphatic endothelial marker Lyve-1 was observed (section 3.2.2.4 and 3.2.2.6). One consistent difference between the stromal cell cultures was protein expression of ICAM-1, expression was seen in spleen, liver, lung and inguinal lymph node cultures. Studies by Cupedo *et al* (45) and Okuda *et al* (198) have highlighted distinct populations of stromal organiser cells within peripheral and mesenteric lymph nodes, that have intermediate or high levels of ICAM-1 and VCAM-1. Whilst both lymph nodes contained the different populations, they were present in different numbers and ratios. The genes differentially expressed in these populations included VCAM-1, ICAM-1, CXCL13, CCL21 and CCL19. This may demonstrate the varied microenvironment present in these lymph nodes and provides evidence as to why they have diverse developmental requirements (section 1.2.1.4). The ICAM-1 expression variation seen in the stromal cell cultures may be indicative of the dominant stromal organiser population present in the spleen, liver, lung and inguinal lymph node cultures.

Following protein expression analysis, whole genome microarrays were used to determine if a specific lymphoid organ fibroblast gene signature could be established. The gene expression observed was able to group the stromal cell cultures into

peripheral and lymphoid sites with expression of 2935 genes being statistically different (figure 3.10). In order to ascertain the biological relevance from this large amount of genes, analysis in the programme DAVID was completed. This produced 16 pathways that had over a two fold enrichment with an FDR of less than 10%. The pathways that were enriched in the peripheral stromal cell cultures were involved in metabolic processes and lipid biosynthesis. Metabolism is a collective term for catabolism, where complex molecules are broken down and anabolism, where complex molecules are made. Cell substrate pathways were also enriched in peripheral cultures over five fold. This may indicate that stromal cells from the peripheral organs have a more active phenotype as there is an increase in the synthesis and degradation of molecules. Interestingly pathways involved in the innate immune response were over four fold enriched in peripheral stromal cell cultures. This is to be expected as peripheral tissues are the first to come into contact with foreign antigen, where the innate immune response is the first defence (1). The lymphoid tissues are mainly involved in the adaptive immune response which is specific to the antigen (2). In the lymphoid tissues pathways involved in cell division, RNA and mRNA processing and splicing, DNA packaging and chromatin organisation, biogenesis and architecture are enriched. This may suggest an increased rate of cell division and translation in the lymphoid stromal cell cultures and all elements that are associated with this process. In immune responses secondary lymphoid organs are continually expanding and contracting as the cell numbers increase and decrease in response to pathogens. This may explain why these pathways are upregulated in the stromal cells of these tissues as appose to those from peripheral sites. During gene expression analysis of the cultured CD45 negative stromal cells, they were also compared to immortalised stromal cell lines and *ex vivo* sorted stromal cells (figure 3.12) Here

principle component analysis found that the *in vitro* cultured CD45 negative stromal cells were more similar to immortalised stromal cell lines than *ex vivo* sorted stromal cells. This raises the issue of *in vitro* cell culture affecting the phenotype of cells. It remains good practice to use the stromal cell cultures at a low passage, therefore minimising the potential differences imposed by culturing the cells (167,199). Contrary to this however, *in vitro* studies have shown that continual passaging up to passage 35 did not effect gene expression in human fibroblasts when assessed by whole genome arrays (152). To further analyse the similarity between the immortalised cell lines and the *in vitro* cultured cells, gene expression from all lymph node stromal cell cultures from both groups were compared (figure 3.13). From SAM analysis, expression of 261 genes was determined to be statistically different. Again these were analysed using DAVID to assess their biological relevance. Five out of the eight pathways enriched in the *in vitro* cultured CD45 negative stromal cells that had over a two fold enrichment with an FDR less than 10%, were apoptosis and cell death related. This may be due to immortalised cell lines having altered growth properties, allowing them to grow and divide indefinitely *in vitro* given the correct culture conditions, which may decrease their rate of apoptosis (200). Pathways in cell development were also enriched by over 9-fold in the *in vitro* cultured lymph node stromal cells. These are involved in formation of the mature cell structure and terminal differentiation. As the *in vitro* grown stromal cells have been in long term culture, it may be that they have a finite life span and therefore express features of an aged cell.

End point PCR was used to validate the microarray gene expression (figure 3.15) Fibroblast indicator genes such as VCAM-1, gp38 and CD248 were shown to be

expressed in all stromal cell cultures, which correlates with microarray and protein expression data. Gene expression indicative of lymphoid tissue organiser (LTo) cells (figure 1.4) LTβR, TRANCE, VCAM-1, ICAM-1, CCL19 and CCL21 was also shown. LTo cells are believed to develop from mesenchymal cells and are important in the formation of lymph nodes, where they interact with lymphoid tissue inducer (LTi) cells (section 1.2.1.3). The stromal cell cultures all have the phenotype of LTo cells, it may be that the stromal cells from non-lymphoid organs have the potential to function as LTo cells given their gene expression. Under the correct conditions, for example chronic inflammation, they may play a role in tertiary lymphoid tissue formation by functioning as LTo cells. In contrast, expression of CD31 and Lyve-1 is present at varying levels in the lymph node stromal cell cultures, the highest in cervical and axillary lymph node stromal cell cultures. The microarray data showed high levels of both markers in all of the lymph node stromal cell cultures. This indicates that the lymph node stromal cultures may in fact be lymphatic endothelial-like stromal cells. The end point PCR gene expression correlated with those genes seen expressed in all stromal cell cultures. However it did not correlate with those shown to be differentially expressed. One explanation for this difference seen between techniques could be the sensitivity of the microarrays. End point PCR provides a positive or negative result whereas the microarray shows quantitative expression, providing information on the extent of the gene expression.

As the CD45 negative lymphoid cultures were unable to be separated using the whole genome arrays, a site specific LDA was used to determine expression of 47 genes indicated by Rinn *et al* who found that primary adult fibroblasts retained many features of the embryonic pattern of expression of Hox genes (151). This profile was

maintained over decades *in vivo* and up to at least passage 35 *in vitro*, suggesting that Hox gene expression is an important source of positional memory (152). Hox genes are a sub group of homeobox genes, in vertebrates these are found in clusters on chromosomes. In mammals four clusters exist, named Hoxa-d. The site specific LDA assessed the gene expression of five Hox genes, namely Hoxa13, Hoxb2, Hoxa11, Hoxd8 and Hoxa5, 4 of which were expressed by our stromal cell cultures with Hoxa13 expression below the threshold level. Hoxa13 is a distal specific Hox gene and disruption leads to hand-foot-genital syndrome in humans (201). Lack of expression in the stromal cell cultures was therefore expected as none were derived from distal organs. Hoxa5, thought to regulate the tumour suppressor p53 in humans (202), had a fairly consistent expression, as did Hoxb2, which functions as a transcription factor involved in development (203), though there was a slight decrease in skin stromal cell cultures. Hoxa11 was expressed in all but the lung stromal cell cultures, which in humans is involved in uterine development and is required for female fertility (204). Hoxd8 showed the greatest variation, with high expression in the lymph nodes, lower in the spleen, liver and thymus and a further decrease in the skin and lung stromal cell cultures. The pattern of Hoxd8 expression could be used to determine if a fibroblast was isolated from a peripheral site or a lymph node as there is over a 10 fold increase in axillary and cervical lymph node derived stromal cells. Loss of the Hoxd gene cluster results in severe limb and genital abnormalities, with Hoxd8 specifically thought to be involved in adult urinary tract function (205). The data here however may suggest it could also be involved in lymph node stromal cell patterning. Other genes assessed by the site specific LDA showed differential expression among sites (figure 3.16b). CD31 and Lyve-1 expression was increased in the lymph node stromal cell cultures, most notably in the Lyve-1 expression,

indicating a lymphatic endothelium genotype as observed with the end point PCR and microarray data. Interestingly, Grem2 which was not observed in the spleen stromal cells, expressed at low levels in the inguinal lymph node stromal cells, at intermediate levels in the thymus, liver and axillary stromal cells and high levels in the cervical lymph node, lung and skin stromal cells, is thought to play a role in regulating organogenesis, body patterning and tissue differentiation (206). This may indicate a novel role in fibroblast regional specificity. Cdh1 and Mmp3 are also differentially expressed between sites. Cdh1 encodes a cell-cell adhesion protein and has a tumour suppressor function (207) and Mmp3 is an enzyme involved in the breakdown of extracellular matrix (194). The differential expression of these genes may represent the specific needs of the microenvironment of that stromal cell population. CD248, Wisp2, FoxF1a, Gulp, Adam9, Fn, Colla1, Bmp4 and Plat all had a lower expression in the peripheral stromal cell cultures compared to lymphoid stromal cell cultures. Again this could be due to the requirements of a specific microenvironment, with peripheral fibroblasts having different extracellular matrix components and supports the differences observed between lymphoid and peripheral stromal cell cultures using whole genome microarrays.

In conclusion, these data highlight major differences between unsorted lymph node stromal cell cultures and those from the spleen, thymus and liver. In CD45 negative sorted cultures a gene signature of lymphoid tissue stromal cells was determined that was different to that from peripheral tissue stromal cells. However this could not differentiate between lymphoid tissue stromal cells. Further studies using LDA showed that Hoxd8, Grem2, Cdh1 and Mmp3 may be used to differentiate between lymphoid tissue stromal cells, although protein expression has yet to be determined so

this data needs further investigation. Finally the gene expression observed indicates that the stromal cell cultures may have the expression profile of LTo cells. This finding needs to be further investigated using functional assays.

Chapter Four

In vitro Function of Fibroblast Populations from Different Sites

CHAPTER FOUR

In vitro Function of Fibroblast Populations from Different Sites

4.1 Introduction

The cross talk between lymphoid tissue inducer (LTi) cells and lymphoid tissue organiser (LTo) cells has been shown to be critical to lymph node organogenesis (35) and involves the ligands and receptors of the tumour necrosis family (TNF) family (36). Lymphotoxin (LT) α, LTβ and TNF are structurally homologous cytokines grouped within the TNF ligand family (37). TNF and LTα can bind to TNF receptors TNFRI and TNFRII. However, LTβ forms a functional heterotrimeric complex, $LT\alpha_1\beta_2$ to bind to its receptor, lymphotoxin β receptor (LTβR) (38,39). The importance of this interaction in functional secondary lymphoid organ formation has been demonstrated by LTα knockout mice. In these mice all lymph nodes and Peyer's patches are absent, with the spleen and nasal-associated lymphoid tissue (NALT) being highly disorganised (40). LTα has been shown to be a key factor in the differentiation of stromal cells into stromal organiser cells, recognised by the upregulated expression of several surface proteins including VCAM-1 and ICAM-1 (35). In this study the gene expression, for example LTβR, TRANCE, VCAM-1, ICAM-1, CCL19 and CCL21, of all the stromal cell cultures is indicative of LTo cells. Therefore the stromal cells were treated with LTα to determine if their functional response was also suggestive of an LTo phenotype.

Another function of the LTo is their interaction with lymphocytes. Previous work has shown that stromal cells co-cultured with lymphocytes results in an increase in lymphocyte survival. This is thought to be mediated by survival factors produced

from the stromal cells and IL-7 was shown to be at least partly responsible for this enhanced survival (67). In this study the gene expression of known lymphocyte survival factors such as IL-6 (208), IL-7 (209,210) and CCL19 (67) were observed in the stromal cell cultures, therefore the co-culture of lymphocytes with cultured stromal cells from different mouse organs was assessed to determine if enhanced survival occurred and if this was affected by the origin of the stromal cell.

In this chapter functional differences were seen between lymphoid and peripheral stromal cell populations in their response to LTα, and also within the lymphoid tissue stromal cells in terms of the degree of their response. Increased lymphocyte survival was observed in co-culture with all stromal cells, however B cells showed only a minimal enhancement of survival with the effect on T cell survival being much greater.

4.2 Results

4.2.1 LTα treatment of stromal cells

Having noted that the phenotype of the stromal cell cultures was similar to that described in the literature as a lymphoid tissue organiser (LTo) cell, the function of these cells was analysed. As LTα has been shown to be a key factor in the differentiation of stromal cells into stromal organiser cells and in LTo interaction with LTi, its effect on the cultured stromal cells was determined. The effect of LTα on VCAM-1 and ICAM-1 expression in stromal cell cultures was assessed by treating splenic stromal cell cultures with LTα at a range of concentrations for 24 hours (figure 4.1a). LTα was shown to increase expression of both VCAM-1 and ICAM-1, with increasing concentrations of LTα also increasing protein expression. Although

2.5µg/ml of LTα increased VCAM-1 expression as compared to 1µg/ml, it did not warrant using a dose 2.5 times higher. ICAM-1 expression increased up to a LTα concentration of 1µg/ml but no further increase in expression was seen with 2.5µg/ml. Therefore, 1µg/ml of LTα was used during a time course to assess dynamics of VCAM-1 and ICAM-1 expression (figure 4.1b). LTα treatment increased ICAM-1 expression up to 24 hours and then decreased by 72 hours. VCAM-1 expression was increased up to 12 hours after LTα treatment, where it remains high to 24 hours and then similar to ICAM-1 decreased by 72 hours. Therefore splenic stromal cells were treated with 1µg/ml of LTα for 24 hours as determined by the titration and time course (figure 4.1c). No effect was seen of LTα treatment on isotype control expression and a clear increase in VCAM-1 and ICAM-1 expression was observed.

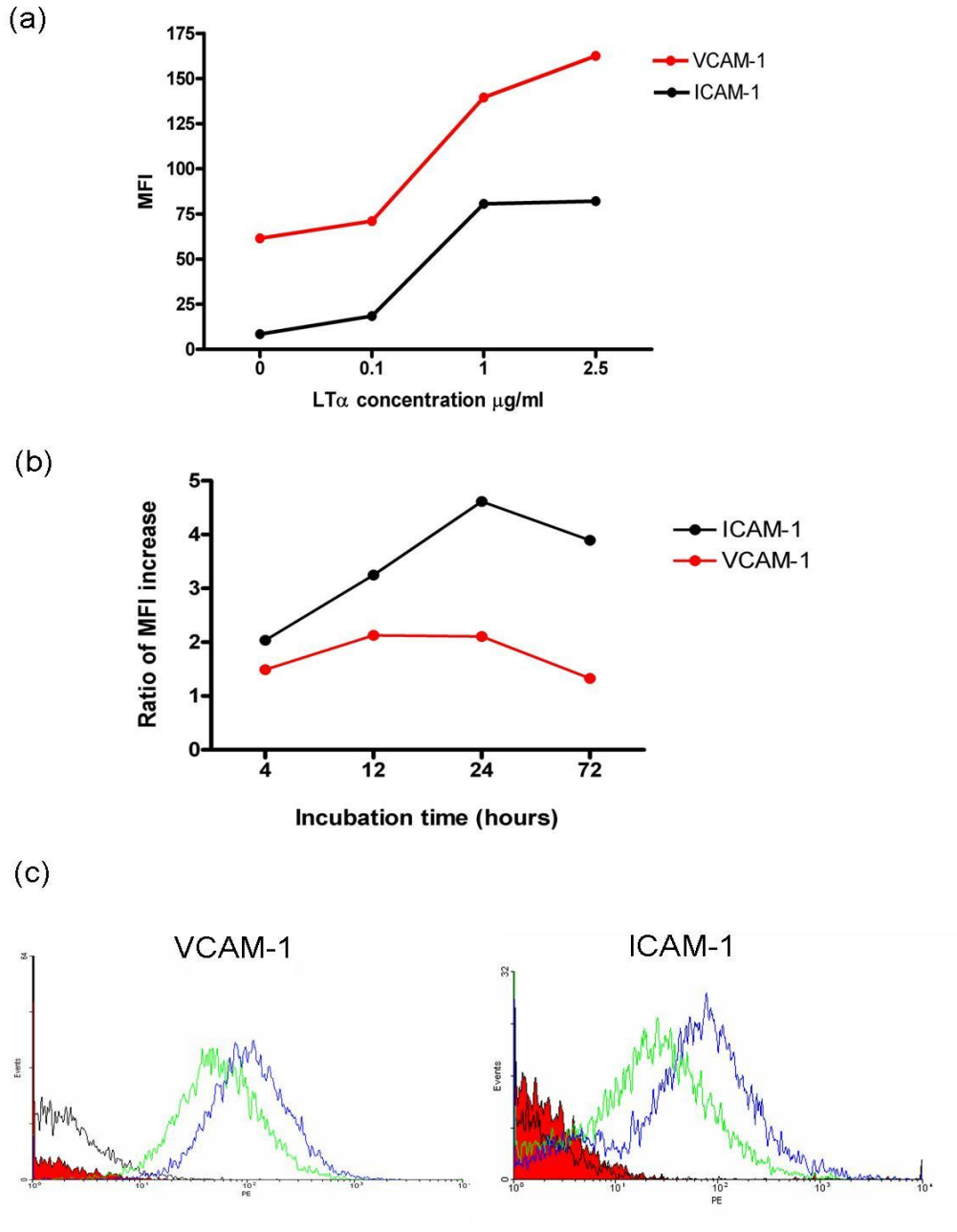

Figure 4.1 LTα increases VCAM-1 and ICAM-1 expression in splenic stromal cells

LTα treatment of splenic stromal cells. (a) Mean fluorescence intensity (MFI) of VCAM-1 (red) and ICAM-1 (black) protein expression assessed by flow cytometry following treatment with LTα for 24 hours (n=1). (b) Time course of treatment with 1μg/ml LTα, data is expressed as a ratio of baseline MFI: MFI following treatment of VCAM-1 (red) and ICAM-1 (black) protein expression (n=1). (c) Effect of treatment with 1μg/ml LTα for 24 hours. Red = baseline isotype control, black outline = LTα treated isotype control, green outline = baseline protein expression and blue outline = LTα treated protein expression. Graphs are representative of 6 independent experiments.

Having observed that 1μg/ml LTα treated for 24 hours was required for maximal increase in VCAM-1 and ICAM-1 expression in splenic stromal cell cultures; this was repeated in all stromal cell lines (figure 4.2). A significant increase ($p<0.05$) in VCAM-1 expression in all but the skin stromal cell cultures was observed. ICAM-1 protein expression was significantly ($p<0.05$) increased in the spleen, inguinal lymph node and lung stromal cell cultures. The thymus, skin and axillary and cervical lymph node stromal cell lines showed little or no increase. However, the corresponding untreated cells of these stromal cells lines also had very little or no ICAM-1 expression. This pattern of ICAM-1 expression correlates with the protein expression assessed by flow cytometry (section 3.3.2.1). These data suggest that LTα can only increase ICAM-1 expression in cells that are already expressing the protein. The significant increase in VCAM-1 expression in all stromal cells but those derived from the skin and in ICAM-1 expression in the spleen, inguinal lymph node and lung stromal cells indicates that these stromal cells may have the ability to function as LTo cells.

During development the function and phenotype of stromal cells differ (50). Therefore, having observed that LTα increases VCAM-1 and ICAM-1 expression in adult splenic stromal cell cultures, cultures derived from E15 and newborn spleens were analysed (figure 4.3). Not only was a difference in VCAM-1 and ICAM-1 expression observed in cultures from different stages in development but also their response to LTα differed. Very little VCAM-1 expression was seen in E15 splenic stromal cells, with a stark increase in the newborn, which then decreased in the adult, although expression still remained high compared with the E15 cultures. Interestingly however, LTα induces a significant increase ($p<0.05$) in VCAM-1 expression only in

the adult derived cultures. Expression of VCAM-1 in newborn cultures does generally increase, however failed to reach significance. ICAM-1 expression followed the same trend as VCAM-1 in the untreated cells, in that ICAM-1 expression was increased in newborn cultures with concomitant decrease in adult cultures, however expression in the adult cultures was lower than in E15. Upon LTα treatment E15, newborn and adult splenic cultures significantly increased ICAM-1 expression ($p<0.05$, $p<0.001$, $p<0.05$ respectively).

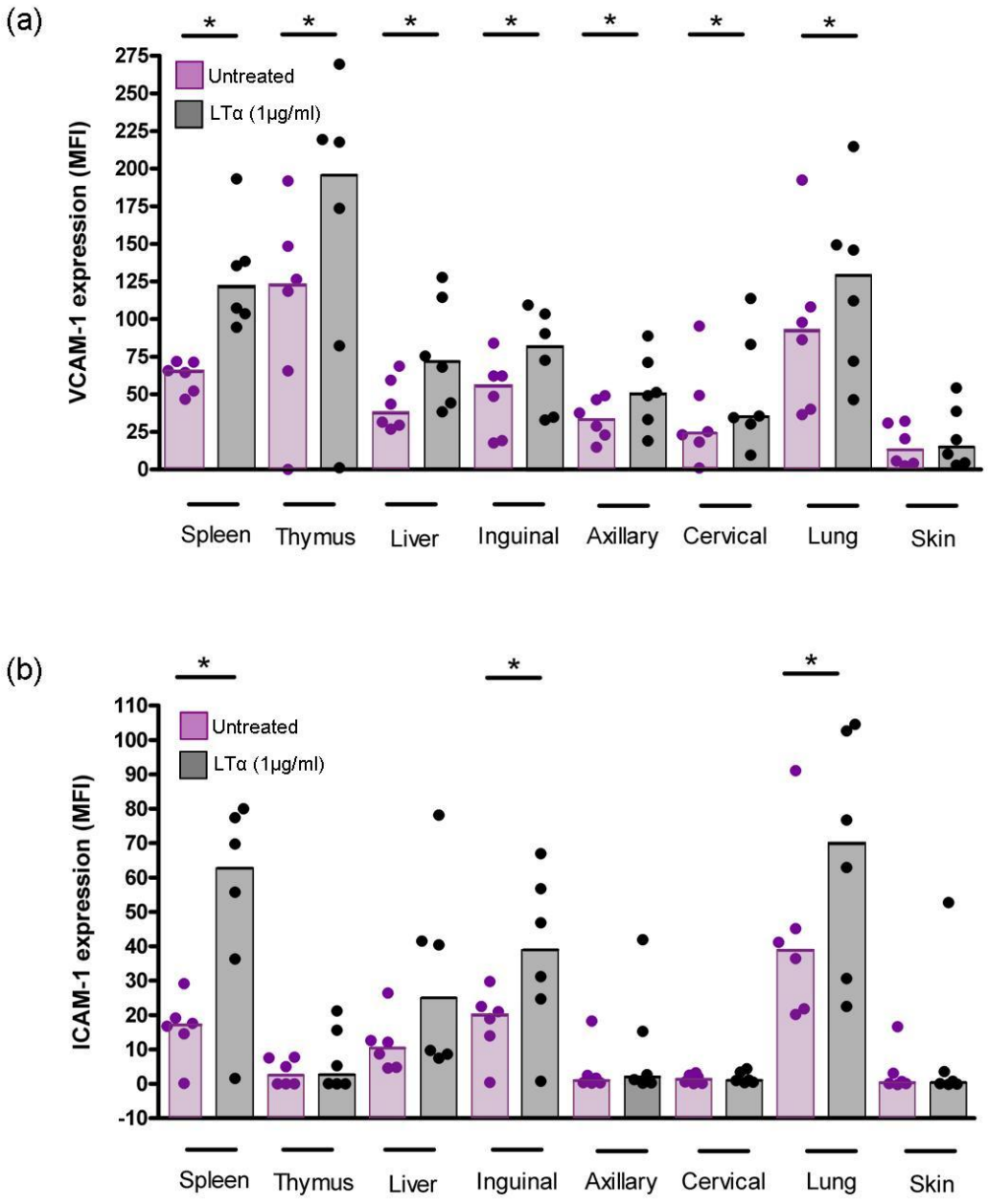

Figure 4.2 Effect of LTα expression on VCAM-1 and ICAM-1 expression on stromal cells

Stromal cells were treated with 1µg/ml LTα for 24 hours, after which (a) VCAM-1 and (b) ICAM-1 expression was determined by flow cytometry. Purple = untreated and black = treated cells, dots represent individual experiments and bars represent the median (n=6). *, $p<0.05$.

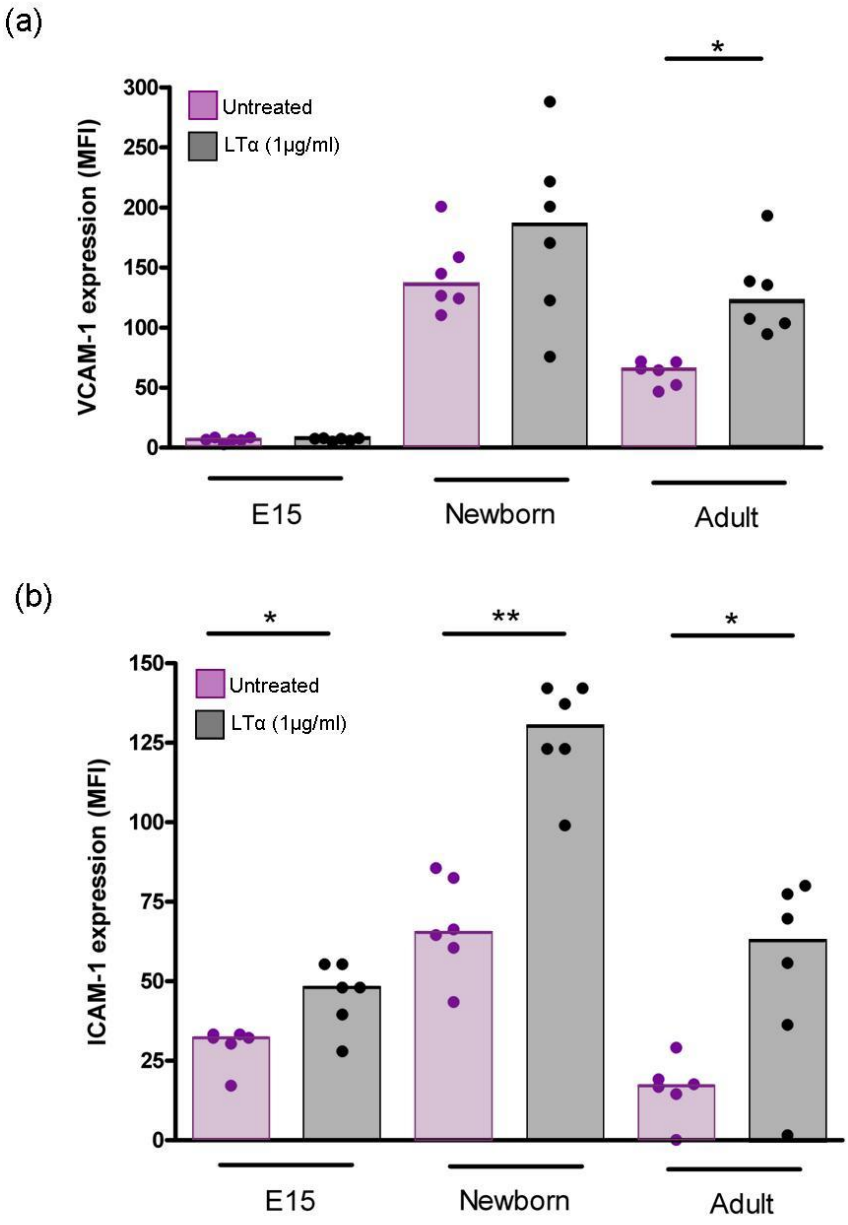

Figure 4.3 Effect of LTα treatment on VCAM-1 and ICAM-1 expression on splenic stromal cell cultures throughout development

Splenic stromal cell cultures from E15, newborn and adult mice were treated with 1µg/ml LTα for 24 hours, after which (a) VCAM-1 and (b) ICAM-1 expression was determined by flow cytometry. Purple = untreated and black = treated cells, dots represent individual experiments and bars represent the median (n=6). *, $p<0.05$ **, $p<0.001$.

4.2.1.1 Gene profile of LTα treated stromal cells

As treatment with LTα affected the protein expression of VCAM-1 and ICAM-1 in lymphoid stromal cell cultures, the effect of LTα on gene expression was also assessed. TNF family members are key in mediating the LTo-LTi interaction (35), as well as production of cytokines such as CCL21 and CCL19 (211). Therefore a TaqMan low density array (LDA) was designed which contained 96 genes (appendix 8.8) including, TNF family ligands, cytokines and chemokines to determine the effect of LTα treatment on stromal cells. All adult stromal cell cultures were treated for 24 hours with 1µg/ml of LTα, after which RNA was extracted and approximately 1µg hybridised to the TNF LDA (appendix 8.9). Significance analysis of microarrays (SAM) analysis found that the expression of 21 of the genes analysed significantly differed between untreated and LTα treated stromal cells (appendix 8.10). Hierarchical clustering based on the SAM analysis grouped the LTα treated and untreated cells together based on their gene expression profile regardless of which organ the stromal cells were derived from (figure 4.4a). The only exception was cultures derived from the inguinal lymph node. Upon treatment the LTα treated stromal cells appeared to converge to a distinct genotype, principle component analysis (PCA) shows the tight clustering of LTα treated stromal cells (figure 4.4b), with downregulation of LTβ, IFN ligand family members, CCL27, CXCL27, IL-12, IL-23 and TNFSF8 and TNFSF15 compared to untreated stromal cells.

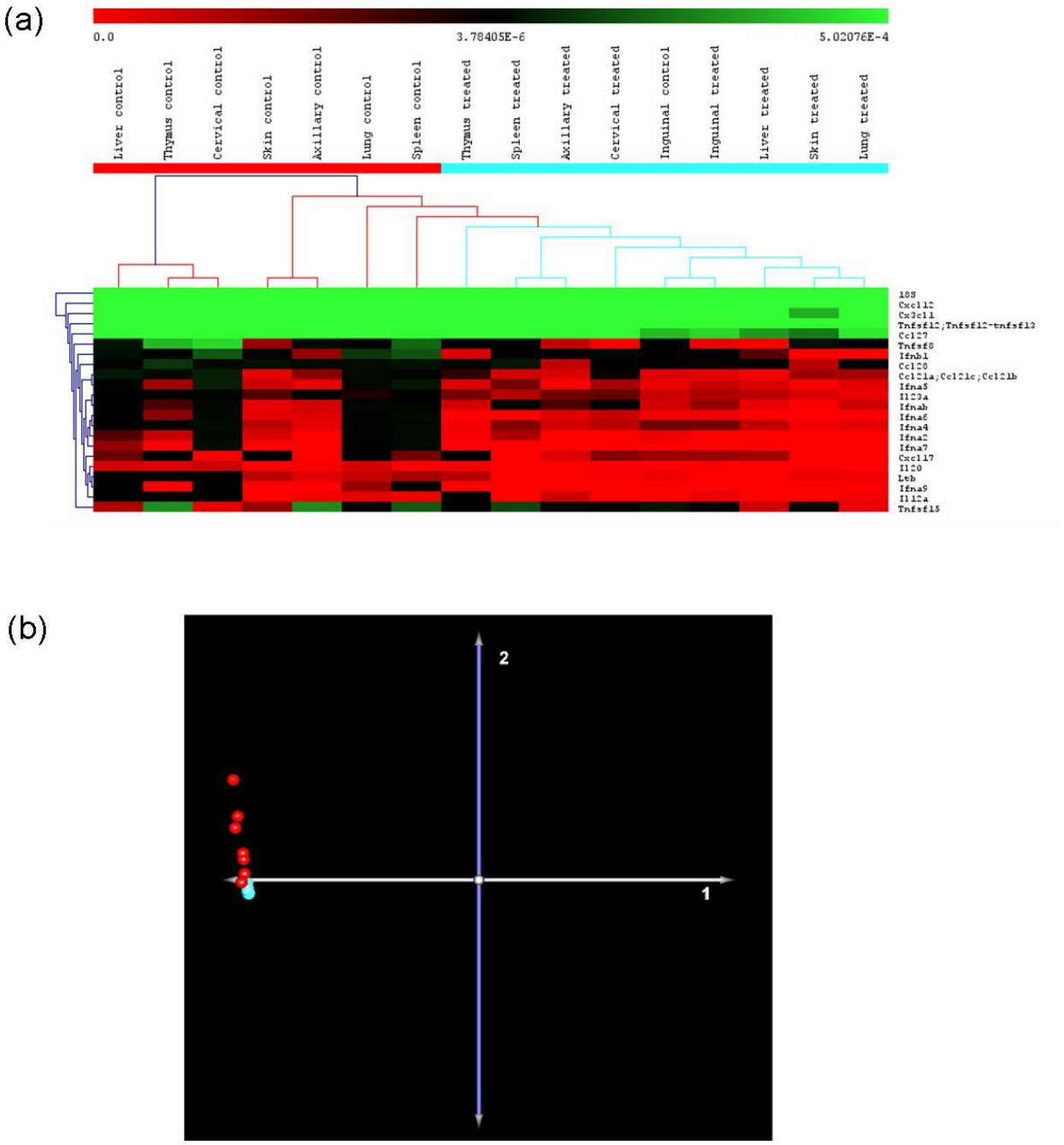

Figure 4.4 Differential gene expression between LTα treated and untreated stromal cells

Total RNA from LTα treated and untreated CD45 negative sorted stromal cells was extracted and gene expression determined using the TNF LDA. (a) Hierarchical clustering of untreated and LTα treated stromal cells. Red = low, green = high and black = medium gene expression (b) PCA analysis based on the 21 significantly different expressed genes from the SAM analysis. Red circles = untreated cells and turquoise circles = LTα treated cells (n=6).

4.2.2 Leucocyte survival in co-culture with stromal cells

Having established that the stromal cell cultures, as assessed by VCAM-1 and ICAM-1 expression, responded to LTα in a manner indicative of LTo-like cells and coupled with the observation that the cultures produced of factors associated with lymphocyte survival, such as IL-6, IL-7 and CCL19 (section 3.2.2.5), lymphocyte survival was assessed in a co-culture system. Whole splenocytes were co-cultured with adult stromal cells derived from lymphoid and peripheral organs, conditioned medium or fresh medium as a control. After four days incubation, the survival of the B cells ($CD19^+$) and T cells ($CD3^+$) was determined by Annexin V using flow cytometry. Annexin V is a marker of cells in an early stage of apoptosis (212). Gates were used to eliminate apoptotic cells by including only Annexin V negative cells. A significant increase in the survival of B cells was observed when cultured with stromal cells from all organs, rather than conditioned or fresh media (figure 4.5). However, the percentage survival was low, generally below 10%, with little or no survival seen when lymphocytes were cultured with conditioned or fresh media. When T cell survival was assessed a significant increase was observed when cultured with all stromal cells, compared to conditioned or fresh media (figure 4.6). Interestingly, the percentage T cell survival was greater than B cell survival with the same stromal cells. In addition, the conditioned media was more effective at increasing T cell survival compared to B cells, suggesting that soluble factors present in the conditioned media may also play a role in T cell survival. The survival experiments were completed twice with three replicates in each. The two different experiments demonstrated variation in survival of both B and T cells, although replicates were tightly clustered.

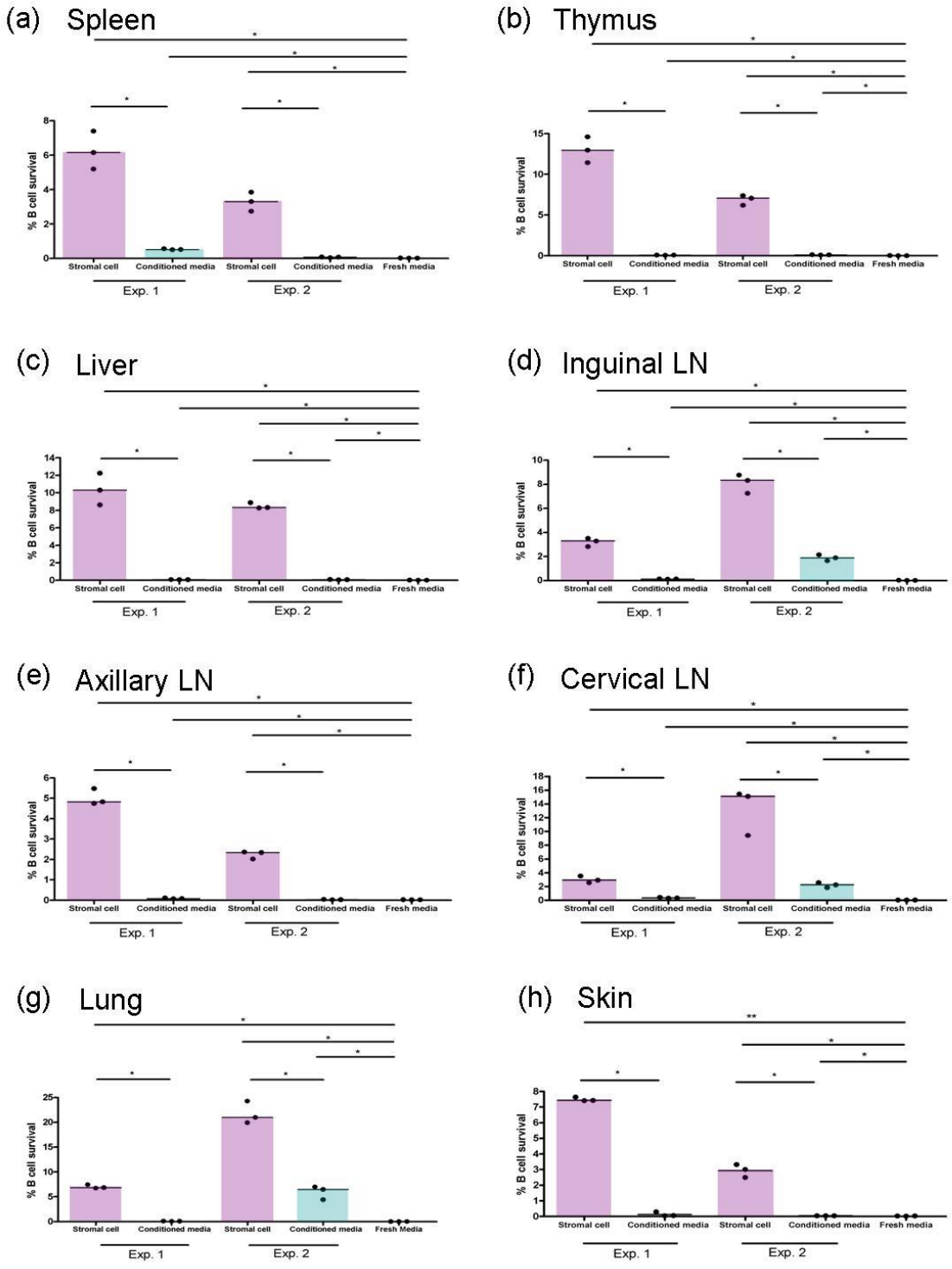

Figure 4.5 Percentage B cell survival in co-culture with stromal cells
One million splenocytes were added to cultured stromal cells (purple bars) or conditioned medium (turquoise bars) from (a) spleen, (b) thymus, (c) liver, (d) inguinal lymph node, (e) axillary lymph node, (f) cervical lymph node, (g) lung and (h) skin, with fresh medium as a control. B cell survival was determined by flow cytometry using Annexin V staining after four days in culture (n=6). *, $p<0.05$. **, $p<0.0001$.

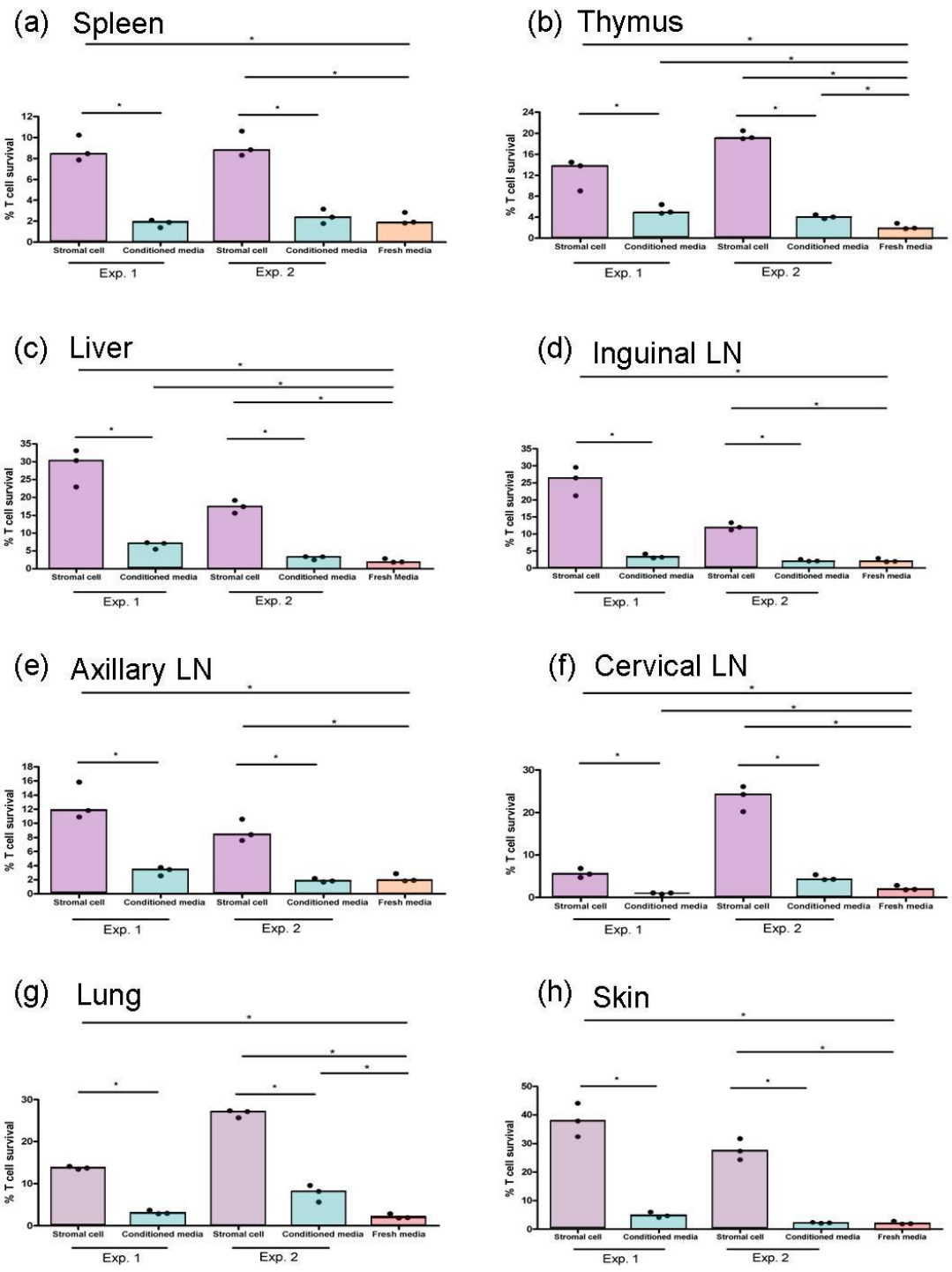

Figure 4.6 Percentage T cell survival in co-culture with stromal cells
One million splenocytes were added to cultured stromal cells (purple bars) or conditioned medium (turquoise bars) from (a) spleen, (b) thymus, (c) liver, (d) inguinal lymph node, (e) axillary lymph node, (f) cervical lymph node, (g) lung and (h) skin with fresh medium as a control (orange bars). T cell survival was determined by flow cytometry using Annexin V staining after four days in culture (n=6). *, $p<0.05$.

4.3 Discussion

Gene expression profiles of all stromal cell cultures, for example LTβR, TRANCE, VCAM-1, ICAM-1, CCL19 and CCL21, suggested a LTo cell phenotype (chapter 3). These cells, in conjunction with LTi cells *in vivo* form secondary lymphoid tissue (35). An important interaction between these two cell types is the activation of LTo by LTα produced by the LTi cell, resulting in an increase in expression of many proteins including VCAM-1 and ICAM-1 (35). Therefore, the response of the stromal cell cultures to LTα was assessed by measuring VCAM-1 and ICAM-1 protein cell surface expression. A significant increase ($p<0.05$) in VCAM-1 expression was seen in all stromal cell cultures except those derived from the skin. The lack of response in the skin stromal cell cultures is not surprising as this is not a secondary lymphoid site and therefore it is reasonable to assume that it would be less likely to respond to LTα. Interestingly however, the lung stromal cell cultures show a significant increase even though it is not a secondary lymphoid site, perhaps indicating its potential for tertiary lymphoid formation under chronic inflammatory conditions (104). Of note, smaller increases in protein expression were seen in the three lymph node stromal cell cultures compared with cell cultures from other lymphoid sites. This may indicate a different phenotype within these stromal cells, which would correlate with the differential gene expression seen in chapter 3, where the lymph node stromal cells had expression of CD31 and Lyve-1, suggesting a lymphatic endothelial-like phenotype. It is tempting to speculate therefore that the different basal levels of VCAM-1 expression in the stromal cell cultures represents the requirements of the specific stromal microenvironment at each site. Conversely, ICAM-1 expression did not follow the same pattern, it was significantly increased ($p<0.05$) only in the spleen, inguinal lymph node and lung stromal cell cultures, which correlates with the protein

expression data (section 3.2.2.2). When analysing the ICAM-1 expression, stromal cell cultures that expressed ICAM-1 when resting could respond to LTα and increase expression. However, in cultures that did not express ICAM-1 in the resting cell, it was unable to be induced upon treatment with LTα. Previous studies have highlighted a variation in ICAM-1 expression in stromal cell populations from different lymphoid tissues, such as Peyer's patches and peripheral and mesenteric lymph nodes (45,198). It is possible that the cultured stromal cells in this study obtained from the different sites are representative of these different populations indicating ICAM-1 expression as a protein that can differentiate different stromal populations.

As the LTo-LTi interaction is key in development, E15 and newborn splenic stromal cell cultures were also treated with LTα. The E15 stromal cell cultures expressed very low levels of VCAM-1 which was not upregulated upon LTα treatment, however ICAM-1 expression was observed and this was significantly upregulated after LTα treatment. Studies by White *et al*, 2007, found that at E15 the largest stromal cell population in the inguinal lymph node was ICAM-1 positive VCAM-1 negative (50), which correlates with the expression found in E15 splenic stromal cultures. In the same study it was shown that as the lymph node develops the single positive stromal cells mature into double positive VCAM-1/ICAM-1 expressing stromal cells by postnatal day 1 (50). Again these findings correlate with this study as in the newborn splenic stromal cell culture both VCAM-1 and ICAM-1 expression was found. The adult splenic stromal cell cultures show lower expression of ICAM-1 and VCAM-1 compared with newborn splenic stromal cell cultures. This may be due to the maturation of the spleen in the adult mouse. However the adult spleen still upregulates expression of both VCAM-1 and ICAM-1 upon treatment with LTα, demonstrating

that the adult stromal cells still have the ability to respond when required. Scandella *et al*, 2008 demonstrated a reactivation of the LTo-LTi relationship seen in development after alterations in the homeostasis of adult secondary lymphoid organs (57). LTi cells, which are not thought to be needed to maintain non-inflammatory secondary lymphoid organ homeostasis, were reactivated upon destruction of the T zone stroma by lymphocytic choriomeningitis virus (LCMV) (57). This study provided evidence that the LTo-LTi interactions are still important in the adult, long after secondary lymphoid organ development has been completed. When analysing gene expression before and after LTα treatment, it was possible to group the adult stromal cell cultures into control and treated populations. The stromal cells seemed to converge into a distinct phenotype, with the treated stromal cells having a more similar gene expression than the untreated group. Significant downregulation of LTβ, IFN ligand family members, CCL27, CXCL27, IL-12, IL-23 and TNFSF8 and TNFSF15 was observed following SAM analysis. Most of these genes are involved in the inflammatory response, either by homing of T cells (CCL27) (213), differentiation of T cells (IL-12) (214) attracting dendritic cells and monocytes (CXCL17) (215), regulating lymphocyte survival (TNFSF8) (216) or promoting upregulation of inflammatory pathways (IL-23) (217). Downregulation of these genes is counterintuitive seeing as LTα is thought to be pro-inflammatory (218) and play a key role tertiary lymphoid formation in chronic inflammatory diseases (219). This could be due to the fact 1µg/ml LTα for 24 hours was not the correct dose or timing to alter gene expression, or it may be that LTα does not effect gene expression, only protein, therefore further investigations such as a luminex assay could assess chemokines/cytokines produced. It could also be due to the requirement for ligation of

other receptors on the stromal cell by mechanisms which would occur *in vivo* such as cell-cell contact between the LTo cells and the LTi cell.

In addition to how the stromal cell cultures are affected by LTα, their own effect on lymphocyte survival was investigated. Previous work by Link *et al*, 2007, has shown an increase in survival with stromal cells via IL-7 and CCL19 (67), for which the cultured stromal cells have all been shown to express the genes (section 3.3.3). A significant increase ($p<0.05$) in B and T cell survival was observed, with T cell survival much greater when cultured with all stromal cell cultures. The difference seen in survival between the two separate experiments could be explained by different proliferation rates of the stromal cells which, in turn is dependant on where in the cell cycle they were when seeded. This could be addressed in future experiments by irradiating the stromal cells before seeding. The percentage B cell survival was comparable with that seen by Link *et al*, 2007 (67). However the percentage T cell survival after 4 days was lower. This highlights that the stromal cell cultures do not keep T cells alive as well as observed this study. It may be due to how the apoptotic cells were identified; in this study Annexin V staining was used by flow cytometry whereas in the study by Link *et al*, trypan blue dye exclusion was used. Annexin V staining by flow cytometry is a less subjective method for determining cell death as the number of apoptotic cells is determined by the flow cytometer using set gates and a large population of the cells.

Previously, phenotypic differences between peripheral and lymphoid stromal cells were observed. In addition, within lymphoid stromal cells, the lymph node cultures showed differences. The aim of this chapter was to see if these phenotypic differences

would be mirrored in function. The response to LTα showed a definite difference between peripheral and lymphoid stromal cell cultures and possibly within lymphoid stromal cell cultures as the lymph node cultures showed a smaller increase in VCAM-1 and ICAM-1 protein expression. Interestingly the lung stromal cells may act more like lymphoid tissue stromal cells when forced. All cultures increased lymphocyte survival indicating a general function of stroma (180). The phenotype of the stromal cell cultures found in chapter 3, for example LTβR, TRANCE, VCAM-1, ICAM-1, CCL19 and CCL21 suggested LTo-like cells. This coupled with the ability to keep T cells alive more successfully than B cells and gp38 gene and protein expression, indicates that the stromal cell cultures are comparable to a population termed fibroblastic reticular cells (FRCs). These are the main stromal cell population from the T zone of secondary lymphoid organs and have a role in the migration and survival of T cells within the T zone (67).

Chapter Five

In vivo Function of Fibroblast Populations from Different Sites

CHAPTER FIVE

In vivo Function of Fibroblast Populations from Different Sites

5.1 Introduction

Stromal cells support the distribution, migration and survival of lymphocytes as well as acting as the structural backbone within lymph nodes. T zone stromal cells, termed fibroblastic reticular cells (FRCs); produce constitutive chemokines and support migrating T cells and dendritic cells (DCs). FRCs are more plentiful than other stromal populations within the lymph node and have been shown to express glycoprotein 38 (gp38 or podoplanin) (section 1.2.2.1.1) (70). They produce extra cellular matrix (ECM) components, which are crucial to the structural stability of the lymph nodes, and CCL21 and CCL19 which attract the CCR7 expressing T cells and DCs to the T zone. In addition, they also enhance the survival of T cells by producing IL-7 (71). In this study, the gene expression of the stromal cell cultures, for example gp38, CCL19 and CCL21, and the increase in T cell survival upon co-culture indicates that the stromal cell cultures are comparable to FRCs (section 1.2.2.1). To determine if the stromal cell cultures function as FRCs, an *in vivo* model was used to assess recruitment and organisation of leucocytes. Previous studies have shown that grafting embryonic lymph nodes under the kidney capsule of adult mice results in the formation of lymphoid tissues containing host lymphocytes which organise into B and T cell areas similar to the adult lymph nodes (50,220). Therefore, in this chapter, stromal cells alone were applied to this technique with reaggregation, host cell recruitment and subsequent organisation analysed.

In this chapter it was established that stromal cells could form reaggregates for use within the kidney capsule transfer model, however structural support was required for consistent survival *in vivo*. Preliminary data suggests that host leucocyte recruitment to the stromal cell reaggregate is possible.

5.2 Results

5.2.1 Pilot kidney capsule model studies using stromal cell reaggregates

To ascertain if the cultured stromal cells from different sites are functionally different *in vivo* a kidney capsule transfer model was used (221). To demonstrate the success of this new technique whole lymphoid organs, which have been shown to work previously (50,222), were grafted under the kidney capsule each time initial surgeries were performed (figure 5.1). The survival and expansion of the embryonic and newborn whole organs after kidney capsule transfer confirmed the success of the technique. This technique was then expanded with the aim of grafting adult stromal cells alone, to assess the functional ability of the stromal cell cultures to recruit and organise host leucocytes. Firstly it was determined if a reaggregate would successfully form using *in vitro* cultured stromal cells. Reaggregates were formed from stromal cells using 100,000 and 150,000 cells using the V-well plate method (section 2.12). Reaggregates of both cell numbers could be removed from the V-well plate and placed in PBS whilst successfully maintaining their globular shape. This was true for all stromal cell lines, examples of liver, spleen and cervical stromal cell reaggregates are shown (figure 5.2).

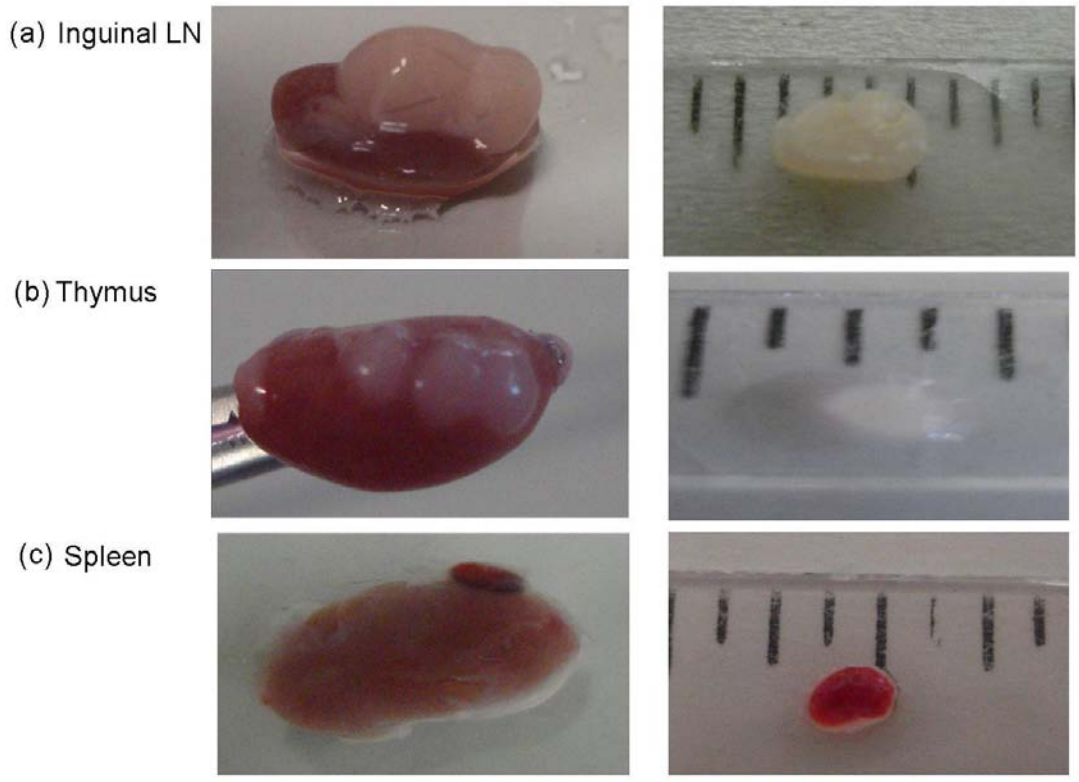

Figure 5.1 Grafting of whole lymphoid organs under the kidney capsule
Whole lymphoid organs dissected from newborn and embryonic C57BL6 mice were grafted under the kidney capsule for 1 week as positive controls (a) Postnatal day 1 inguinal lymph nodes, (b) E15 thymus, (c) E15 spleen. Left panel shows dissected kidneys, right panel shows the size of the organs recovered in millimeters (n=3).

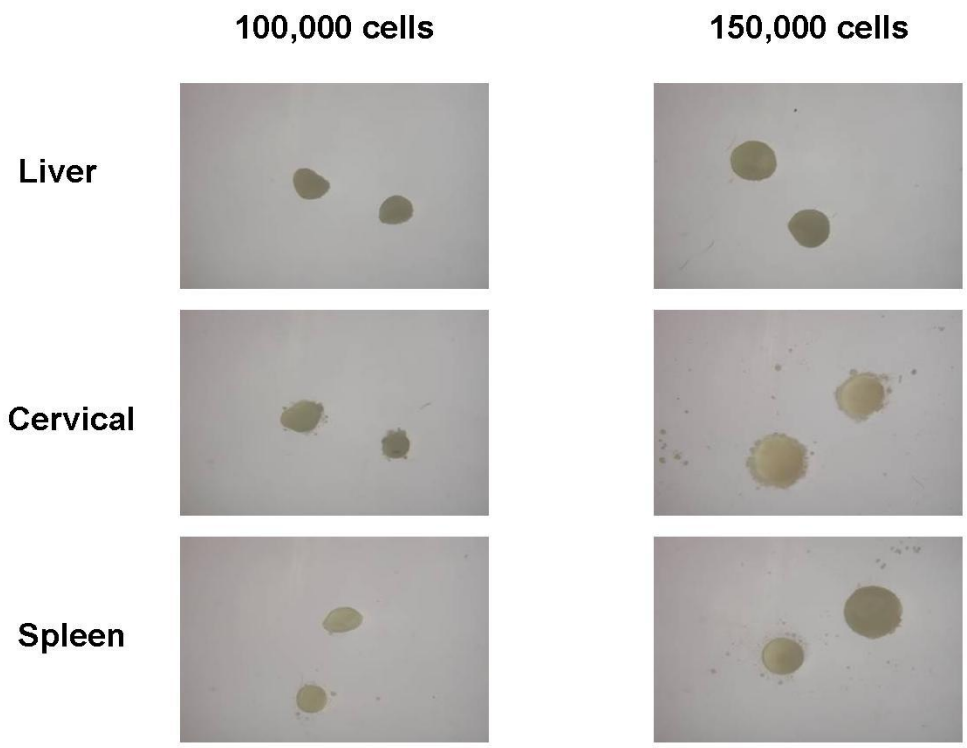

Figure 5.2 Stromal cell reaggregate formation
Reaggregates were formed from 100,000 and 150,000 CD45 negative stromal cells. Cells were centrifuged at 900g for 5 minutes, then 225g for 5 minutes in a V-well plate and placed at 37°C, 5% CO_2 for 24 hours. The reaggregates were removed placed into PBS where they maintained their structure. Pictures are representative reaggregates from two independent cultures.

Having demonstrated that the stromal cells successfully formed reaggregates, cervical lymph node and liver stromal cell reaggregates, formed from 100,000 cells, were grafted under the kidney capsule of an adult C57BL6 mouse. Stromal cells derived from these sites were chosen initially to compare recruitment and organisation of leucocytes by stromal cells from a lymph node against stromal cells from a non-lymph node organ. When kidney capsule surgery was performed a postnatal day one inguinal lymph node or an E15 spleen or thymus was grafted into a separate mouse to ensure the technique was successful. The reaggregates were incubated for four weeks following grafting, a length of time used in previous kidney capsule transfer studies (222). After four weeks, the stromal cell reaggregate grafts had enlarged, as they were then clearly visible by eye (figure 5.3). The reaggregates were then dissected from the kidney, snap frozen and cryogenically sectioned. Immunofluorescent staining was performed using stromal cell markers including CD248, gp38 and VCAM-1 as well as markers for infiltrating host cells such as macrophage (F4/80), dendritic cells (CD11c), B cells (B220) and T cells (CD3). The CD45 negative stromal cells derived from the liver maintained their phenotype from the *in vitro* culture (section 3.2.2.2); high CD248, gp38 and VCAM-1 expression was observed in the liver stromal cell graft (figure 5.4). However, the staining of the stromal cell markers was not homogeneous and may indicate organisation of these cells within the graft. The positive collagen type I staining suggests that the stromal cells are functional, producing ECM components. The punctate PDGFRα staining indicates vascularisation of the graft (223). The protein expression from the liver CD45 negative stromal cell reaggregate shows a recruitment of F4/80, CD11c, CD3 and small population of B220 positive cells. This suggests that host macrophages, dendritic cells, T cells and a small number of host B cells have been recruited into the

graft. Interestingly, there may be some structural organisation as there were regions where CD11c and CD3 positive cells clustered. Specifically, there were areas where CD248 was not expressed and CD3 and gp38 expression were high (figure 5.4c,d). This suggests a T zone area may have formed as gp38 has been shown to be expressed on FRC of the T zone stroma (section 1.2.2.1.1). Of note, there was a population of cells observed that were CD3 and CD248 positive (figure 5.4d), CD248 expression has been restricted to stromal cells in the previous studies (224,225), this may be due to the close proximity of the cell membranes of the T cell and stromal cells. Further staining and higher magnification images could answer this question. The protein expression observed from the cervical CD45 negative stromal cell graft showed expression of stromal markers CD248 and gp38 but this was mostly restricted to a capsular like structure around the edge of the graft (figure 5.5). Interestingly, VCAM-1 expression was not seen within the graft, even though the cervical stromal cells in culture showed high VCAM-1 expression (section 3.2.2.2). Collagen type I expression again indicated that the stromal cells were functional by producing ECM components. Punctate PDGFRα was present indicating vascularisation of the graft. Recruitment of host macrophage, dendritic cells, T cells and B cells was observed but to a lesser extent than the liver stromal cell graft. F4/80 positive staining was throughout the graft where as CD11c, CD3 and B220 seemed to be restricted to the subcapsular area. Again B220 staining was rarely seen which concurs with the low B cell survival observed during *in vitro* co-culture with the stromal cells. The outer capsule which was gp38, CD248 and collagen type I positive may indicate that the stromal cells were attempting to form a lymph node type structure although there was no evidence of T and B cell compartmentalisation. Gene expression from sections of the recovered grafts showed expression of T cell marker CD3 and B cell marker

CD19 in both grafts and confirmed the recruitment of T and B cells observed by immunofluorescent staining (figure 5.6).

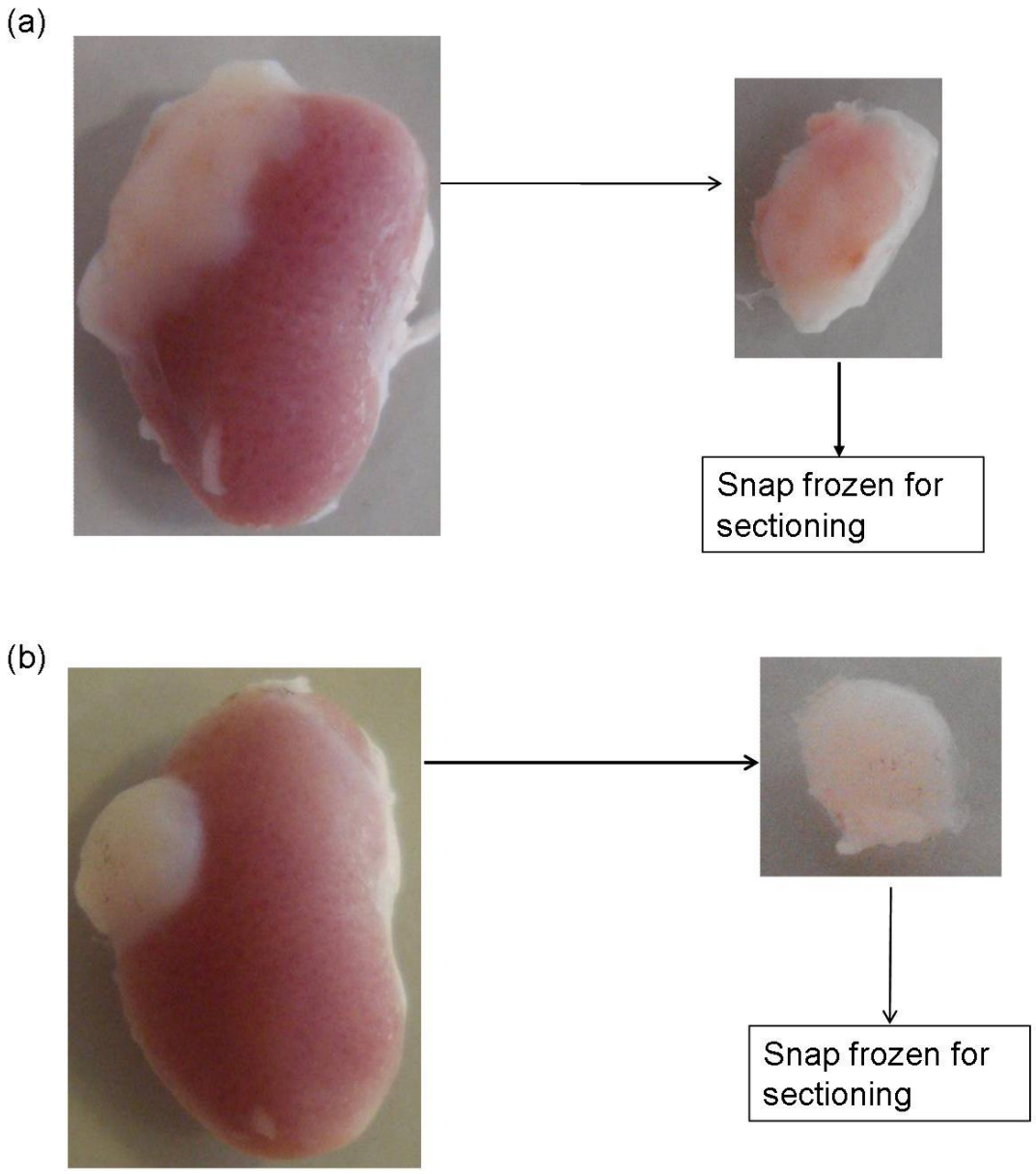

Figure 5.3 Grafting of CD45 negative stromal cell reaggregates under the kidney capsule

Reaggregates formed from 100,000 stromal cells derived from (a) liver and (b) cervical lymph node were grafted under the kidney capsule for 4 weeks, after which the kidney was harvested and the graft dissected and snap frozen (n=1).

(a)

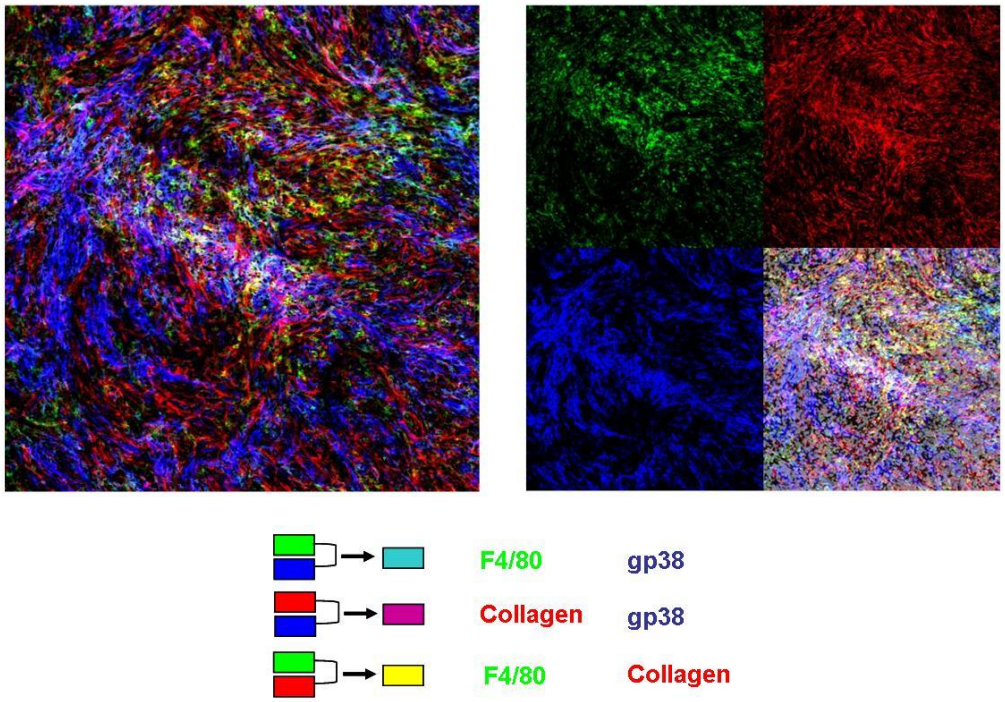
F4/80 gp38
Collagen gp38
F4/80 Collagen

(b)

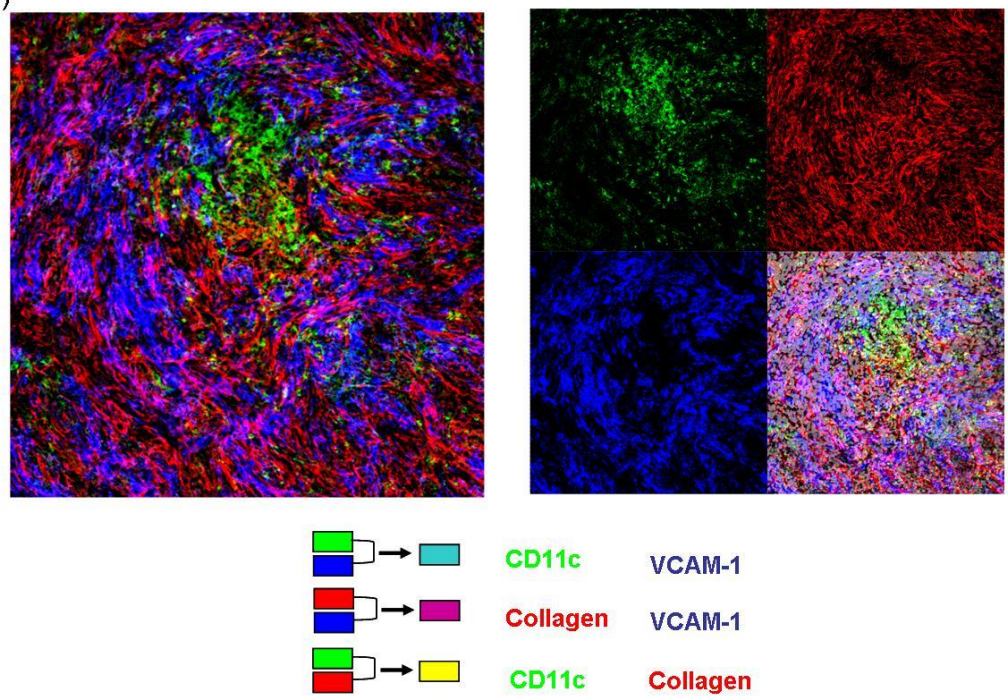
CD11c VCAM-1
Collagen VCAM-1
CD11c Collagen

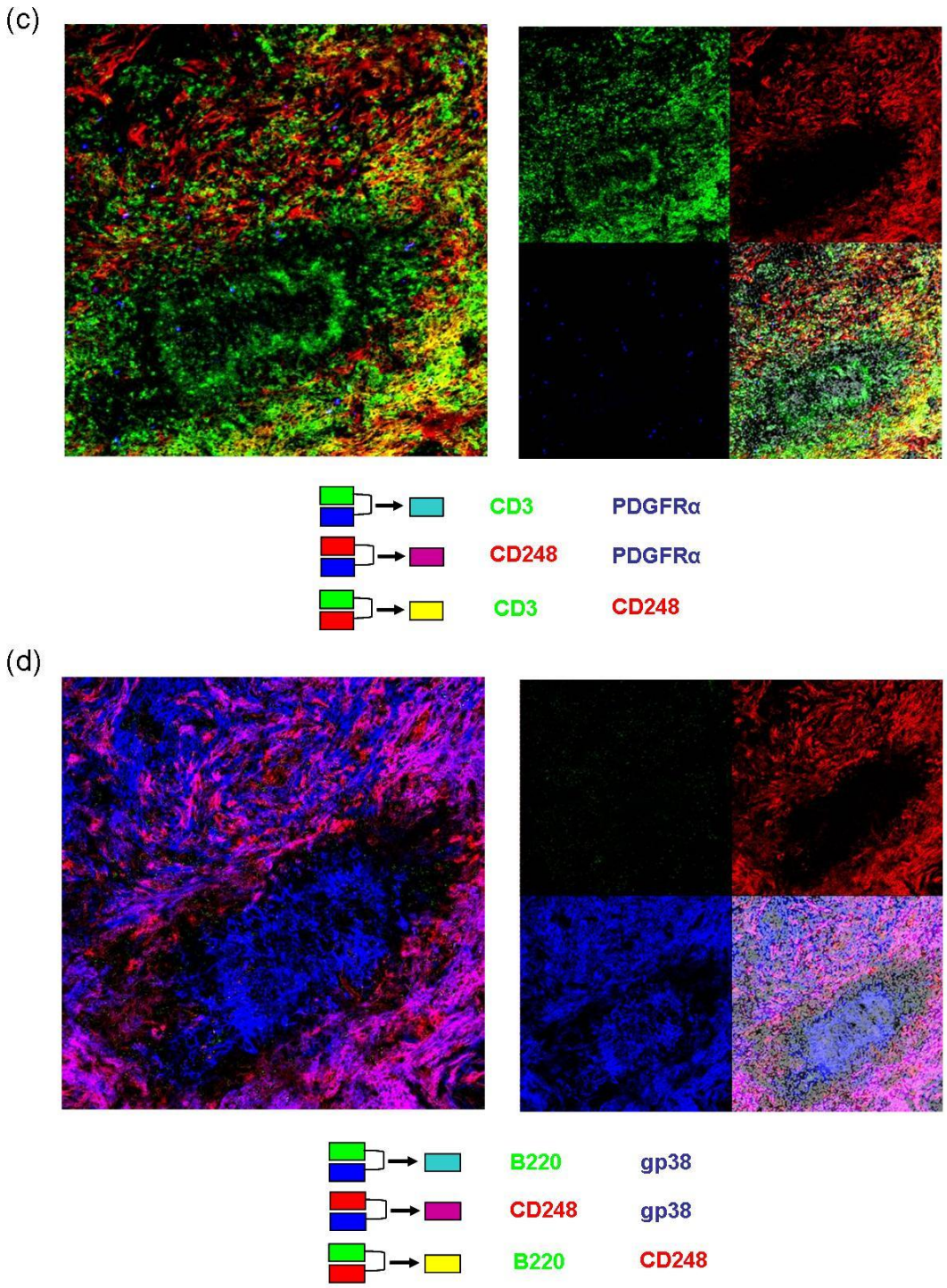

Figure 5.4 Content and structure of a grafted liver stromal cell reaggregate
A reaggregate was formed from 100,000 CD45 negative liver stromal cells and grafted under the kidney capsule for four weeks. The graft was then fixed, frozen, sectioned and co-stained as above with cell nuclei in grey (a-d). Images taken at x40 (n=1).

(a)

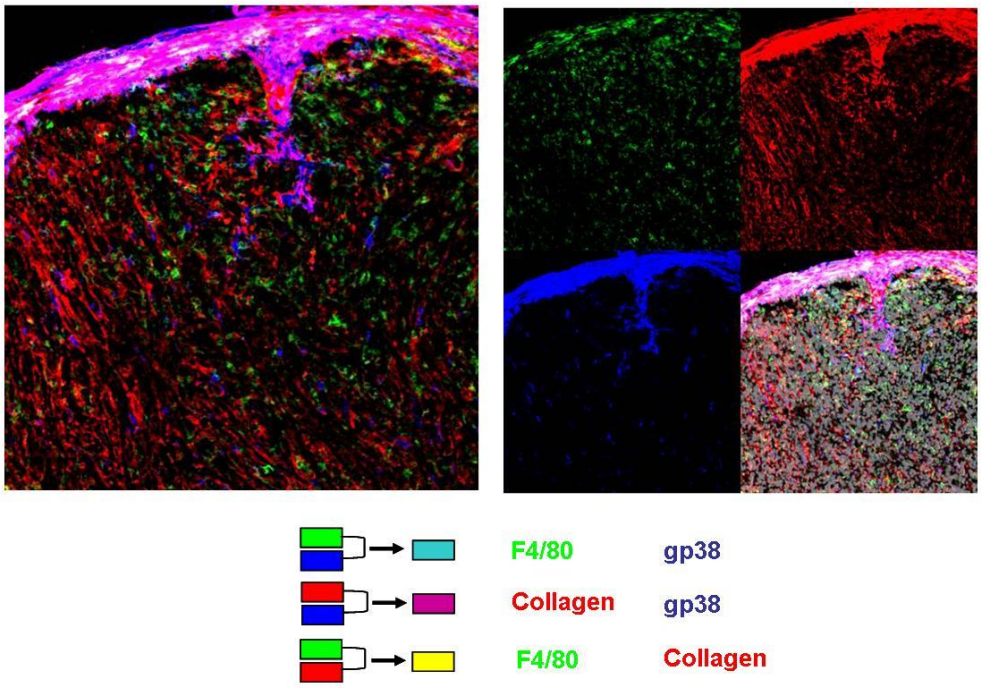
F4/80 gp38
Collagen gp38
F4/80 Collagen

(b)

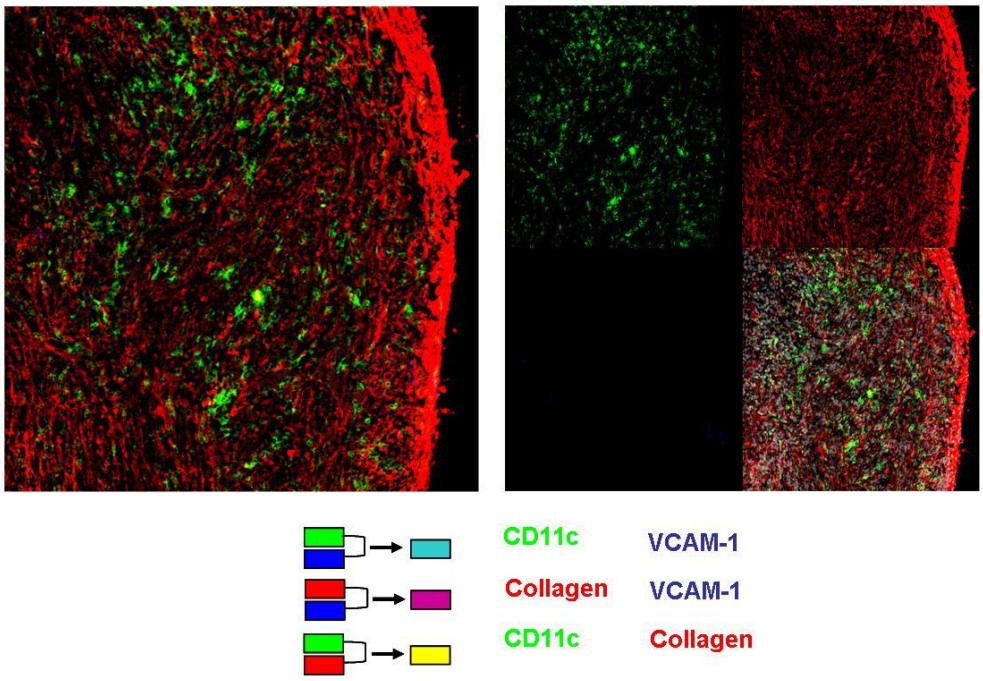
CD11c VCAM-1
Collagen VCAM-1
CD11c Collagen

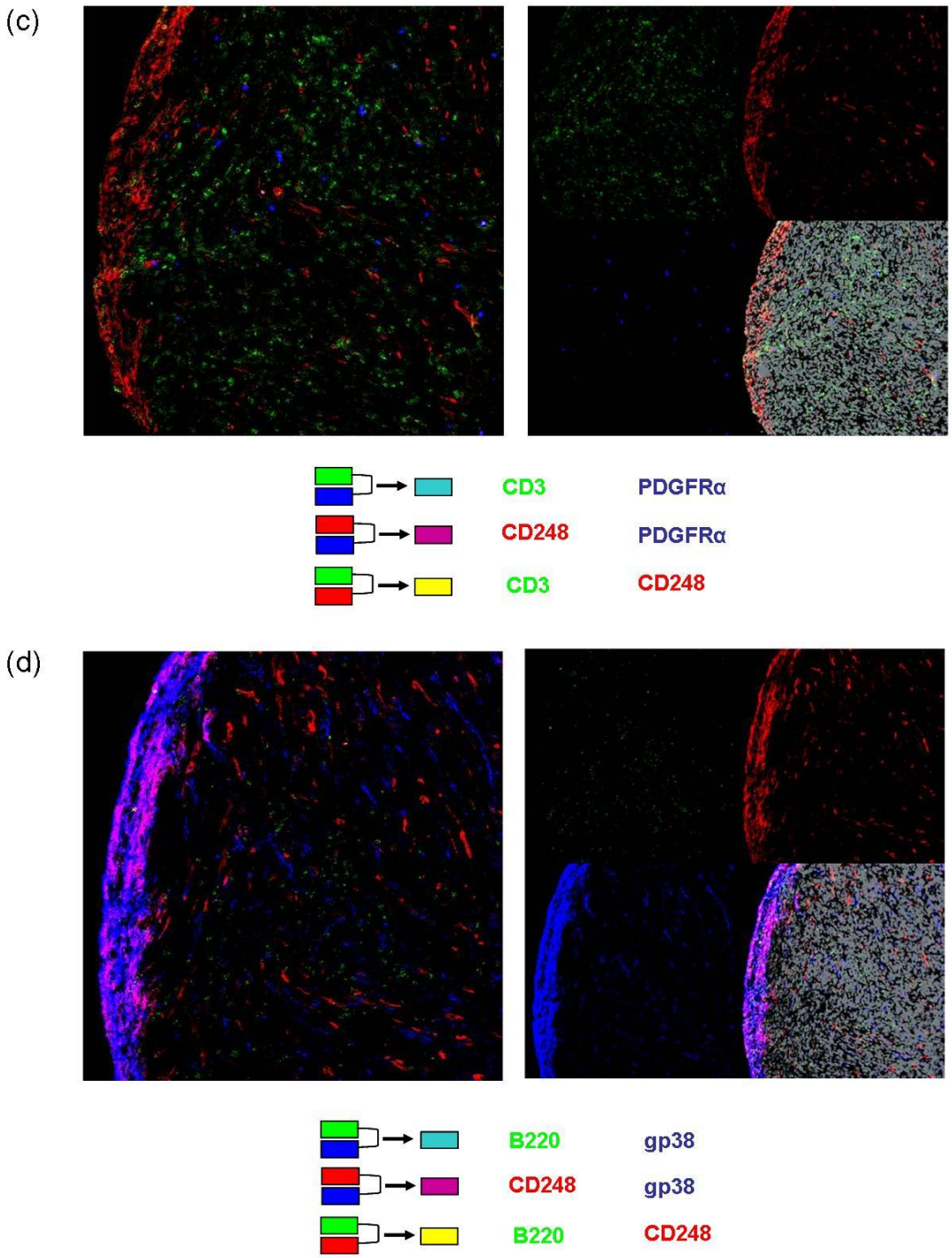

Figure 5.5 Content and structure of a grafted cervical stromal cell reaggregate
A reaggregate was formed from 100,000 CD45 negative cervical stromal cells and grafted under the kidney capsule for four weeks. The graft was then fixed, frozen, sectioned and co-stained as above with cell nuclei in grey (a-d). Images taken at x40 (n=1).

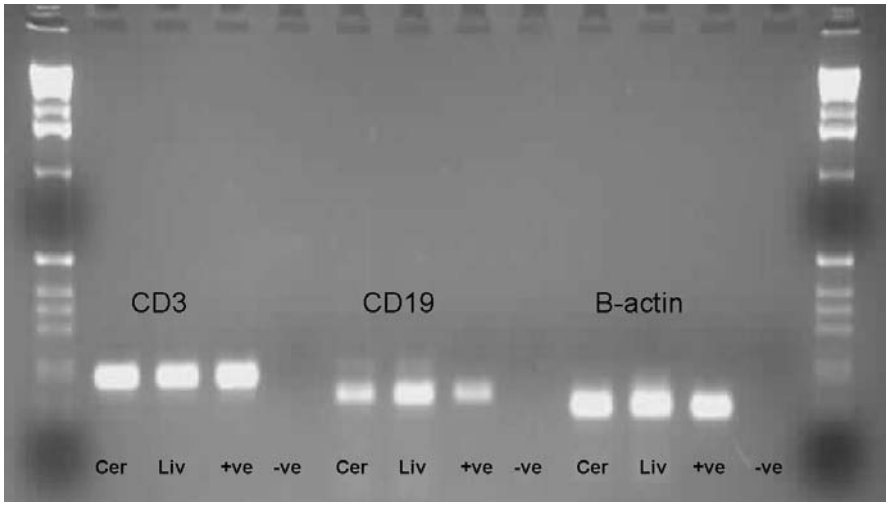

Figure 5.6 End point PCR from recovered kidney capsule grafts
A reaggregate was formed from 100,000 CD45 negative stromal cells and grafted under the kidney capsule for four weeks. The graft was then fixed, frozen, sectioned. Total RNA was extracted from five 5µm sections and end point PCR performed. Cer = stromal cells derived from the cervical lymph node, Liv = stromal cells derived from the liver, +ve = positive control and –ve = negative control (n=1).

5.2.2 Development of the kidney capsule transfer model

Having observed the clear survival and expansion of liver and cervical lymph node stromal cell reaggregates in the pilot study, the technique was then repeated with the remaining stromal cell cultures. As initial surgeries were completed in male and female mice successfully, the sex of the host mice was not thought to be an issue and subsequent surgeries were carried out using mostly male mice due to the ease of access to the kidney without the presence of ovaries. However, the successful growth of the other stromal cell culture reaggregates was not observed, nor could the successful liver and cervical lymph node stromal cell grafts be repeated, with no reaggregates present four weeks after grafting. To determine why the kidney capsule of stromal cells alone could not be repeated the quality of the reaggregate was first assessed. Reaggregates were made from all stromal cell cultures and instead of grafting under the kidney capsule were sectioned, fixed and immunofluoresently stained for early apoptosis marker active-caspase 3, to assess cell death within the reaggregates (figure 5.7). Very little or no active-caspase 3 staining was observed in reaggregates from all stromal cell lines. The lack of grafting success therefore, does not seem to be due to the increased cell death in the reaggregate. As well as active-caspase 3, the reaggregate sections were co-stained with gp38 and VCAM-1. High gp38 expression was also present in all reaggregates; however VCAM-1 expression was not consistent. Expression of VCAM-1 was highest in spleen and inguinal lymph node reaggregates with little or no expression observed in the thymus, liver, skin, lung and axillary and cervical lymph node stromal reaggregates.

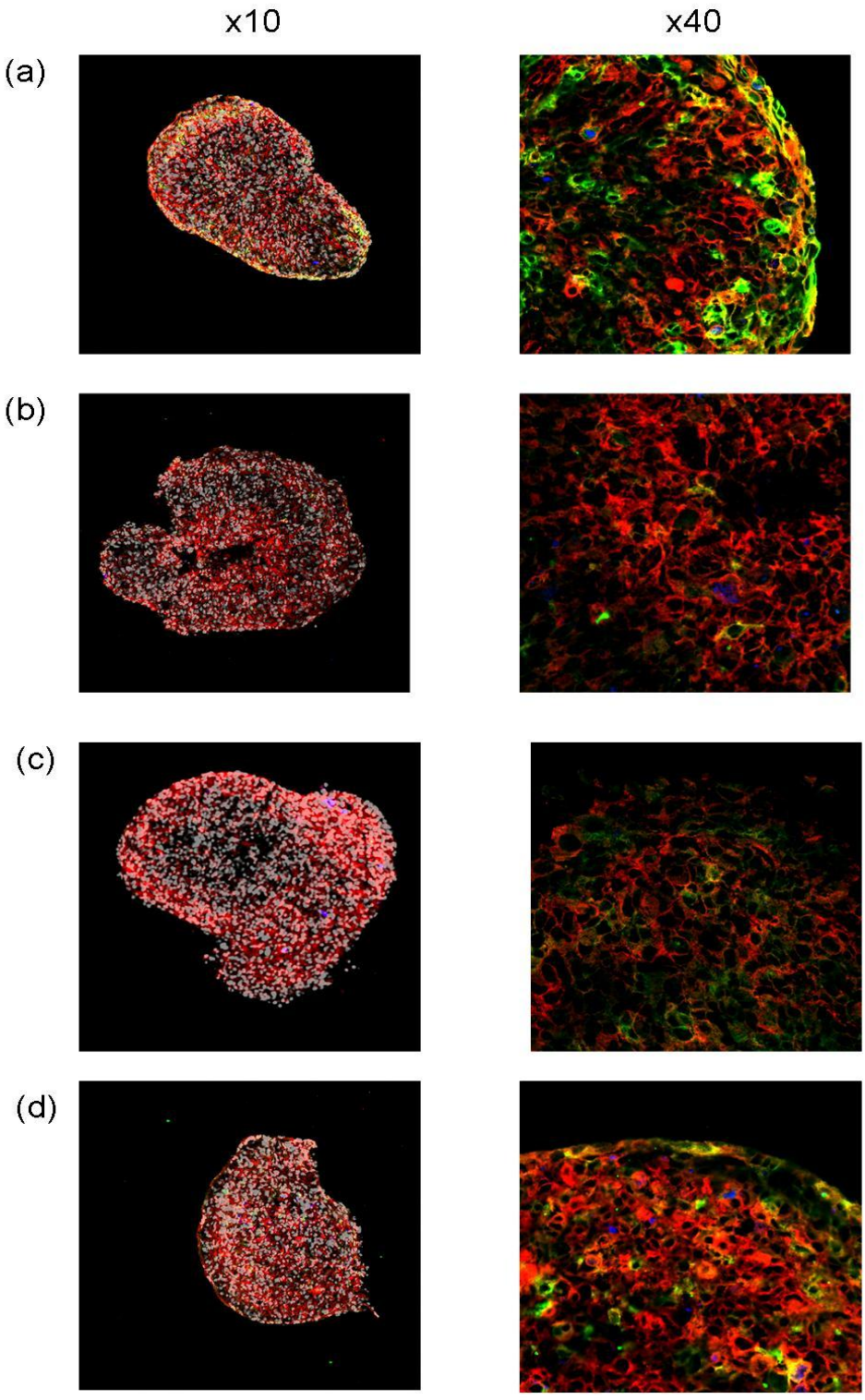
x10
x40
(a)
(b)
(c)
(d)

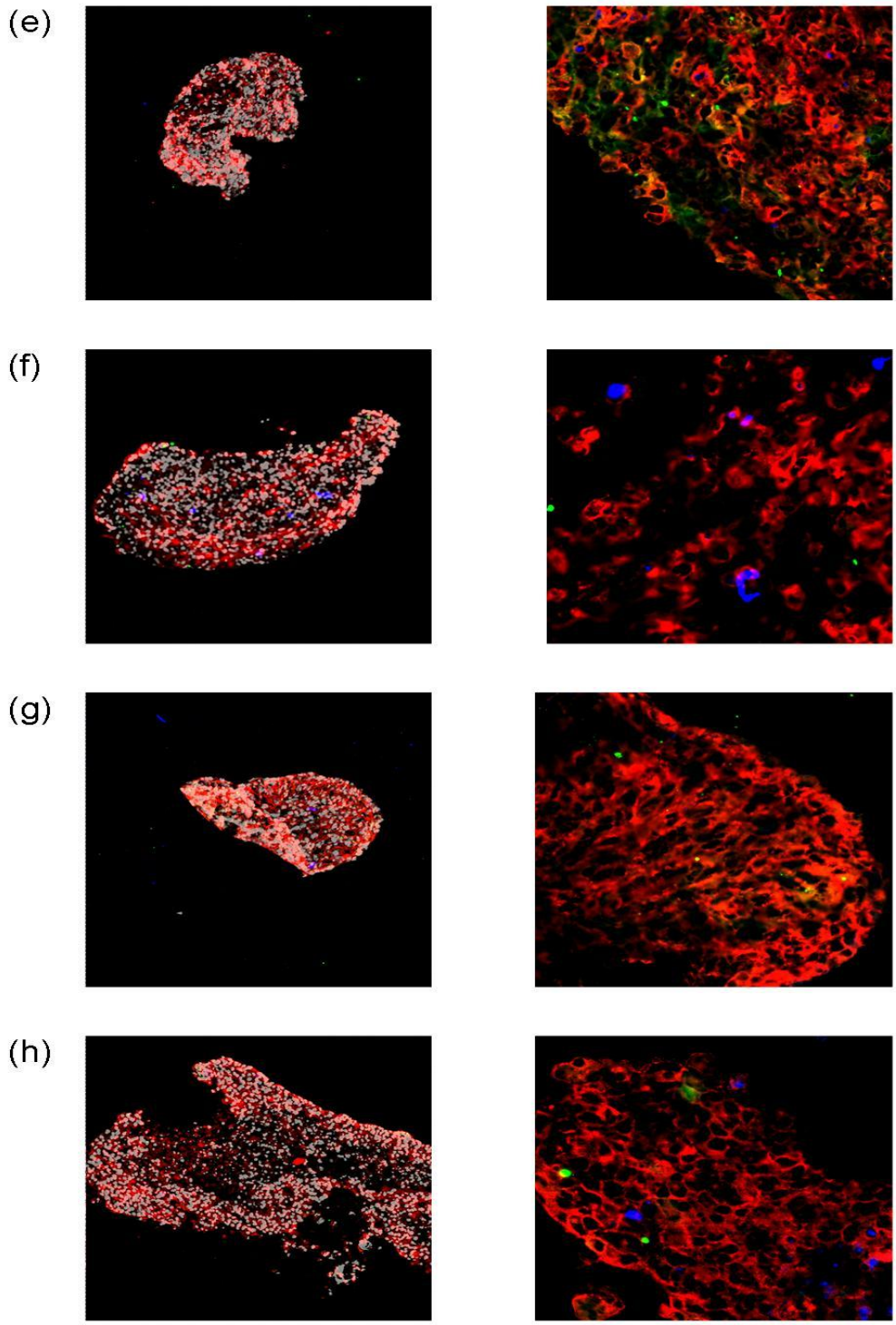

Figure 5.7 Structure and viability of stromal cell reaggregates
Reaggregates formed from 100,000 stromal cells derived from the (a) spleen, (b) thymus, (c) liver, (d) inguinal lymph node, (e) axillary lymph node, (f) cervical lymph node, (g) lung and (h) skin, were snap frozen, sectioned, fixed and stained using immunofluorescence. Red = gp38, blue = active caspase-3, green = VCAM-1, yellow = co-localisation of VCAM-1 and gp38 and grey = cell nuclei. Images taken at x10, left panel and x40 without nuclei staining, right panel (images representative of two independent reaggregates).

Studies have suggested that expression of VCAM-1 is low under baseline conditions (24), which is in agreement with the expression levels seen in the reaggregates and cultured cells by immunofluorescence (section 3.2.2.3). VCAM-1 mediates leucocyte-endothelial cell adhesion and signal transduction (226) and so may be important in attracting/retaining host cells within the graft. It has already been shown that treatment of the stromal cell cultures with LTα increases VCAM-1 expression in all stromal cell lines except the skin (section 4.2.1). Therefore, splenic stromal cell reaggregates were treated with LTα to determine if this would increase VCAM-1 expression within the reaggregate and thus the success of grafting. Treatment with LTα showed a dose dependent increase in VCAM-1 expression in the splenic stromal cell reaggregate (figure 5.8). The grafted LTα treated CD45 negative splenic stromal cells have maintained their phenotype from the *in vitro* culture (section 3.2.2.2); high CD248 and gp38 expression was observed (figure 5.9). Very low PDGFRα staining was seen indicating little or no vascularisation of the graft. The protein expression of F4/80, CD11c, CD3 and small population of B220 positive cells, suggests recruitment of host macrophages, dendritic cells, T cells and a small number of host B cells. The protein expression within the graft was similar to that seen in the untreated stromal cell grafts in terms of recruitment of host cells (section 5.2.1) conversely, no outer capsule formation or T zone organisation was seen. However, as with the grafting of untreated stromal cell reaggreagtes, this could not be repeated successfully when grafts of all other LTα-treated stromal cell cultures were attempted and no reaggregates were present seven days after grafting.

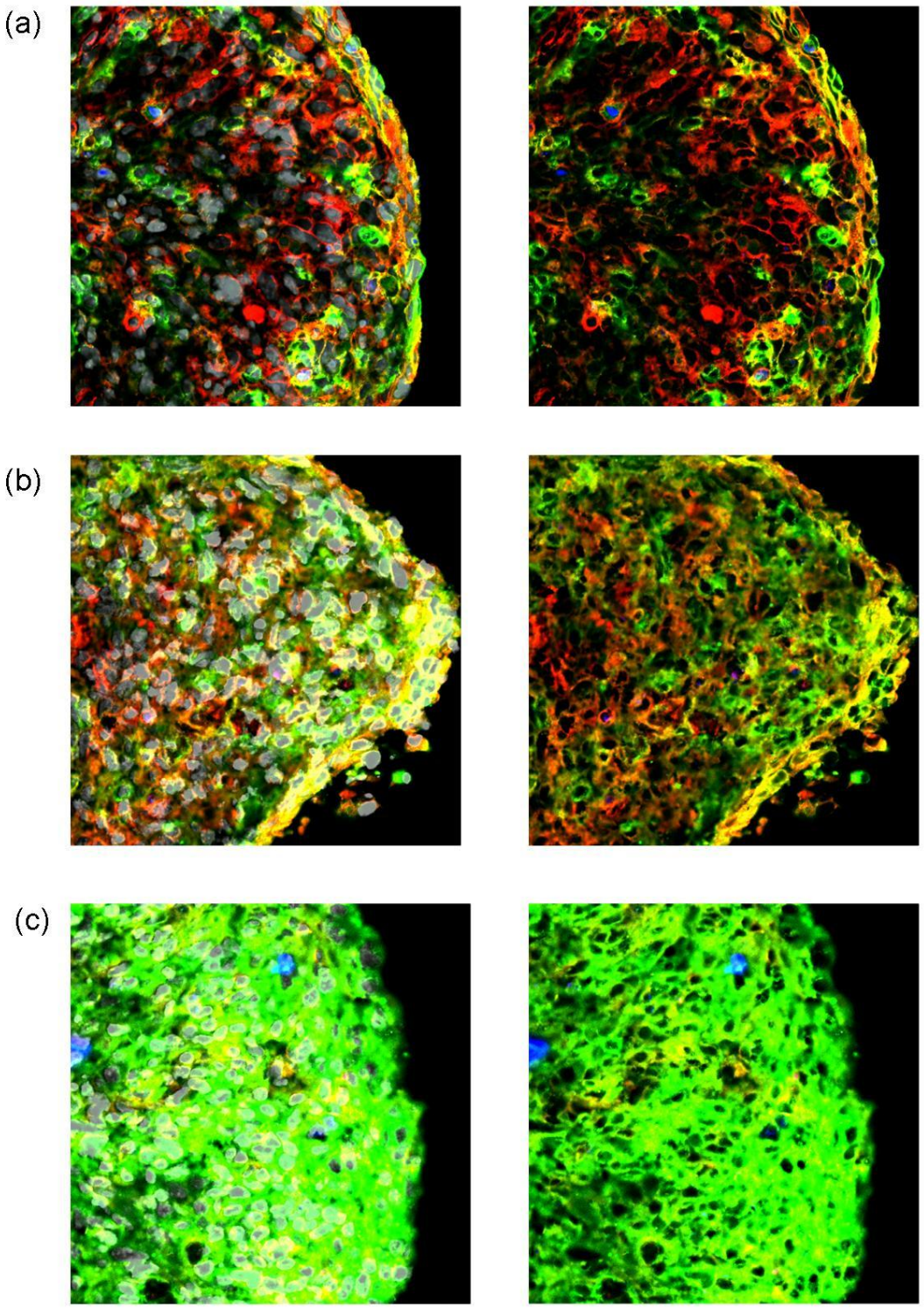

Figure 5.8 Lymphotoxin α treated splenic stromal cell reaggregates
Reaggreagtes formed from 100,000 splenic stromal cells were treated with LTα for 24 hours, (a) untreated, (b) 1µg/ml and (c) 2µg/ml, after which they were snap frozen, sectioned, fixed and stained using immunofluorescence. Red = gp38, blue = caspase-3, green = VCAM-1, yellow = co-localisation of VCAM-1 and gp38 and grey = cell nuclei. Images taken at x40 (images representative of two independent reaggregates).

(a)

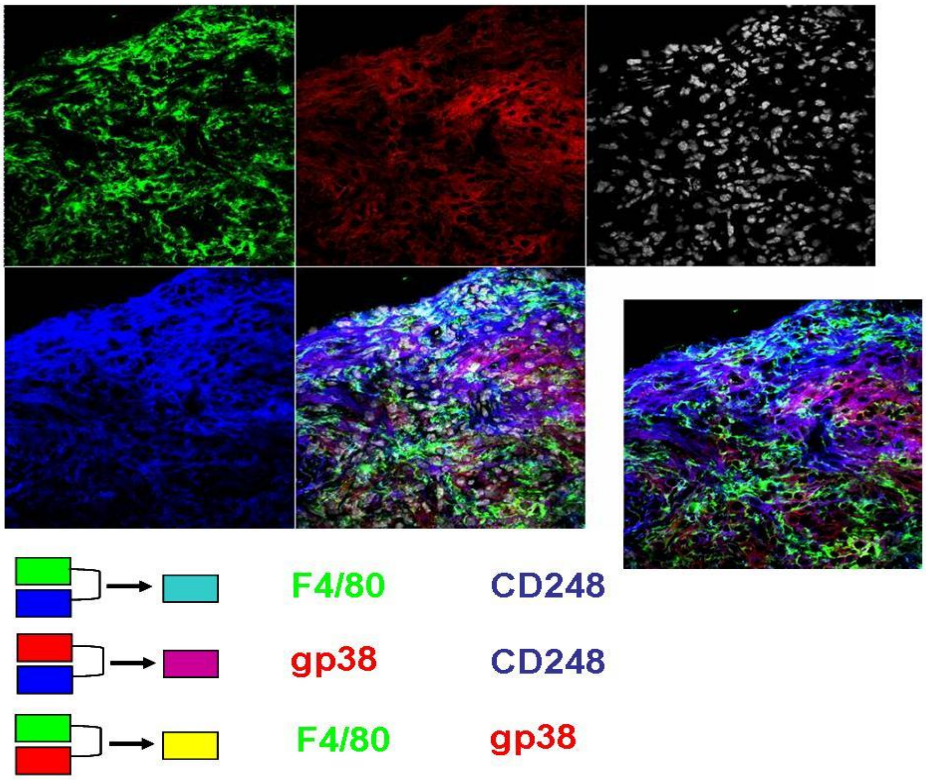
F4/80 CD248
gp38 CD248
F4/80 gp38

(b)

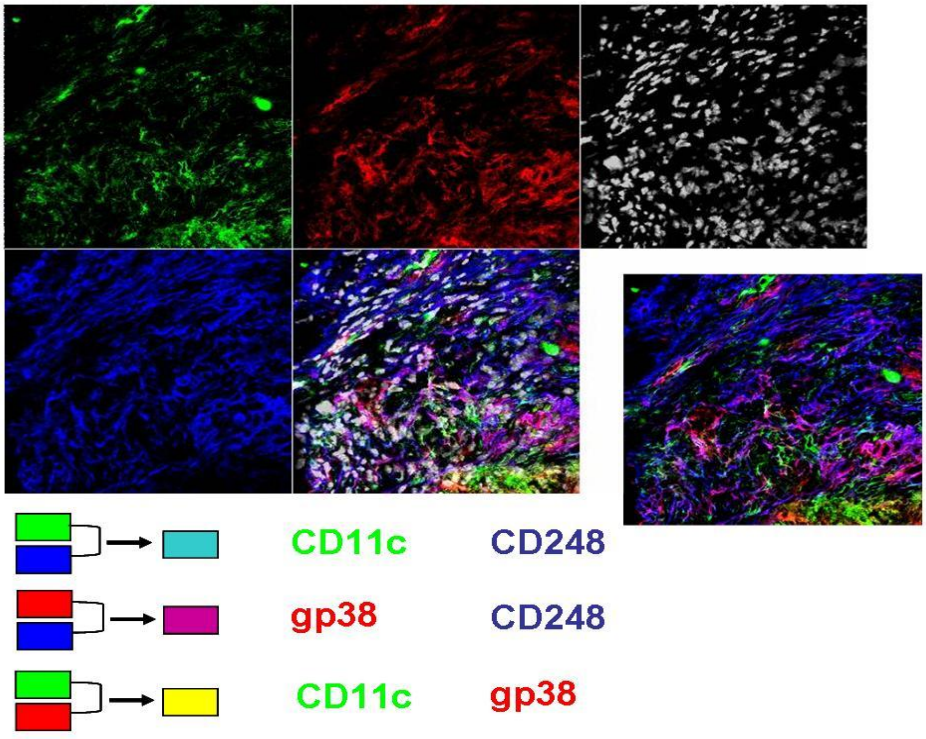
CD11c CD248
gp38 CD248
CD11c gp38

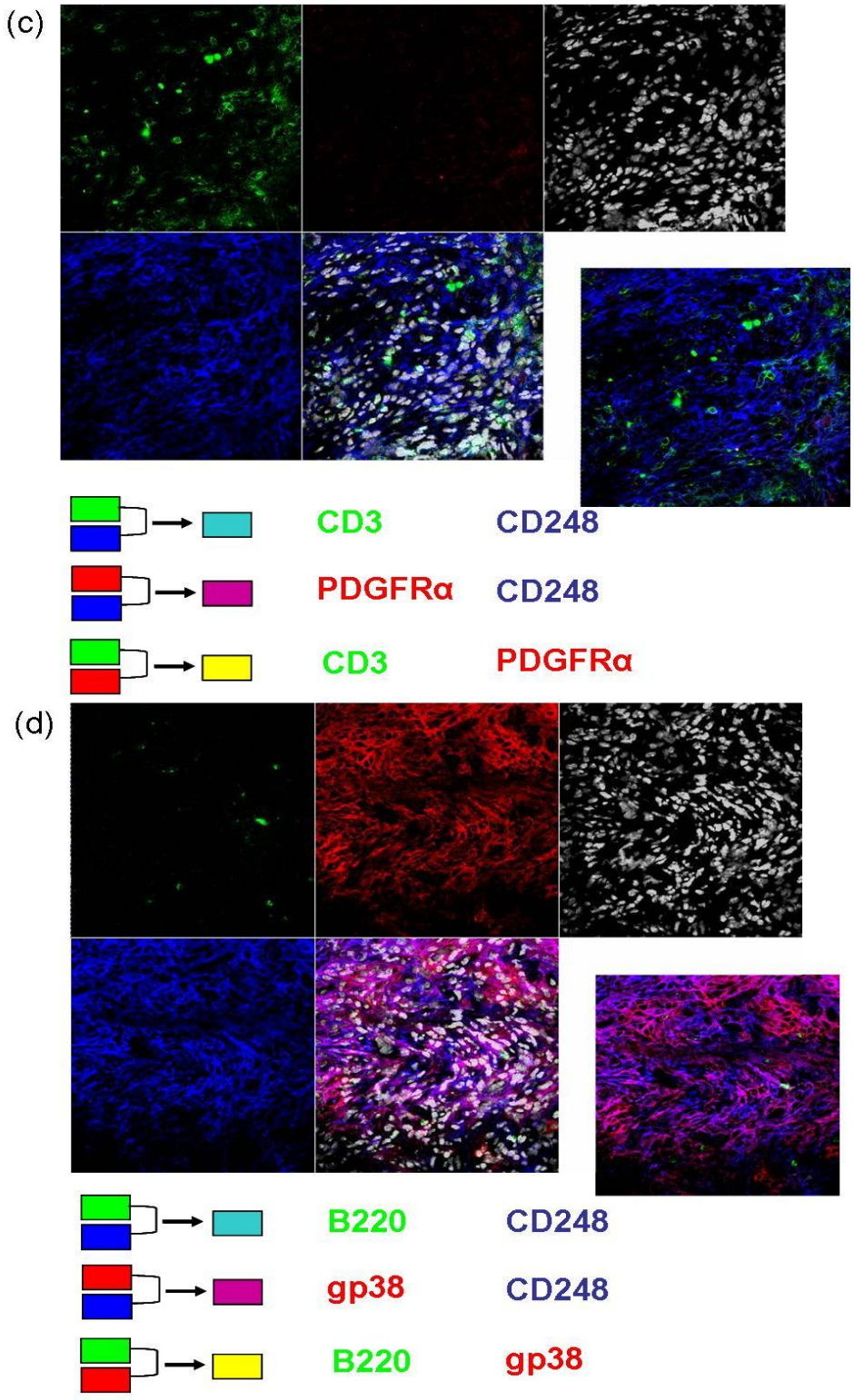

Figure 5.9 Seven day grafted, LTα treated splenic stromal cell reaggregate
A reaggregate formed from 100,000 CD45 negative splenic stromal cells was treated with 1µg/ml LTα for 24 hours and grafted under the kidney capsule for seven days. The graft was then snap frozen, sectioned, fixed and co-stained as above (a-d) with cell nuclei in grey. Images taken at x40 (n=1).

5.2.3 Kidney capsule transfer using gelatine sponge supported stromal cells

Having observed that stromal cells alone and LTα treated stromal cells had failed to give consistent results in kidney capsule transfer, addition of physical support was tried. Seemayer *et al*, 2003 and Suematsu *et al*, 2004 have previously reported successful use of a 3D-sponge to provide structure for stromal cells within kidney capsule surgery (69,227). Therefore, the *in vitro* cultured splenic stromal cells were suspended in a gelatine sponge, instead of forming a reaggregate, prior to surgery. Kidney capsule transfer was then completed using stromal cells present within a collagen sponge. Encouragingly, after 7 and 14 days the sponges remained present under the kidney capsule, although they did not appear to have increased in size. The grafts were removed, cryosectioned, fixed and stained using immunofluorescence for donor stromal cell marker expression, such as gp38 and CD248, and infiltrating host cells, such as macrophage (F4/80), dendritic cells (CD11c), B cells (B220) and T cells (CD3). The morphology observed after grafting for 7 days was different to that of the stromal cells alone, spaces could be seen without cells, presumably where the sponge was present (figure 5.10). However cells were retained in the sponge and expression of gp38 and CD248 were high confirming stromal cell presence. There was also evidence of recruitment of host cells, with CD11c and F4/80 expression found. However in contrast to the pilot and LTα treated grafts, no CD3 or B220 positive staining was observed, suggesting that no T or B cell recruitment had occurred. Although this was on day seven, therefore it may occur at a later time point as the pilot grafts were at week four. The protein expression seen after 7 days was the comparable with that after 14 days under the kidney capsule, with an increase in F4/80 expression observed, indicating further macrophage recruitment (figure 5.11). Using the collagen sponge as structure for the stromal cells under the kidney capsule

provided more consistent results with successful repeats of both seven and fourteen day grafts.

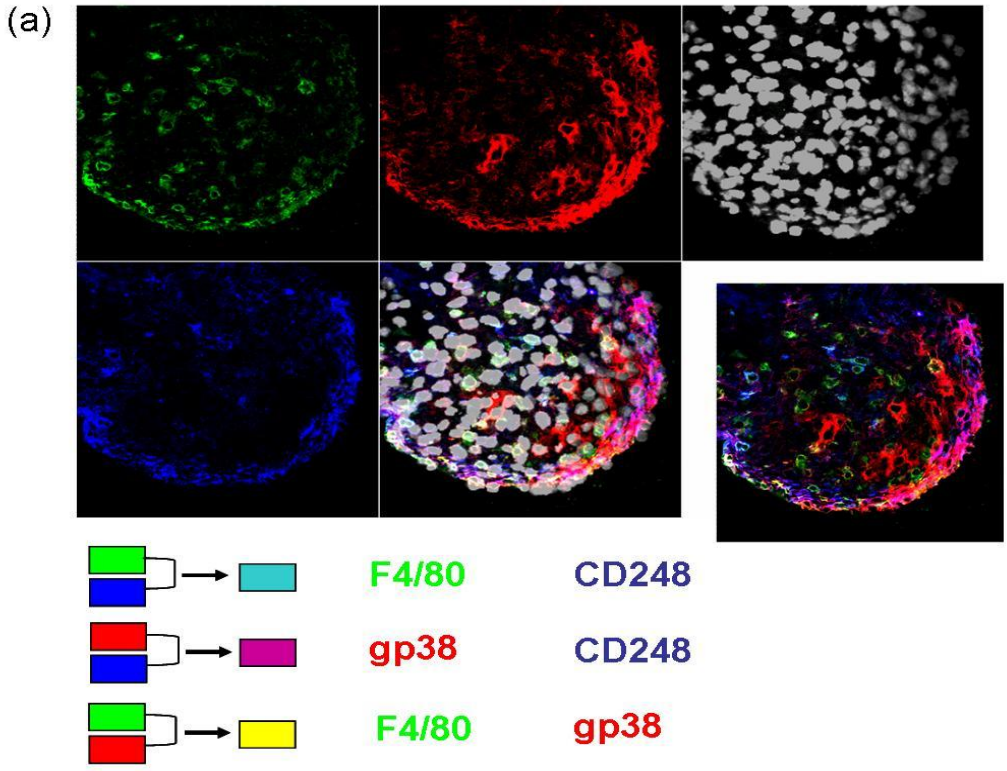
(a)
F4/80
CD248
gp38
CD248
F4/80
gp38

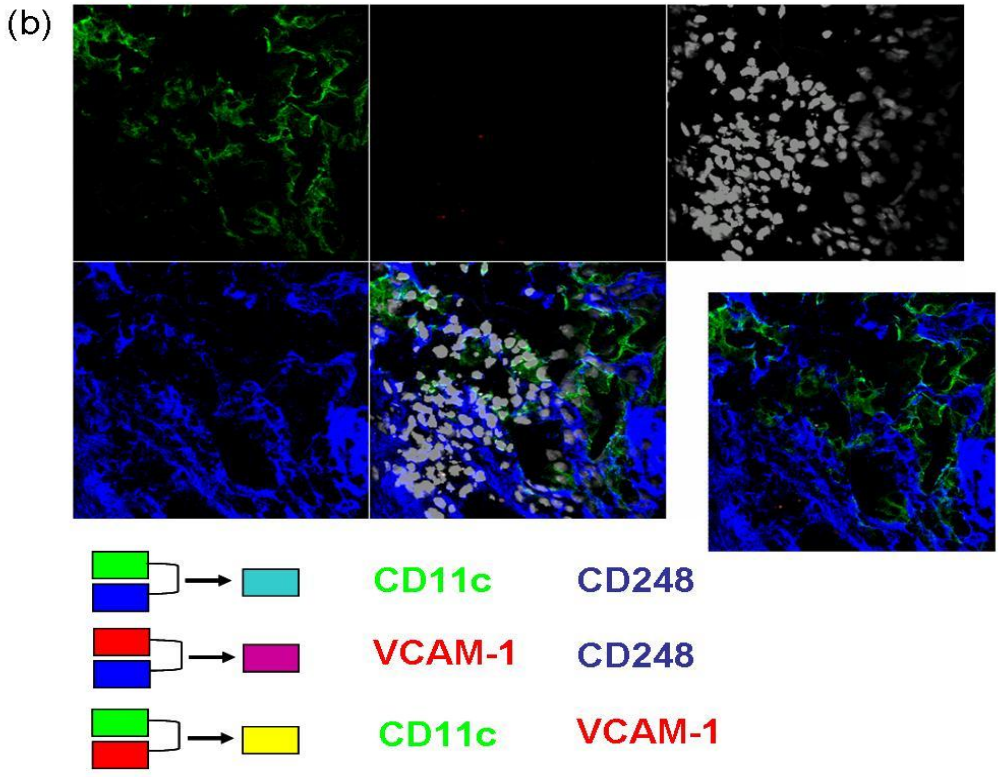
(b)
CD11c
CD248
VCAM-1
CD248
CD11c
VCAM-1

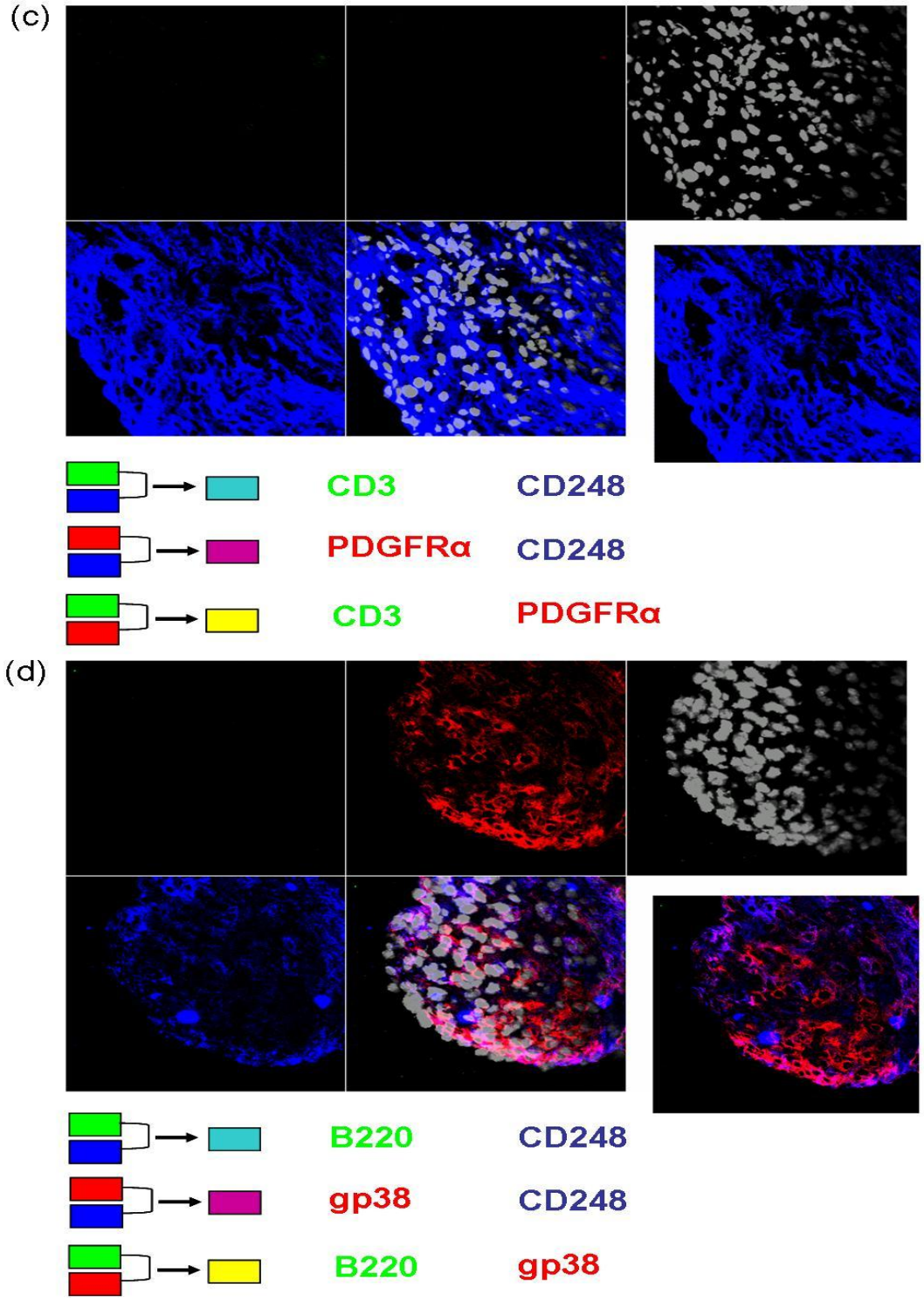

Figure 5.10 Seven day grafted, splenic stromal cells suspended in a gelatine sponge

A gelatine sponge (2-3mm^3) was placed in 50µl complete fibroblast media with 100,000 CD45 negative splenic stromal cells for 2 hours prior to surgery, after which it was grafted under the kidney capsule for seven days. The graft was then fixed, frozen, sectioned and co-stained as above (a-d) with cell nuclei in grey. Images taken at x40 (n=2).

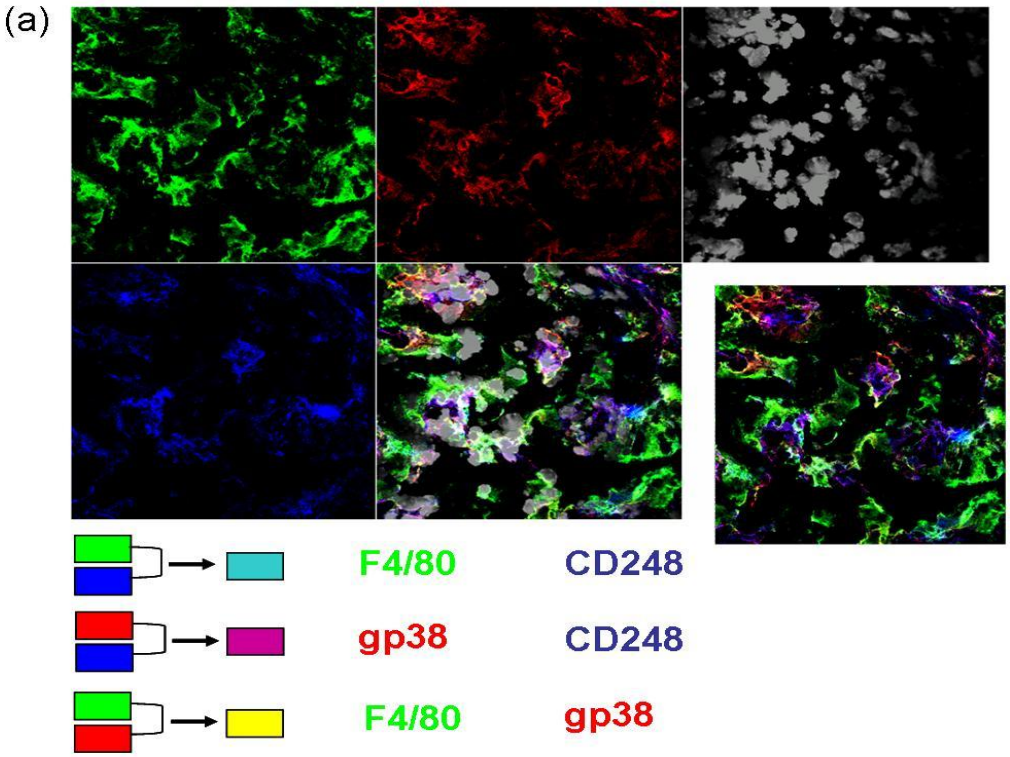
(a)
F4/80
CD248
gp38
CD248
F4/80
gp38

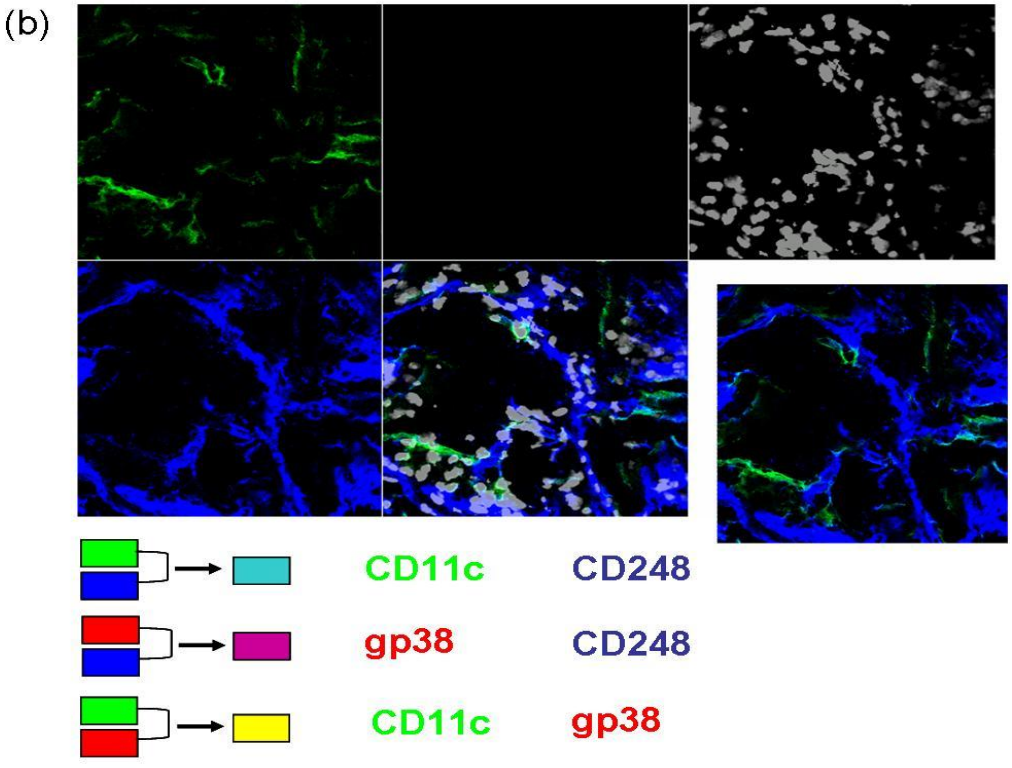
(b)
CD11c
CD248
gp38
CD248
CD11c
gp38

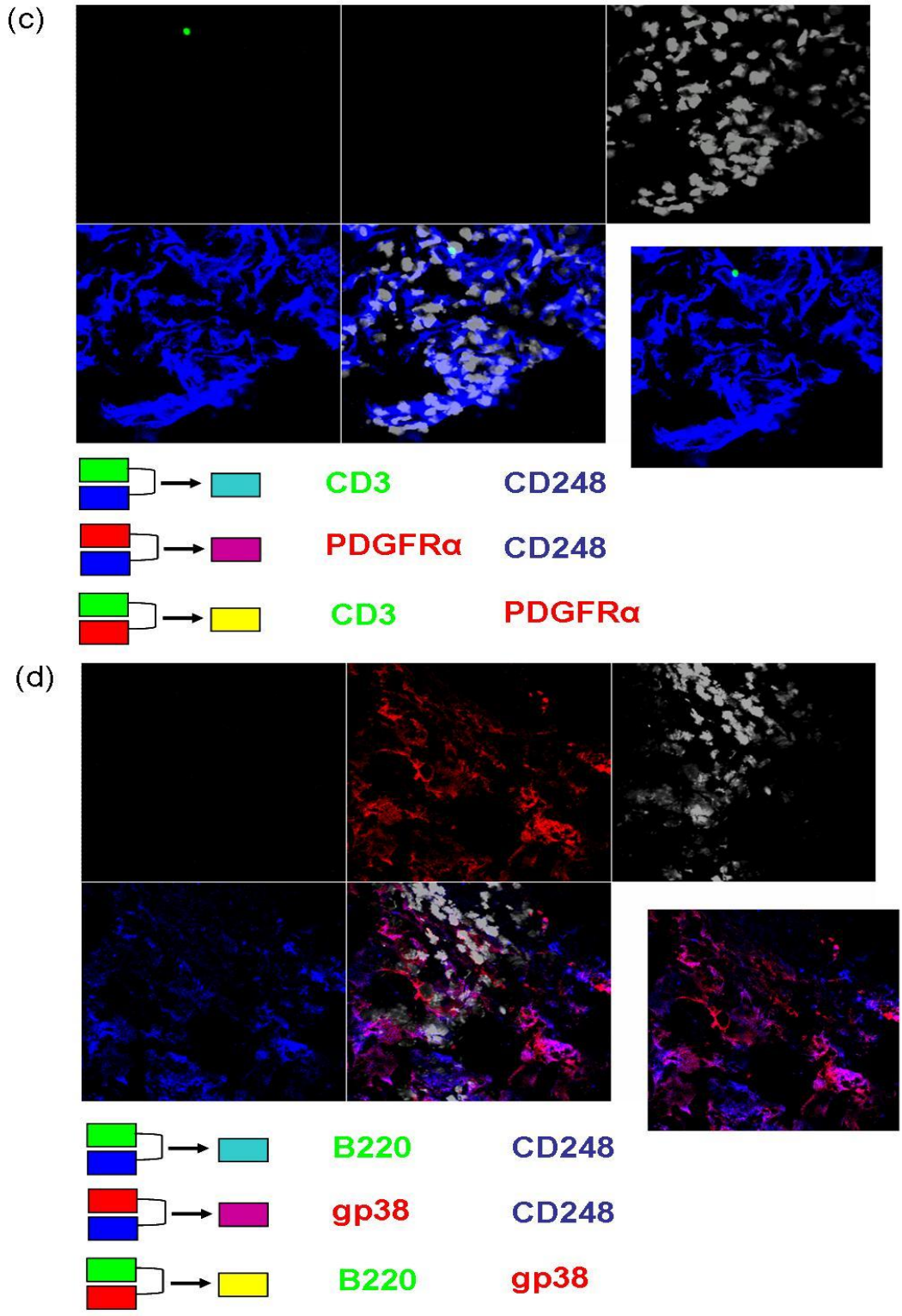

Figure 5.11 Fourteen day grafted, splenic stromal cells suspended in a gelatine sponge

A gelatine sponge (2-3mm^3) was placed in 50µl complete fibroblast media with 100,000 CD45 negative splenic stromal cells for 2 hours prior to surgery, after which it was grafted under the kidney capsule for fourteen days. The graft was then fixed, frozen, sectioned and co-stained as above (a-d) with cell nuclei in grey. Images taken at x40 (n=2).

5.3 Discussion

Gene and protein data suggested that not only are adult CD45 negative stromal cells cultured from peripheral and lymphoid organs different but also that lymph node cultures had different profiles when compared to other lymphoid organs tested (chapter 3). These differences were also upheld when *in vitro* functional studies were performed (chapter 4). Moreover, these data highlighted that the stromal cell cultures maybe similar to the FRCs due to their ability to differentially keep CD3 positive cells alive (section 4.2.2). Therefore, the kidney capsule transfer model was utilised to examine whether these stromal cells, *in vivo*, were able to survive, organise and recruit host leucocytes, differentially depending on these differences observed.

An initial pilot study demonstrated that it was possible to form reaggregates from the CD45 negative stromal cells using the V-well plate method, which grew successfully when grafted under the kidney capsule. This study suggested that these grafts were able to recruit host dendritic cells, macrophages, T and B cells into the reaggregate. It was also indicated that there may be differences between the stromal cells used with the liver stromal cell reaggregate organising the T cells into areas where there was low expression of CD248 or collagen type I. Interestingly, these T cell areas had a high expression of gp38, which is thought to be expressed on T zone stromal cells (72). In contrast, the cervical stromal cell graft was quite different; there was little evidence of any host cell organisation but CD248, gp38 and collagen type I expressing stromal cells formed a capsule-like structure around the edges of the graft. Protein expression within the capsule agrees with that seen previously by Lax *et al* (2007) where CD248 expression was observed in the lymph node caspsule (140) and also by Katakai *et al* (2004) where gp38 expression was seen the lymph node capsule

(71). However, the data could not be repeated nor was it successful with the remaining stromal cell lines. Therefore, the quality of the stromal cell reaggregates was assessed by active-caspase 3 expression, which confirmed that the reaggregates did not contain many apoptotic cells. To further ensure the quality of the grafts, the quantity of necrotic cells could also be assessed using haematoxylin and eosin staining. VCAM-1 expression in these reaggregates was low and as VCAM-1 is thought to be important in the interaction between stromal cells and lymphocytes (226), it was reasoned that increasing VCAM-1 expression could make a more successful reaggregate. LTα treatment has been shown to increase VCAM-1 expression in cultured stromal cells, therefore the reaggreagates were treated with LTα (1μg/ml) for 24 hours. The preliminary LTα treated splenic stromal cell reaggregate was successful and after seven days had recruited host macrophage, dendritic cells, T and B cells, although less stromal organisation was appreciated compared to the pilot grafts. However, when repeated again, as with untreated LTα stromal cells, the grafts were unsuccessful. A technique used by Seemayer *et al* (2003) is to use a 3D-sponge as structure for the implanted cells (227). Cells are trypsinised and added onto the sponge, which is then co-implanted with pieces of human cartilage under the renal capsule of SCID mice to analyse the invasion of the cartilage by fibroblasts. Therefore, this technique was adopted for use with the stromal cells. Importantly, the kidney capsule grafting using the gelatine sponge structural support were successful with grafts analysed after seven and fourteen days post implantation. The data from these grafts showed consistent growth and survival, with expression of stromal cell markers CD248 and gp38 but not VCAM-1. Host macrophage and dendritic cells but no T or B cells were recruited unlike unsupported

grafts. T and B cell entry may occur after fourteen days as the pilot grafts were incubated for four weeks.

In conclusion, data in this chapter provides a method for analysing the function of cultured stromal cells *in vivo*. This involves using a gelatine sponge as structural support for the implanted stromal cells. Using this technique, adult splenic stromal cells for the first time have been shown to form a structure which is able to recruit and support host CD11c and F4/80 positive leucocytes. It will be interesting in the future to repeat with all cultured stromal cells and look for possible differences between peripheral and lymphoid sites in the recruitment of leucocytes.

Chapter Six

General Discussion

CHAPTER SIX

General Discussion

Stroma is an important structural component of vertebrate animals. It consists of extracellular matrix (ECM), mesenchymal cells and a scaffold consisting of nerves and blood and lymphatic vessels (119). The most abundant cell type of tissue stroma is the fibroblast (120). In recent years it has become clear that fibroblasts play not only an active role in defining the structure of tissue microenvironments but also modulating immune cell behaviour by conditioning the local cellular content and cytokine production, specifically tailoring the response to the cause of the damage (113). Fibroblast gene expression in humans has been studied by many groups (119,136,150,151,228). It has become apparent that there is considerable positional memory and topographic differentiation as defined by their gene expression profiles. Interestingly, a set of 337 human fibroblast genes has been found which varies according to three anatomical divisions: anterior-posterior, proximal-distal and dermal-nondermal. These genes were involved in pattern formation, cell-cell signalling and matrix remodelling (151). It is therefore reasonable to hypothesise that this may also be the case among mouse fibroblasts, in particular for this study within the murine lymphoid organs. In addition, given the degree of homology between many human and murine genes, it could be possible that the site defining genes found in the human are also important in the mouse.

In this thesis, stromal cells from different lymphoid and peripheral sites were cultured and characterised in terms of morphology, protein expression and gene expression to define site specific profiles within the populations. In addition, following phenotypic

and genotypic analysis functional differences between the cultured stromal cells were investigated. These analyses confirmed the diversity of morphology, gene and protein expression between the cultured stromal cells. Furthermore, preliminary functional assays also confirm that fibroblasts from different sites differ in their ability to not only to respond to lymphotoxin α (LTα) *in vitro*, but also form tissue reaggregates and recruit host leucocytes *in vivo*.

6.1 Fibroblast reticular cell phenotype

In this study a method of successfully culturing stromal cells and sorting these into a homogenous fibroblast population based on CD45 protein expression was developed. Fibroblast populations were defined by their ability to adhere to plastic, expression cell surface proteins (CD248, VCAM-1 and gp38) and gene expression (CCL19, CCL21, CD248, VCAM-1, ICAM-1, gp38, CXCL12 and LTβR) with a lack of expression of other cell lineage markers. Previous studies have described a stromal cell type called a fibroblast reticular cell (FRC) from the T zones of lymph nodes. These cells highly express gp38, PDGFRα, LTβR and VCAM-1 amongst others and were also found to be a major source of IL-7 (67,71). This phenotype is very similar to the cultured stromal cells described in chapter three. Importantly a consistent finding was that the lymph node stromal cells had differential gene expression of CD31 and Lyve-1 when compared to the stromal cells from other sites, which may suggest a lymphatic endothelial population from the lymph nodes. In addition to the FRC cell type, a gp38, CD31, Lyve-1, VCAM-1 and LTβR positive population was also described (67), termed lymphatic endothelial cells (LECs), which closely matches that seen in the lymph node stromal cell populations. Therefore, these data indicate that two different populations are being isolated from the different sites using

the same method. More recently, a stromal cell population, termed marginal reticular cells (MRCs) was found in the outer follicular region immediately underneath the subcapsular sinus of lymph nodes in adult mice. These cells expressed VCAM-1, ICAM-1, MadCAM-1, CXCL13, TRANCE, BP-3 and gp38 and have been described as specialised reticular fibroblasts (69). The stromal cells in this study express little or no CXCL13 but given the similarity in gene expression to the MRCs, it is possible that they are present in the stromal cell cultures. In chapter four, *in vitro* functional studies showed that all cultured stromal cells increased the survival of T cells more so than B cells in a co-culture system. Preliminary results from the *in vivo* kidney caspsule transfer pilot studies in chapter five also showed a preferential recruitment of T cells to B cells into the stromal cell grafts. Taken together, these data indicate that the cultured lymphoid stromal cells in this study are comparable to FRCs. As FRCs are found in the T zones of secondary lymphoid organs, the FRC-like cells derived from non-lymphoid sites may have the potential to form tertiary lymphoid structures should the correct conditions arise, for example chronic inflammation.

6.2 Fibroblast heterogeneity exists between murine lymphoid organs

Primary adult human fibroblasts have been shown to retain many features of the embryonic pattern of the expression of HOX genes (119,151). It is thought that the expression of these genes may dictate positional identity. The stability of HOX gene expression was shown over 35 passages by Rinn *et al* in 2008. Gene expression patterns were assessed by culturing fibroblasts from one site in conditioned media from another and also culturing two sets of fibroblasts from different sites together. Neither of these altered the gene expression significantly and the fibroblasts were still able to be clustered site specifically based on their gene expression. However it was

reported that gene expression of cultured fibroblasts can be altered by treatment with a histone deacetylase inhibitor. These results are consistent with earlier findings that site specific HOX expression is epigenetically maintained by chromatin modifications in fibroblasts (152,229). Stability was also observed in the cultured murine stromal cell cultures in this study with regard to their protein and gene expression over many passages. A gene signature from CD45 negative stromal cells was determined using whole genome microarrays, which was able to differentiate lymphoid tissue stromal cells from peripheral tissue stromal cells. However, this could not differentiate between stromal cells from different lymphoid tissues. Further studies using low density arrays (LDAs) containing genes found to be important in grouping human fibroblasts indicated that Hoxd8, Grem2, Cdh1 and Mmp3 may differentiate between lymphoid tissue derived stromal cells, although protein expression has yet to be determined and requires further investigation. Functional data from *in vitro* LTα treatment in chapter four confirmed a definite difference between peripheral and lymphoid stromal cell cultures, where LTα was able to induce a significant increase in VCAM-1 protein expression in all stromal cell cultures but not in those derived from the skin. Differences were also seen within lymphoid stromal cell cultures as the lymph node cultures showed lesser response to LTα treatment in comparison to other sites. Pilot *in vivo* kidney capsule studies in chapter five demonstrated a difference in organisation of donor stromal cells and host recruited leucocytes between liver and cervical lymph node derived stromal cell grafts. These data illustrate that differences observed in gene and protein expression may also be relevant when considering function of stromal cells derived from different sites.

Previous work by this group has suggested a stromal area postcode regulates leucocyte survival, retention, proliferation and differentiation within lymphoid tissues. This thesis supports this hypothesis, with peripheral tissues, lymphoid tissues and lymph node stromal cells having distinct phenotypes and preliminary functional data showing differences in their response to LTα and in the recruitment and survival of leucocytes. Many inflammatory diseases have site specific manifestations, for example rheumatoid arthritis mainly in the synovium and psoriasis in the skin. Inappropriate expression of all or parts of the code may therefore play a key role in the instigation or continuance of disease and make stromal cells a therapeutic target. Specific medication targeting 'activation markers' of stromal cells could alter the phenotype of the cell to a more 'resting state', thereby modifying the function of the stromal cells as an anti-inflammatory therapy.

6.3 Future work leading from this study

The investigations within this thesis have examined the hypothesis of a stromal area postcode within murine lymphoid tissues. The genes found to be differentially expressed by the TNF LDA between the stromal cell cultures from different sites, require further investigation, such as completion of protein expression of these genes to confirm they are differentially expressed. Should these genes be able to differentiate between stromal cells from different sites it would be interesting to manipulate the genes involved. For example using a gene knock-in to induce expression or RNA interference to silence the gene, to analyse whether one particular stromal cell then becomes more phenotypically like another. To assess functionality, cultured stromal cells from different sites of eYFP expressing mice could be adoptively transferred to determine if they traffic back to their organ of origin, this

would be a key experiment to answer the question of the stability of regional identity. Combining these two experiments and altering the gene expression of the stromal cells before adoptive transfer would show whether it is possible to then change stromal cell function by modifying its phenotype and analysing the trafficking of that altered stromal cell.

The *in vitro* cultured stromal cell genotype was more similar to an immortalised stromal cell than an *ex vivo* sorted stromal cell, suggesting that *in vitro* culture affects the stromal cell gene expression. Although *ex vivo* stromal cell numbers are low, it would be interesting to sort stromal cells from different sites and compare their gene expression. Resting and inflamed tissue could also be compared to determine if regional identity is maintained in an inflammatory response.

The kidney capsule transfer model using the structural support of the gelatine sponge can be used to analyse *in vivo* recruitment and survival of host leucocytes from splenic stromal cell cultures. This model can now be used as an *in vivo* functional readout for the role of stromal cells and other cell types in the formation of lymphoid-like structures. Kidney capsule transfers for all stromal cell cultures should be completed to confirm the technique and look for differences in recruitment and survival of leucocytes. eYFP mice should next be used to confirm that the stromal cells found in the recovered grafts are from the donor cell cultures and the leucocytes found are host derived, as there is the possibility of host stromal cell invasion. This model could then be expanded, by creating reaggregates for grafting of stromal cells from different sites with lymphoid tissue inducer (LTi) cells from the same or other

sites to see if these can recruit leucocytes and organise them into classical T and B cell compartments.

Taken together these data emphasise the phenotypic and functional differences of stromal cells derived from peripheral tissues, lymphoid tissues and lymph nodes and consolidate stromal cells as more than just a structural component within organs.

Chapter Seven

Reference List

CHAPTER SEVEN

Reference List

1. Janeway, C. J., P. Travers, M. Walport, and M. J. Sholmchik. 2005. *Immunobiology*, 6 ed. Garland Science Publishing, New York.

2. Lawrence, T., D. A. Willoughby, and D. W. Gilroy. 2002. Anti-inflammatory lipid mediators and insights into the resolution of inflammation. *Nat. Rev. Immunol.* 2: 787-795.

3. Medzhitov, R., and C. Janeway, Jr. 2000. Innate immunity. *N. Engl. J. Med.* 343: 338-344.

4. Borregaard, N., and J. B. Cowland. 1997. Granules of the human neutrophilic polymorphonuclear leukocyte. *Blood* 89: 3503-3521.

5. Steinman, R. M. 2006. Linking innate to adaptive immunity through dendritic cells. *Novartis. Found. Symp.* 279: 101-109.

6. Alberts, B., A. Johnson, J. Lewis, M. Raff, K. Roberts, and P. Walter. 2002. *Molecular Biology of the cell*, 4 ed. Garland Science Publishing, New York.

7. Kemper, C., and J. P. Atkinson. 2007. T-cell regulation: with complements from innate immunity. *Nat. Rev. Immunol.* 7: 9-18.

8. Fujita, T. 2002. Evolution of the lectin-complement pathway and its role in innate immunity. *Nat. Rev. Immunol.* 2: 346-353.

9. Medzhitov, R. 2001. Toll-like receptors and innate immunity. *Nat. Rev. Immunol.* 1: 135-145.

10. Akira, S., K. Takeda, and T. Kaisho. 2001. Toll-like receptors: critical proteins linking innate and acquired immunity. *Nat. Immunol.* 2: 675-680.

11. Akira, S., and K. Takeda. 2004. Toll-like receptor signalling. *Nat. Rev. Immunol.* 4: 499-511.

12. Kuma, V., A. K. Abbas, and N. Fausto. 2004. *Robbins and Cotran's Pathologic Basis of Disease*, 7 ed. Saunders Co Ltd.

13. Geginat, J., F. Sallusto, and A. Lanzavecchia. 2001. Cytokine-driven proliferation and differentiation of human naive, central memory, and effector memory CD4(+) T cells. *J. Exp. Med.* 194: 1711-1719.

14. McBride, J. M., and C. G. Fathman. 2002. A complicated relationship: fulfilling the interactive needs of the T lymphocyte and the dendritic cell. *Pharmacogenomics. J.* 2: 367-376.

15. O'garra, A., and N. Arai. 2000. The molecular basis of T helper 1 and T helper 2 cell differentiation. *Trends Cell Biol.* 10: 542-550.

16. Takahashi, T., Y. Kuniyasu, M. Toda, N. Sakaguchi, M. Itoh, M. Iwata, J. Shimizu, and S. Sakaguchi. 1998. Immunologic self-tolerance maintained by CD25+CD4+ naturally anergic and suppressive T cells: induction of autoimmune disease by breaking their anergic/suppressive state. *Int. Immunol.* 10: 1969-1980.

17. Read, S., and F. Powrie. 2001. CD4(+) regulatory T cells. *Curr. Opin. Immunol.* 13: 644-649.

18. Marrack, P., and J. Kappler. 1987. The T cell receptor. *Science* 238: 1073-1079.

19. Barry, M., and R. C. Bleackley. 2002. Cytotoxic T lymphocytes: all roads lead to death. *Nat. Rev. Immunol.* 2: 401-409.

20. Surh, C. D., and J. Sprent. 1994. T-cell apoptosis detected in situ during positive and negative selection in the thymus. *Nature* 372: 100-103.

21. Mackay, C. R., W. Marston, and L. Dudler. 1992. Altered patterns of T cell migration through lymph nodes and skin following antigen challenge. *Eur. J. Immunol.* 22: 2205-2210.

22. Geginat, J., F. Sallusto, and A. Lanzavecchia. 2001. Cytokine-driven proliferation and differentiation of human naive, central memory, and effector memory CD4(+) T cells. *J. Exp. Med.* 194: 1711-1719.

23. Westermann, J., B. Engelhardt, and J. C. Hoffmann. 2001. Migration of T cells in vivo: molecular mechanisms and clinical implications. *Ann. Intern. Med.* 135: 279-295.

24. Ley, K., C. Laudanna, M. I. Cybulsky, and S. Nourshargh. 2007. Getting to the site of inflammation: the leukocyte adhesion cascade updated. *Nat. Rev. Immunol.* 7: 678-689.

25. Bradley, L. M., and S. R. Watson. 1996. Lymphocyte migration into tissue: the paradigm derived from CD4 subsets. *Curr. Opin. Immunol.* 8: 312-320.

26. Johnson-Leger, C., M. Aurrand-Lions, and B. A. Imhof. 2000. The parting of the endothelium: miracle, or simply a junctional affair? *J. Cell Sci.* 113 (Pt 6): 921-933.

27. Gunn, M. D., S. Kyuwa, C. Tam, T. Kakiuchi, A. Matsuzawa, L. T. Williams, and H. Nakano. 1999. Mice lacking expression of secondary lymphoid organ chemokine have defects in lymphocyte homing and dendritic cell localization. *J. Exp. Med.* 189: 451-460.

28. Jackson, D. G. 2003. The lymphatics revisited: new perspectives from the hyaluronan receptor LYVE-1. *Trends Cardiovasc. Med.* 13: 1-7.

29. Mebius, R. E. 2003. Organogenesis of lymphoid tissues. *Nat. Rev. Immunol.* 3: 292-303.

30. Sabin, F. R. 1916. The method of growth of the lymphatic system. *Science* 44: 145-158.

31. Wigle, J. T., and G. Oliver. 1999. Prox1 function is required for the development of the murine lymphatic system. *Cell* 98: 769-778.

32. Hoch, R. V., and P. Soriano. 2003. Roles of PDGF in animal development. *Development* 130: 4769-4784.

33. Ornitz, D. M., and N. Itoh. 2001. Fibroblast growth factors. *Genome Biol.* 2: REVIEWS3005.

34. Mummery, C. L. 2001. Transforming growth factor beta and mouse development. *Microsc. Res. Tech.* 52: 374-386.

35. Cupedo, T., and R. E. Mebius. 2005. Cellular interactions in lymph node development. *J. Immunol.* 174: 21-25.

36. Rennert, P. D., D. James, F. Mackay, J. L. Browning, and P. S. Hochman. 1998. Lymph node genesis is induced by signaling through the lymphotoxin beta receptor. *Immunity.* 9: 71-79.

37. Smith, C. A., T. Farrah, and R. G. Goodwin. 1994. The TNF receptor superfamily of cellular and viral proteins: activation, costimulation, and death. *Cell* 76: 959-962.

38. Ware, C. F., T. L. VanArsdale, P. D. Crowe, and J. L. Browning. 1995. The ligands and receptors of the lymphotoxin system. *Curr. Top. Microbiol. Immunol.* 198: 175-218.

39. Force, W. R., B. N. Walter, C. Hession, R. Tizard, C. A. Kozak, J. L. Browning, and C. F. Ware. 1995. Mouse lymphotoxin-beta receptor. Molecular genetics, ligand binding, and expression. *J. Immunol.* 155: 5280-5288.

40. Banks, T. A., B. T. Rouse, M. K. Kerley, P. J. Blair, V. L. Godfrey, N. A. Kuklin, D. M. Bouley, J. Thomas, S. Kanangat, and M. L. Mucenski. 1995. Lymphotoxin-alpha-deficient mice. Effects on secondary lymphoid organ development and humoral immune responsiveness. *J. Immunol.* 155: 1685-1693.

41. Sacca, R., S. Turley, L. Soong, I. Mellman, and N. H. Ruddle. 1997. Transgenic expression of lymphotoxin restores lymph nodes to lymphotoxin-alpha-deficient mice. *J. Immunol.* 159: 4252-4260.

42. Rennert, P. D., J. L. Browning, R. Mebius, F. Mackay, and P. S. Hochman. 1996. Surface lymphotoxin alpha/beta complex is required for the development of peripheral lymphoid organs. *J. Exp. Med.* 184: 1999-2006.

43. Alimzhanov, M. B., D. V. Kuprash, M. H. Kosco-Vilbois, A. Luz, R. L. Turetskaya, A. Tarakhovsky, K. Rajewsky, S. A. Nedospasov, and K. Pfeffer.

1997. Abnormal development of secondary lymphoid tissues in lymphotoxin beta-deficient mice. *Proc. Natl. Acad. Sci. U. S. A* 94: 9302-9307.

44. Koni, P. A., R. Sacca, P. Lawton, J. L. Browning, N. H. Ruddle, and R. A. Flavell. 1997. Distinct roles in lymphoid organogenesis for lymphotoxins alpha and beta revealed in lymphotoxin beta-deficient mice. *Immunity.* 6: 491-500.

45. Cupedo, T., M. F. Vondenhoff, E. J. Heeregrave, A. E. De Weerd, W. Jansen, D. G. Jackson, G. Kraal, and R. E. Mebius. 2004. Presumptive lymph node organizers are differentially represented in developing mesenteric and peripheral nodes. *J. Immunol.* 173: 2968-2975.

46. Futterer, A., K. Mink, A. Luz, M. H. Kosco-Vilbois, and K. Pfeffer. 1998. The lymphotoxin beta receptor controls organogenesis and affinity maturation in peripheral lymphoid tissues. *Immunity.* 9: 59-70.

47. Kim, D., R. E. Mebius, J. D. MacMicking, S. Jung, T. Cupedo, Y. Castellanos, J. Rho, B. R. Wong, R. Josien, N. Kim, P. D. Rennert, and Y. Choi. 2000. Regulation of peripheral lymph node genesis by the tumor necrosis factor family member TRANCE. *J. Exp. Med.* 192: 1467-1478.

48. Yoshida, H., A. Naito, J. Inoue, M. Satoh, S. M. Santee-Cooper, C. F. Ware, A. Togawa, S. Nishikawa, and S. Nishikawa. 2002. Different cytokines induce surface lymphotoxin-alphabeta on IL-7 receptor-alpha cells that differentially engender lymph nodes and Peyer's patches. *Immunity.* 17: 823-833.

49. Adachi, S., H. Yoshida, K. Honda, K. Maki, K. Saijo, K. Ikuta, T. Saito, and S. I. Nishikawa. 1998. Essential role of IL-7 receptor alpha in the formation of Peyer's patch anlage. *Int. Immunol.* 10: 1-6.

50. White, A., D. Carragher, S. Parnell, A. Msaki, N. Perkins, P. Lane, E. Jenkinson, G. Anderson, and J. H. Caamano. 2007. Lymphotoxin a-dependent and -independent signals regulate stromal organizer cell homeostasis during lymph node organogenesis. *Blood* 110: 1950-1959.

51. Muller, J. R., and U. Siebenlist. 2003. Lymphotoxin beta receptor induces sequential activation of distinct NF-kappa B factors via separate signaling pathways. *J. Biol. Chem.* 278: 12006-12012.

52. Cupedo, T., W. Jansen, G. Kraal, and R. E. Mebius. 2004. Induction of secondary and tertiary lymphoid structures in the skin. *Immunity.* 21: 655-667.

53. Yoshida, H., K. Honda, R. Shinkura, S. Adachi, S. Nishikawa, K. Maki, K. Ikuta, and S. I. Nishikawa. 1999. IL-7 receptor alpha+ CD3(-) cells in the embryonic intestine induces the organizing center of Peyer's patches. *Int. Immunol.* 11: 643-655.

54. Kim, M. Y., F. M. Gaspal, H. E. Wiggett, F. M. McConnell, A. Gulbranson-Judge, C. Raykundalia, L. S. Walker, M. D. Goodall, and P. J. Lane. 2003. CD4(+)CD3(-) accessory cells costimulate primed CD4 T cells through OX40

and CD30 at sites where T cells collaborate with B cells. *Immunity.* 18: 643-654.

55. Gaspal, F. M., M. Y. Kim, F. M. McConnell, C. Raykundalia, V. Bekiaris, and P. J. Lane. 2005. Mice deficient in OX40 and CD30 signals lack memory antibody responses because of deficient CD4 T cell memory. *J. Immunol.* 174: 3891-3896.

56. Kim, M. Y., F. M. McConnell, F. M. Gaspal, A. White, S. H. Glanville, V. Bekiaris, L. S. Walker, J. Caamano, E. Jenkinson, G. Anderson, and P. J. Lane. 2007. Function of CD4+CD3- cells in relation to B- and T-zone stroma in spleen. *Blood* 109: 1602-1610.

57. Scandella, E., B. Bolinger, E. Lattmann, S. Miller, S. Favre, D. R. Littman, D. Finke, S. A. Luther, T. Junt, and B. Ludewig. 2008. Restoration of lymphoid organ integrity through the interaction of lymphoid tissue-inducer cells with stroma of the T cell zone. *Nat. Immunol.* 9: 667-675.

58. Cella, M., A. Fuchs, W. Vermi, F. Facchetti, K. Otero, J. K. Lennerz, J. M. Doherty, J. C. Mills, and M. Colonna. 2009. A human natural killer cell subset provides an innate source of IL-22 for mucosal immunity. *Nature* 457: 722-725.

59. Moretta, A., R. Biassoni, C. Bottino, M. C. Mingari, and L. Moretta. 2000. Natural cytotoxicity receptors that trigger human NK-cell-mediated cytolysis. *Immunol. Today* 21: 228-234.

60. Takatori, H., Y. Kanno, W. T. Watford, C. M. Tato, G. Weiss, I. I. Ivanov, D. R. Littman, and J. J. O'Shea. 2009. Lymphoid tissue inducer-like cells are an innate source of IL-17 and IL-22. *J. Exp. Med.* 206: 35-41.

61. Vivier, E., H. Spits, and T. Cupedo. 2009. Interleukin-22-producing innate immune cells: new players in mucosal immunity and tissue repair? *Nat. Rev. Immunol.* 9: 229-234.

62. Drayton, D. L., S. Liao, R. H. Mounzer, and N. H. Ruddle. 2006. Lymphoid organ development: from ontogeny to neogenesis. *Nat. Immunol.* 7: 344-353.

63. Oliver, G. 2004. Lymphatic vasculature development. *Nat. Rev. Immunol.* 4: 35-45.

64. Berlin, C., E. L. Berg, M. J. Briskin, D. P. Andrew, P. J. Kilshaw, B. Holzmann, I. L. Weissman, A. Hamann, and E. C. Butcher. 1993. Alpha 4 beta 7 integrin mediates lymphocyte binding to the mucosal vascular addressin MAdCAM-1. *Cell* 74: 185-195.

65. Blum, K. S., and R. Pabst. 2006. Keystones in lymph node development. *J. Anat.* 209: 585-595.

66. Cyster, J. G. 2003. Lymphoid organ development and cell migration. *Immunol. Rev.* 195: 5-14.

67. Link, A., T. K. Vogt, S. Favre, M. R. Britschgi, H. Acha-Orbea, B. Hinz, J. G. Cyster, and S. A. Luther. 2007. Fibroblastic reticular cells in lymph nodes regulate the homeostasis of naive T cells. *Nat. Immunol.* 8: 1255-1265.

68. Allen, C. D., and J. G. Cyster. 2008. Follicular dendritic cell networks of primary follicles and germinal centers: phenotype and function. *Semin. Immunol.* 20: 14-25.

69. Katakai, T., H. Suto, M. Sugai, H. Gonda, A. Togawa, S. Suematsu, Y. Ebisuno, K. Katagiri, T. Kinashi, and A. Shimizu. 2008. Organizer-like reticular stromal cell layer common to adult secondary lymphoid organs. *J. Immunol.* 181: 6189-6200.

70. Luther, S. A., H. L. Tang, P. L. Hyman, A. G. Farr, and J. G. Cyster. 2000. Coexpression of the chemokines ELC and SLC by T zone stromal cells and deletion of the ELC gene in the plt/plt mouse. *Proc. Natl. Acad. Sci. U. S. A* 97: 12694-12699.

71. Katakai, T., T. Hara, M. Sugai, H. Gonda, and A. Shimizu. 2004. Lymph node fibroblastic reticular cells construct the stromal reticulum via contact with lymphocytes. *J. Exp. Med.* 200: 783-795.

72. Farr, A. G., M. L. Berry, A. Kim, A. J. Nelson, M. P. Welch, and A. Aruffo. 1992. Characterization and cloning of a novel glycoprotein expressed by stromal cells in T-dependent areas of peripheral lymphoid tissues. *J. Exp. Med.* 176: 1477-1482.

73. Breiteneder-Geleff, S., K. Matsui, A. Soleiman, P. Meraner, H. Poczewski, R. Kalt, G. Schaffner, and D. Kerjaschki. 1997. Podoplanin, novel 43-kd membrane protein of glomerular epithelial cells, is down-regulated in puromycin nephrosis. *Am. J. Pathol.* 151: 1141-1152.

74. Schacht, V., M. I. Ramirez, Y. K. Hong, S. Hirakawa, D. Feng, N. Harvey, M. Williams, A. M. Dvorak, H. F. Dvorak, G. Oliver, and M. Detmar. 2003. T1alpha/podoplanin deficiency disrupts normal lymphatic vasculature formation and causes lymphedema. *EMBO J.* 22: 3546-3556.

75. Farr, A., A. Nelson, and S. Hosier. 1992. Characterization of an antigenic determinant preferentially expressed by type I epithelial cells in the murine thymus. *J. Histochem. Cytochem.* 40: 651-664.

76. Mahtab, E. A., M. C. Wijffels, N. M. Van Den Akker, N. D. Hahurij, H. Lie-Venema, L. J. Wisse, M. C. DeRuiter, P. Uhrin, J. Zaujec, B. R. Binder, M. J. Schalij, R. E. Poelmann, and A. C. Gittenberger-de Groot. 2008. Cardiac malformations and myocardial abnormalities in podoplanin knockout mouse embryos: Correlation with abnormal epicardial development. *Dev. Dyn.* 237: 847-857.

77. Ngo, V. N., R. J. Cornall, and J. G. Cyster. 2001. Splenic T zone development is B cell dependent. *J. Exp. Med.* 194: 1649-1660.

78. Bekiaris, V., D. Withers, S. H. Glanville, F. M. McConnell, S. M. Parnell, M. Y. Kim, F. M. Gaspal, E. Jenkinson, C. Sweet, G. Anderson, and P. J. Lane. 2007. Role of CD30 in B/T segregation in the spleen. *J. Immunol.* 179: 7535-7543.

79. Rademakers, L. H. 1991. Follicular dendritic cells in germinal centre development. *Res. Immunol.* 142: 257-260.

80. Lindhout, E., M. van Eijk, M. van Pel, J. Lindeman, H. J. Dinant, and C. de Groot. 1999. Fibroblast-like synoviocytes from rheumatoid arthritis patients have intrinsic properties of follicular dendritic cells. *J. Immunol.* 162: 5949-5956.

81. Park, C. S., and Y. S. Choi. 2005. How do follicular dendritic cells interact intimately with B cells in the germinal centre? *Immunology* 114: 2-10.

82. Hase, H., Y. Kanno, M. Kojima, K. Hasegawa, D. Sakurai, H. Kojima, N. Tsuchiya, K. Tokunaga, N. Masawa, M. Azuma, K. Okumura, and T. Kobata. 2004. BAFF/BLyS can potentiate B-cell selection with the B-cell coreceptor complex. *Blood* 103: 2257-2265.

83. Nolte, M. A., J. A. Belien, I. Schadee-Eestermans, W. Jansen, W. W. Unger, N. van Rooijen, G. Kraal, and R. E. Mebius. 2003. A conduit system distributes chemokines and small blood-borne molecules through the splenic white pulp. *J. Exp. Med.* 198: 505-512.

84. Gretz, J. E., A. O. Anderson, and S. Shaw. 1997. Cords, channels, corridors and conduits: critical architectural elements facilitating cell interactions in the lymph node cortex. *Immunol. Rev.* 156: 11-24.

85. Sixt, M., N. Kanazawa, M. Selg, T. Samson, G. Roos, D. P. Reinhardt, R. Pabst, M. B. Lutz, and L. Sorokin. 2005. The conduit system transports soluble antigens from the afferent lymph to resident dendritic cells in the T cell area of the lymph node. *Immunity.* 22: 19-29.

86. Bajenoff, M., J. G. Egen, L. Y. Koo, J. P. Laugier, F. Brau, N. Glaichenhaus, and R. N. Germain. 2006. Stromal cell networks regulate lymphocyte entry, migration, and territoriality in lymph nodes. *Immunity.* 25: 989-1001.

87. Hayakawa, M., M. Kobayashi, and T. Hoshino. 1988. Direct contact between reticular fibers and migratory cells in the paracortex of mouse lymph nodes: a morphological and quantitative study. *Arch. Histol. Cytol.* 51: 233-240.

88. Gretz, J. E., C. C. Norbury, A. O. Anderson, A. E. Proudfoot, and S. Shaw. 2000. Lymph-borne chemokines and other low molecular weight molecules reach high endothelial venules via specialized conduits while a functional barrier limits access to the lymphocyte microenvironments in lymph node cortex. *J. Exp. Med.* 192: 1425-1440.

89. Hecksher-Sorensen, J., R. P. Watson, L. A. Lettice, P. Serup, L. Eley, C. De Angelis, U. Ahlgren, and R. E. Hill. 2004. The splanchnic mesodermal plate

directs spleen and pancreatic laterality, and is regulated by Bapx1/Nkx3.2. *Development* 131: 4665-4675.

90. Green, M. C. 1967. A defect of the splanchnic mesoderm caused by the mutant gene dominant hemimelia in the mouse. *Dev. Biol.* 15: 62-89.

91. Seifert, M. F., and S. C. Marks, Jr. 1985. The regulation of hemopoiesis in the spleen. *Experientia* 41: 192-199.

92. Mebius, R. E., and G. Kraal. 2005. Structure and function of the spleen. *Nat. Rev. Immunol.* 5: 606-616.

93. Lenox, L. E., L. Shi, S. Hegde, and R. F. Paulson. 2009. Extramedullary erythropoiesis in the adult liver requires BMP-4/Smad5-dependent signaling. *Exp. Hematol.* 37: 549-558.

94. Lopez-Guillermo, A., F. Cervantes, M. Bruguera, A. Pereira, E. Feliu, and C. Rozman. 1991. Liver dysfunction following splenectomy in idiopathic myelofibrosis: a study of 10 patients. *Acta Haematol.* 85: 184-188.

95. Sainte-Marie, G., and F. S. Peng. 1986. Diffusion of a lymph-carried antigen in the fiber network of the lymph node of the rat. *Cell Tissue Res.* 245: 481-486.

96. Ngo, V. N., H. Korner, M. D. Gunn, K. N. Schmidt, D. S. Riminton, M. D. Cooper, J. L. Browning, J. D. Sedgwick, and J. G. Cyster. 1999. Lymphotoxin alpha/beta and tumor necrosis factor are required for stromal cell expression of homing chemokines in B and T cell areas of the spleen. *J. Exp. Med.* 189: 403-412.

97. Ansel, K. M., V. N. Ngo, P. L. Hyman, S. A. Luther, R. Forster, J. D. Sedgwick, J. L. Browning, M. Lipp, and J. G. Cyster. 2000. A chemokine-driven positive feedback loop organizes lymphoid follicles. *Nature* 406: 309-314.

98. Ngo, V. N., H. Korner, M. D. Gunn, K. N. Schmidt, D. S. Riminton, M. D. Cooper, J. L. Browning, J. D. Sedgwick, and J. G. Cyster. 1999. Lymphotoxin alpha/beta and tumor necrosis factor are required for stromal cell expression of homing chemokines in B and T cell areas of the spleen. *J. Exp. Med.* 189: 403-412.

99. Ngo, V. N., H. Korner, M. D. Gunn, K. N. Schmidt, D. S. Riminton, M. D. Cooper, J. L. Browning, J. D. Sedgwick, and J. G. Cyster. 1999. Lymphotoxin alpha/beta and tumor necrosis factor are required for stromal cell expression of homing chemokines in B and T cell areas of the spleen. *J. Exp. Med.* 189: 403-412.

100. Matsumoto, M., Y. X. Fu, H. Molina, and D. D. Chaplin. 1997. Lymphotoxin-alpha-deficient and TNF receptor-I-deficient mice define developmental and functional characteristics of germinal centers. *Immunol. Rev.* 156: 137-144.

101. Ansel, K. M., V. N. Ngo, P. L. Hyman, S. A. Luther, R. Forster, J. D. Sedgwick, J. L. Browning, M. Lipp, and J. G. Cyster. 2000. A chemokine-driven positive feedback loop organizes lymphoid follicles. *Nature* 406: 309-314.

102. Matsumoto, M., Y. X. Fu, H. Molina, and D. D. Chaplin. 1997. Lymphotoxin-alpha-deficient and TNF receptor-I-deficient mice define developmental and functional characteristics of germinal centers. *Immunol. Rev.* 156: 137-144.

103. Amlot, P. L., and A. E. Hayes. 1985. Impaired human antibody response to the thymus-independent antigen, DNP-Ficoll, after splenectomy. Implications for post-splenectomy infections. *Lancet* 1: 1008-1011.

104. Kratz, A., A. Campos-Neto, M. S. Hanson, and N. H. Ruddle. 1996. Chronic inflammation caused by lymphotoxin is lymphoid neogenesis. *J. Exp. Med.* 183: 1461-1472.

105. Haworth, O., and C. D. Buckley. 2007. Resolving the problem of persistence in the switch from acute to chronic inflammation. *Proc. Natl. Acad. Sci. U. S. A* 104: 20647-20648.

106. Maddox, J. F., S. P. Colgan, C. B. Clish, N. A. Petasis, V. V. Fokin, and C. N. Serhan. 1998. Lipoxin B4 regulates human monocyte/neutrophil adherence and motility: design of stable lipoxin B4 analogs with increased biologic activity. *FASEB J.* 12: 487-494.

107. Soyombo, O., B. W. Spur, and T. H. Lee. 1994. Effects of lipoxin A4 on chemotaxis and degranulation of human eosinophils stimulated by platelet-activating factor and N-formyl-L-methionyl-L-leucyl-L-phenylalanine. *Allergy* 49: 230-234.

108. Gilroy, D. W., P. R. Colville-Nash, D. Willis, J. Chivers, M. J. Paul-Clark, and D. A. Willoughby. 1999. Inducible cyclooxygenase may have anti-inflammatory properties. *Nat. Med.* 5: 698-701.

109. Salmon, M., D. Scheel-Toellner, A. P. Huissoon, D. Pilling, N. Shamsadeen, H. Hyde, A. D. D'Angeac, P. A. Bacon, P. Emery, and A. N. Akbar. 1997. Inhibition of T cell apoptosis in the rheumatoid synovium. *J. Clin. Invest* 99: 439-446.

110. Pilling, D., A. N. Akbar, J. Girdlestone, C. H. Orteu, N. J. Borthwick, N. Amft, D. Scheel-Toellner, C. D. Buckley, and M. Salmon. 1999. Interferon-beta mediates stromal cell rescue of T cells from apoptosis. *Eur. J. Immunol.* 29: 1041-1050.

111. Buckley, C. D., N. Amft, P. F. Bradfield, D. Pilling, E. Ross, F. Arenzana-Seisdedos, A. Amara, S. J. Curnow, J. M. Lord, D. Scheel-Toellner, and M. Salmon. 2000. Persistent induction of the chemokine receptor CXCR4 by TGF-beta 1 on synovial T cells contributes to their accumulation within the rheumatoid synovium. *J. Immunol.* 165: 3423-3429.

112. Shiow, L. R., D. B. Rosen, N. Brdickova, Y. Xu, J. An, L. L. Lanier, J. G. Cyster, and M. Matloubian. 2006. CD69 acts downstream of interferon-alpha/beta to inhibit S1P1 and lymphocyte egress from lymphoid organs. *Nature* 440: 540-544.

113. Buckley, C. D., D. Pilling, J. M. Lord, A. N. Akbar, D. Scheel-Toellner, and M. Salmon. 2001. Fibroblasts regulate the switch from acute resolving to chronic persistent inflammation. *Trends Immunol.* 22: 199-204.

114. Schroder, A. E., A. Greiner, C. Seyfert, and C. Berek. 1996. Differentiation of B cells in the nonlymphoid tissue of the synovial membrane of patients with rheumatoid arthritis. *Proc. Natl. Acad. Sci. U. S. A* 93: 221-225.

115. Ghosh, S., A. C. Steere, B. D. Stollar, and B. T. Huber. 2005. In situ diversification of the antibody repertoire in chronic Lyme arthritis synovium. *J. Immunol.* 174: 2860-2869.

116. Baddoura, F. K., I. W. Nasr, B. Wrobel, Q. Li, N. H. Ruddle, and F. G. Lakkis. 2005. Lymphoid neogenesis in murine cardiac allografts undergoing chronic rejection. *Am. J. Transplant.* 5: 510-516.

117. Hjelmstrom, P. 2001. Lymphoid neogenesis: de novo formation of lymphoid tissue in chronic inflammation through expression of homing chemokines. *J. Leukoc. Biol.* 69: 331-339.

118. Paavonen, K., J. Mandelin, T. Partanen, L. Jussila, T. F. Li, A. Ristimaki, K. Alitalo, and Y. T. Konttinen. 2002. Vascular endothelial growth factors C and D and their VEGFR-2 and 3 receptors in blood and lymphatic vessels in healthy and arthritic synovium. *J. Rheumatol.* 29: 39-45.

119. Chang, H. Y., J. T. Chi, S. Dudoit, C. Bondre, R. M. van de, D. Botstein, and P. O. Brown. 2002. Diversity, topographic differentiation, and positional memory in human fibroblasts. *Proc. Natl. Acad. Sci. U. S. A* 99: 12877-12882.

120. Filer, A., C. Pitzalis, and C. D. Buckley. 2006. Targeting the stromal microenvironment in chronic inflammation. *Curr. Opin. Pharmacol.* 6: 393-400.

121. Tarin, D., and C. B. Croft. 1969. Ultrastructural features of wound healing in mouse skin. *J. Anat.* 105: 189-190.

122. Sabatelli, P., P. Bonaldo, G. Lattanzi, P. Braghetta, N. Bergamin, C. Capanni, E. Mattioli, M. Columbaro, A. Ognibene, G. Pepe, E. Bertini, L. Merlini, N. M. Maraldi, and S. Squarzoni. 2001. Collagen VI deficiency affects the organization of fibronectin in the extracellular matrix of cultured fibroblasts. *Matrix Biol.* 20: 475-486.

123. Marinkovich, M. P., D. R. Keene, C. S. Rimberg, and R. E. Burgeson. 1993. Cellular origin of the dermal-epidermal basement membrane. *Dev. Dyn.* 197: 255-267.

124. Tomita, T., T. Nakase, M. Kaneko, K. Shi, K. Takahi, T. Ochi, and H. Yoshikawa. 2002. Expression of extracellular matrix metalloproteinase inducer and enhancement of the production of matrix metalloproteinases in rheumatoid arthritis. *Arthritis Rheum.* 46: 373-378.

125. Dahm, R., and M. Kiebler. 2005. Cell biology: silenced RNA on the move. *Nature* 438: 432-435.

126. Iwano, M., D. Plieth, T. M. Danoff, C. Xue, H. Okada, and E. G. Neilson. 2002. Evidence that fibroblasts derive from epithelium during tissue fibrosis. *J. Clin. Invest* 110: 341-350.

127. Kalluri, R., and E. G. Neilson. 2003. Epithelial-mesenchymal transition and its implications for fibrosis. *J. Clin. Invest* 112: 1776-1784.

128. Zeisberg, M., G. Bonner, Y. Maeshima, P. Colorado, G. A. Muller, F. Strutz, and R. Kalluri. 2001. Renal fibrosis: collagen composition and assembly regulates epithelial-mesenchymal transdifferentiation. *Am. J. Pathol.* 159: 1313-1321.

129. Zeisberg, M., J. Hanai, H. Sugimoto, T. Mammoto, D. Charytan, F. Strutz, and R. Kalluri. 2003. BMP-7 counteracts TGF-beta1-induced epithelial-to-mesenchymal transition and reverses chronic renal injury. *Nat. Med.* 9: 964-968.

130. Garrett, D. M., and G. W. Conrad. 1979. Fibroblast-like cells from embryonic chick cornea, heart, and skin are antigenically distinct. *Dev. Biol.* 70: 50-70.

131. Schor, S. L., and A. M. Schor. 1987. Clonal heterogeneity in fibroblast phenotype: implications for the control of epithelial-mesenchymal interactions. *Bioessays* 7: 200-204.

132. Dugina, V., A. Alexandrova, C. Chaponnier, J. Vasiliev, and G. Gabbiani. 1998. Rat fibroblasts cultured from various organs exhibit differences in alpha-smooth muscle actin expression, cytoskeletal pattern, and adhesive structure organization. *Exp. Cell Res.* 238: 481-490.

133. Abe, R., S. C. Donnelly, T. Peng, R. Bucala, and C. N. Metz. 2001. Peripheral blood fibrocytes: differentiation pathway and migration to wound sites. *J. Immunol.* 166: 7556-7562.

134. Bucala, R., L. A. Spiegel, J. Chesney, M. Hogan, and A. Cerami. 1994. Circulating fibrocytes define a new leukocyte subpopulation that mediates tissue repair. *Mol. Med.* 1: 71-81.

135. Pilling, D., C. D. Buckley, M. Salmon, and R. H. Gomer. 2003. Inhibition of fibrocyte differentiation by serum amyloid P. *J. Immunol.* 171: 5537-5546.

136. Parsonage, G., A. D. Filer, O. Haworth, G. B. Nash, G. E. Rainger, M. Salmon, and C. D. Buckley. 2005. A stromal address code defined by fibroblasts. *Trends Immunol.* 26: 150-156.

137. Postlethwaite, A. E., H. Shigemitsu, and S. Kanangat. 2004. Cellular origins of fibroblasts: possible implications for organ fibrosis in systemic sclerosis. *Curr. Opin. Rheumatol.* 16: 733-738.

138. Kalluri, R., and M. Zeisberg. 2006. Fibroblasts in cancer. *Nat. Rev. Cancer* 6: 392-401.

139. MacFadyen, J. R., O. Haworth, D. Roberston, D. Hardie, M. T. Webster, H. R. Morris, M. Panico, M. Sutton-Smith, A. Dell, G. P. van der, D. Wienke, C. D. Buckley, and C. M. Isacke. 2005. Endosialin (TEM1, CD248) is a marker of stromal fibroblasts and is not selectively expressed on tumour endothelium. *FEBS Lett.* 579: 2569-2575.

140. Lax, S., T. Z. Hou, E. Jenkinson, M. Salmon, J. R. MacFadyen, C. M. Isacke, G. Anderson, A. F. Cunningham, and C. D. Buckley. 2007. CD248/Endosialin is dynamically expressed on a subset of stromal cells during lymphoid tissue development, splenic remodeling and repair. *FEBS Lett.* 581: 3550-3556.

141. Hirschi, K. K., S. A. Rohovsky, L. H. Beck, S. R. Smith, and P. A. D'Amore. 1999. Endothelial cells modulate the proliferation of mural cell precursors via platelet-derived growth factor-BB and heterotypic cell contact. *Circ. Res.* 84: 298-305.

142. Norsworthy, P. J., L. Fossati-Jimack, J. Cortes-Hernandez, P. R. Taylor, A. E. Bygrave, R. D. Thompson, S. Nourshargh, M. J. Walport, and M. Botto. 2004. Murine CD93 (C1qRp) contributes to the removal of apoptotic cells in vivo but is not required for C1q-mediated enhancement of phagocytosis. *J. Immunol.* 172: 3406-3414.

143. Conway, E. M., W. M. Van de, S. Pollefeyt, K. Jurk, H. Van Aken, A. De Vriese, J. I. Weitz, H. Weiler, P. W. Hellings, P. Schaeffer, J. M. Herbert, D. Collen, and G. Theilmeier. 2002. The lectin-like domain of thrombomodulin confers protection from neutrophil-mediated tissue damage by suppressing adhesion molecule expression via nuclear factor kappaB and mitogen-activated protein kinase pathways. *J. Exp. Med.* 196: 565-577.

144. Bagley, R. G., N. Honma, W. Weber, P. Boutin, C. Rouleau, S. Shankara, S. Kataoka, I. Ishida, B. L. Roberts, and B. A. Teicher. 2008. Endosialin/TEM 1/CD248 is a pericyte marker of embryonic and tumor neovascularization. *Microvasc. Res.* 76: 180-188.

145. MacFadyen, J., K. Savage, D. Wienke, and C. M. Isacke. 2007. Endosialin is expressed on stromal fibroblasts and CNS pericytes in mouse embryos and is downregulated during development. *Gene Expr. Patterns.* 7: 363-369.

146. Christian, S., R. Winkler, I. Helfrich, A. M. Boos, E. Besemfelder, D. Schadendorf, and H. G. Augustin. 2008. Endosialin (Tem1) is a marker of tumor-associated myofibroblasts and tumor vessel-associated mural cells. *Am. J. Pathol.* 172: 486-494.

147. Nanda, A., B. Karim, Z. Peng, G. Liu, W. Qiu, C. Gan, B. Vogelstein, B. St Croix, K. W. Kinzler, and D. L. Huso. 2006. Tumor endothelial marker 1 (Tem1) functions in the growth and progression of abdominal tumors. *Proc. Natl. Acad. Sci. U. S. A* 103: 3351-3356.

148. Bagley, R. G., W. Weber, C. Rouleau, M. Yao, N. Honma, S. Kataoka, I. Ishida, B. L. Roberts, and B. A. Teicher. 2009. Human mesenchymal stem cells from bone marrow express tumor endothelial and stromal markers. *Int. J. Oncol.* 34: 619-627.

149. Fries, K. M., T. Blieden, R. J. Looney, G. D. Sempowski, M. R. Silvera, R. A. Willis, and R. P. Phipps. 1994. Evidence of fibroblast heterogeneity and the role of fibroblast subpopulations in fibrosis. *Clin. Immunol. Immunopathol.* 72: 283-292.

150. Parsonage, G., F. Falciani, A. Burman, A. Filer, E. Ross, M. Bofill, S. Martin, M. Salmon, and C. D. Buckley. 2003. Global gene expression profiles in fibroblasts from synovial, skin and lymphoid tissue reveals distinct cytokine and chemokine expression patterns. *Thromb. Haemost.* 90: 688-697.

151. Rinn, J. L., C. Bondre, H. B. Gladstone, P. O. Brown, and H. Y. Chang. 2006. Anatomic demarcation by positional variation in fibroblast gene expression programs. *PLoS. Genet.* 2: e119.

152. Rinn, J. L., J. K. Wang, N. Allen, S. A. Brugmann, A. J. Mikels, H. Liu, T. W. Ridky, H. S. Stadler, R. Nusse, J. A. Helms, and H. Y. Chang. 2008. A dermal HOX transcriptional program regulates site-specific epidermal fate. *Genes Dev.* 22: 303-307.

153. Nash, G. B., C. D. Buckley, and R. G. Ed. 2004. The local physicochemical environment conditions the proinflammatory response of endothelial cells and thus modulates leukocyte recruitment. *FEBS Lett.* 569: 13-17.

154. Rinn, J. L., J. K. Wang, H. Liu, K. Montgomery, R. M. van de, and H. Y. Chang. 2008. A systems biology approach to anatomic diversity of skin. *J. Invest Dermatol.* 128: 776-782.

155. Pap, T., U. Muller-Ladner, R. E. Gay, and S. Gay. 2000. Fibroblast biology. Role of synovial fibroblasts in the pathogenesis of rheumatoid arthritis. *Arthritis Res.* 2: 361-367.

156. Smith, R. S., T. J. Smith, T. M. Blieden, and R. P. Phipps. 1997. Fibroblasts as sentinel cells. Synthesis of chemokines and regulation of inflammation. *Am. J. Pathol.* 151: 317-322.

157. Zhang, Y., H. J. Cao, B. Graf, H. Meekins, T. J. Smith, and R. P. Phipps. 1998. CD40 engagement up-regulates cyclooxygenase-2 expression and prostaglandin E2 production in human lung fibroblasts. *J. Immunol.* 160: 1053-1057.

158. Mueller, D. L. 2000. T cells: A proliferation of costimulatory molecules. *Curr. Biol.* 10: R227-R230.

159. Tlsty, T. D. 2001. Stromal cells can contribute oncogenic signals. *Semin. Cancer Biol.* 11: 97-104.

160. Postlethwaite, A. E., M. A. Holness, H. Katai, and R. Raghow. 1992. Human fibroblasts synthesize elevated levels of extracellular matrix proteins in response to interleukin 4. *J. Clin. Invest* 90: 1479-1485.

161. Illsley, M. C., J. H. Peacock, R. J. McAnulty, and J. R. Yarnold. 2000. Increased collagen production in fibroblasts cultured from irradiated skin and effect of TGF beta(1)- clinical study. *Br. J. Cancer* 83: 650-654.

162. Khurana, R., and S. M. Berney. 2005. Clinical aspects of rheumatoid arthritis. *Pathophysiology.* 12: 153-165.

163. Firestein, G. S. 2003. Evolving concepts of rheumatoid arthritis. *Nature* 423: 356-361.

164. Khurana, R., and S. M. Berney. 2005. Clinical aspects of rheumatoid arthritis. *Pathophysiology.* 12: 153-165.

165. Goronzy, J. J., and C. M. Weyand. 2005. Rheumatoid arthritis. *Immunol. Rev.* 204: 55-73.

166. Fassbender, H. G. 1983. Histomorphological basis of articular cartilage destruction in rheumatoid arthritis. *Coll. Relat Res.* 3: 141-155.

167. Muller-Ladner, U., J. Kriegsmann, B. N. Franklin, S. Matsumoto, T. Geiler, R. E. Gay, and S. Gay. 1996. Synovial fibroblasts of patients with rheumatoid arthritis attach to and invade normal human cartilage when engrafted into SCID mice. *Am. J. Pathol.* 149: 1607-1615.

168. Aidinis, V., P. Carninci, M. Armaka, W. Witke, V. Harokopos, N. Pavelka, D. Koczan, C. Argyropoulos, M. M. Thwin, S. Moller, K. Waki, P. Gopalakrishnakone, P. Ricciardi-Castagnoli, H. J. Thiesen, Y. Hayashizaki, and G. Kollias. 2005. Cytoskeletal rearrangements in synovial fibroblasts as a novel pathophysiological determinant of modeled rheumatoid arthritis. *PLoS. Genet.* 1: e48.

169. Firestein, G. S. 1996. Invasive fibroblast-like synoviocytes in rheumatoid arthritis. Passive responders or transformed aggressors? *Arthritis Rheum.* 39: 1781-1790.

170. Sund, M., and R. Kalluri. 2009. Tumor stroma derived biomarkers in cancer. *Cancer Metastasis Rev.* 28: 177-183.

171. Ronnov-Jessen, L., O. W. Petersen, and M. J. Bissell. 1996. Cellular changes involved in conversion of normal to malignant breast: importance of the stromal reaction. *Physiol Rev.* 76: 69-125.

172. Dvorak, H. F. 1986. Tumors: wounds that do not heal. Similarities between tumor stroma generation and wound healing. *N. Engl. J. Med.* 315: 1650-1659.

173. Schedin, P., and A. Elias. 2004. Multistep tumorigenesis and the microenvironment. *Breast Cancer Res.* 6: 93-101.

174. Rodemann, H. P., and G. A. Muller. 1991. Characterization of human renal fibroblasts in health and disease: II. In vitro growth, differentiation, and collagen synthesis of fibroblasts from kidneys with interstitial fibrosis. *Am. J. Kidney Dis.* 17: 684-686.

175. Thiery, J. P. 2001. [Role of growth factor signaling in epithelial cell plasticity during development and in carcinogenesis]. *Bull. Acad. Natl. Med.* 185: 1279-1292.

176. Finak, G., N. Bertos, F. Pepin, S. Sadekova, M. Souleimanova, H. Zhao, H. Chen, G. Omeroglu, S. Meterissian, A. Omeroglu, M. Hallett, and M. Park. 2008. Stromal gene expression predicts clinical outcome in breast cancer. *Nat. Med.* 14: 518-527.

177. da Silva, M. L., P. C. Chagastelles, and N. B. Nardi. 2006. Mesenchymal stem cells reside in virtually all post-natal organs and tissues. *J. Cell Sci.* 119: 2204-2213.

178. Campagnoli, C., I. A. Roberts, S. Kumar, P. R. Bennett, I. Bellantuono, and N. M. Fisk. 2001. Identification of mesenchymal stem/progenitor cells in human first-trimester fetal blood, liver, and bone marrow. *Blood* 98: 2396-2402.

179. Pittenger, M. F., A. M. Mackay, S. C. Beck, R. K. Jaiswal, R. Douglas, J. D. Mosca, M. A. Moorman, D. W. Simonetti, S. Craig, and D. R. Marshak. 1999. Multilineage potential of adult human mesenchymal stem cells. *Science* 284: 143-147.

180. Jones, S., N. Horwood, A. Cope, and F. Dazzi. 2007. The antiproliferative effect of mesenchymal stem cells is a fundamental property shared by all stromal cells. *J. Immunol.* 179: 2824-2831.

181. Haniffa, M. A., X. N. Wang, U. Holtick, M. Rae, J. D. Isaacs, A. M. Dickinson, C. M. Hilkens, and M. P. Collin. 2007. Adult human fibroblasts are potent immunoregulatory cells and functionally equivalent to mesenchymal stem cells. *J. Immunol.* 179: 1595-1604.

182. Haniffa, M. A., M. P. Collin, C. D. Buckley, and F. Dazzi. 2009. Mesenchymal stem cells: the fibroblasts' new clothes? *Haematologica* 94: 258-263.

183. Jones, E., and D. McGonagle. 2008. Human bone marrow mesenchymal stem cells in vivo. *Rheumatology. (Oxford)* 47: 126-131.

184. Criswell, L. A., K. A. Pfeiffer, R. F. Lum, B. Gonzales, J. Novitzke, M. Kern, K. L. Moser, A. B. Begovich, V. E. Carlton, W. Li, A. T. Lee, W. Ortmann, T. W. Behrens, and P. K. Gregersen. 2005. Analysis of families in the multiple autoimmune disease genetics consortium (MADGC) collection: the PTPN22 620W allele associates with multiple autoimmune phenotypes. *Am. J. Hum. Genet.* 76: 561-571.

185. Freeman, G. J., G. S. Gray, C. D. Gimmi, D. B. Lombard, L. J. Zhou, M. White, J. D. Fingeroth, J. G. Gribben, and L. M. Nadler. 1991. Structure, expression, and T cell costimulatory activity of the murine homologue of the human B lymphocyte activation antigen B7. *J. Exp. Med.* 174: 625-631.

186. Freeman, G. J., J. G. Gribben, V. A. Boussiotis, J. W. Ng, V. A. Restivo, Jr., L. A. Lombard, G. S. Gray, and L. M. Nadler. 1993. Cloning of B7-2: a CTLA-4 counter-receptor that costimulates human T cell proliferation. *Science* 262: 909-911.

187. Vliagoftis, H., A. S. Worobec, and D. D. Metcalfe. 1997. The protooncogene c-kit and c-kit ligand in human disease. *J. Allergy Clin. Immunol.* 100: 435-440.

188. Bogen, S. A., H. S. Baldwin, S. C. Watkins, S. M. Albelda, and A. K. Abbas. 1992. Association of murine CD31 with transmigrating lymphocytes following antigenic stimulation. *Am. J. Pathol.* 141: 843-854.

189. Nakano, A., T. Harada, S. Morikawa, and Y. Kato. 1990. Expression of leukocyte common antigen (CD45) on various human leukemia/lymphoma cell lines. *Acta Pathol. Jpn.* 40: 107-115.

190. Lin, H. H., D. E. Faunce, M. Stacey, A. Terajewicz, T. Nakamura, J. Zhang-Hoover, M. Kerley, M. L. Mucenski, S. Gordon, and J. Stein-Streilein. 2005. The macrophage F4/80 receptor is required for the induction of antigen-specific efferent regulatory T cells in peripheral tolerance. *J. Exp. Med.* 201: 1615-1625.

191. Banchereau, J., and R. M. Steinman. 1998. Dendritic cells and the control of immunity. *Nature* 392: 245-252.

192. Im, J., H. Kim, S. Kim, and E. H. Jho. 2007. Wnt/beta-catenin signaling regulates expression of PRDC, an antagonist of the BMP-4 signaling pathway. *Biochem. Biophys. Res. Commun.* 354: 296-301.

193. Bacani, J. T., M. Soares, R. Zwingerman, N. di Nicola, J. Senz, R. Riddell, D. G. Huntsman, and S. Gallinger. 2006. CDH1/E-cadherin germline mutations in early-onset gastric cancer. *J. Med. Genet.* 43: 867-872.

194. Mott, J. D., and Z. Werb. 2004. Regulation of matrix biology by matrix metalloproteinases. *Curr. Opin. Cell Biol.* 16: 558-564.

195. Gordon, J. R., and S. J. Galli. 1994. Promotion of mouse fibroblast collagen gene expression by mast cells stimulated via the Fc epsilon RI. Role for mast cell-derived transforming growth factor beta and tumor necrosis factor alpha. *J. Exp. Med.* 180: 2027-2037.

196. Chiaradonna, F., D. Gaglio, M. Vanoni, and L. Alberghina. 2006. Expression of transforming K-Ras oncogene affects mitochondrial function and morphology in mouse fibroblasts. *Biochim. Biophys. Acta* 1757: 1338-1356.

197. Strutz, F., H. Okada, C. W. Lo, T. Danoff, R. L. Carone, J. E. Tomaszewski, and E. G. Neilson. 1995. Identification and characterization of a fibroblast marker: FSP1. *J. Cell Biol.* 130: 393-405.

198. Okuda, M., A. Togawa, H. Wada, and S. Nishikawa. 2007. Distinct activities of stromal cells involved in the organogenesis of lymph nodes and Peyer's patches. *J. Immunol.* 179: 804-811.

199. Filer, A., M. Bik, G. N. Parsonage, J. Fitton, E. Trebilcock, K. Howlett, M. Cook, K. Raza, D. L. Simmons, A. M. Thomas, M. Salmon, D. Scheel-Toellner, J. M. Lord, G. A. Rabinovich, and C. D. Buckley. 2009. Galectin 3 induces a distinctive pattern of cytokine and chemokine production in rheumatoid synovial fibroblasts via selective signaling pathways. *Arthritis Rheum.* 60: 1604-1614.

200. Wang, Y., D. D. Belsham, and M. Glogauer. 2009. Rac1 and Rac2 in Osteoclastogenesis: A Cell Immortalization Model. *Calcif. Tissue Int.*

201. Mortlock, D. P., and J. W. Innis. 1997. Mutation of HOXA13 in hand-foot-genital syndrome. *Nat. Genet.* 15: 179-180.

202. Stasinopoulos, I. A., Y. Mironchik, A. Raman, F. Wildes, P. Winnard, Jr., and V. Raman. 2005. HOXA5-twist interaction alters p53 homeostasis in breast cancer cells. *J. Biol. Chem.* 280: 2294-2299.

203. Prabagaran, E., A. H. Bandivdekar, V. Dighe, and V. P. Raghavan. 2007. HOXBES2: a novel epididymal HOXB2 homeoprotein and its domain-specific association with spermatozoa. *Biol. Reprod.* 76: 314-326.

204. Connell, K. A., M. K. Guess, H. W. Chen, T. Lynch, R. Bercik, and H. S. Taylor. 2009. HOXA11 promotes fibroblast proliferation and regulates p53 in uterosacral ligaments. *Reprod. Sci.* 16: 694-700.

205. Di Poi, N., J. Zakany, and D. Duboule. 2007. Distinct roles and regulations for HoxD genes in metanephric kidney development. *PLoS. Genet.* 3: e232.

206. Zuniga, A., O. Michos, F. Spitz, A. P. Haramis, L. Panman, A. Galli, K. Vintersten, C. Klasen, W. Mansfield, S. Kuc, D. Duboule, R. Dono, and R. Zeller. 2004. Mouse limb deformity mutations disrupt a global control region within the large regulatory landscape required for Gremlin expression. *Genes Dev.* 18: 1553-1564.

207. Semb, H., and G. Christofori. 1998. The tumor-suppressor function of E-cadherin. *Am. J. Hum. Genet.* 63: 1588-1593.

208. Teague, T. K., P. Marrack, J. W. Kappler, and A. T. Vella. 1997. IL-6 rescues resting mouse T cells from apoptosis. *J. Immunol.* 158: 5791-5796.

209. Vella, A., T. K. Teague, J. Ihle, J. Kappler, and P. Marrack. 1997. Interleukin 4 (IL-4) or IL-7 prevents the death of resting T cells: stat6 is probably not required for the effect of IL-4. *J. Exp. Med.* 186: 325-330.

210. Akbar, A. N., N. J. Borthwick, R. G. Wickremasinghe, P. Panayoitidis, D. Pilling, M. Bofill, S. Krajewski, J. C. Reed, and M. Salmon. 1996. Interleukin-2 receptor common gamma-chain signaling cytokines regulate activated T cell apoptosis in response to growth factor withdrawal: selective induction of anti-apoptotic (bcl-2, bcl-xL) but not pro-apoptotic (bax, bcl-xS) gene expression. *Eur. J. Immunol.* 26: 294-299.

211. Luther, S. A., A. Bidgol, D. C. Hargreaves, A. Schmidt, Y. Xu, J. Paniyadi, M. Matloubian, and J. G. Cyster. 2002. Differing activities of homeostatic chemokines CCL19, CCL21, and CXCL12 in lymphocyte and dendritic cell recruitment and lymphoid neogenesis. *J. Immunol.* 169: 424-433.

212. Bacso, Z., R. B. Everson, and J. F. Eliason. 2000. The DNA of annexin V-binding apoptotic cells is highly fragmented. *Cancer Res.* 60: 4623-4628.

213. Homey, B., H. Alenius, A. Muller, H. Soto, E. P. Bowman, W. Yuan, L. McEvoy, A. I. Lauerma, T. Assmann, E. Bunemann, M. Lehto, H. Wolff, D. Yen, H. Marxhausen, W. To, J. Sedgwick, T. Ruzicka, P. Lehmann, and A. Zlotnik. 2002. CCL27-CCR10 interactions regulate T cell-mediated skin inflammation. *Nat. Med.* 8: 157-165.

214. Schulz, E. G., L. Mariani, A. Radbruch, and T. Hofer. 2009. Sequential polarization and imprinting of type 1 T helper lymphocytes by interferon-gamma and interleukin-12. *Immunity.* 30: 673-683.

215. Pisabarro, M. T., B. Leung, M. Kwong, R. Corpuz, G. D. Frantz, N. Chiang, R. Vandlen, L. J. Diehl, N. Skelton, H. S. Kim, D. Eaton, and K. N. Schmidt. 2006. Cutting edge: novel human dendritic cell- and monocyte-attracting chemokine-like protein identified by fold recognition methods. *J. Immunol.* 176: 2069-2073.

216. Duckett, C. S., and C. B. Thompson. 1997. CD30-dependent degradation of TRAF2: implications for negative regulation of TRAF signaling and the control of cell survival. *Genes Dev.* 11: 2810-2821.

217. Zelante, T., A. De Luca, P. Bonifazi, C. Montagnoli, S. Bozza, S. Moretti, M. L. Belladonna, C. Vacca, C. Conte, P. Mosci, F. Bistoni, P. Puccetti, R. A. Kastelein, M. Kopf, and L. Romani. 2007. IL-23 and the Th17 pathway promote inflammation and impair antifungal immune resistance. *Eur. J. Immunol.* 37: 2695-2706.

218. Ruddle, N. H., and R. Homer. 1988. The role of lymphotoxin in inflammation. *Prog. Allergy* 40: 162-182.

219. Ruddle, N. H. 1999. Lymphoid neo-organogenesis: lymphotoxin's role in inflammation and development. *Immunol. Res.* 19: 119-125.

220. Rothkotter, H. J., and R. Pabst. 1990. Autotransplantation of lymph node fragments. Structure and function of regenerated tissue. *Scand. J. Plast. Reconstr. Surg. Hand Surg.* 24: 101-105.

221. Yamada, K., A. Shimizu, R. Utsugi, F. L. Ierino, P. Gargollo, G. W. Haller, R. B. Colvin, and D. H. Sachs. 2000. Thymic transplantation in miniature swine. II. Induction of tolerance by transplantation of composite thymokidneys to thymectomized recipients. *J. Immunol.* 164: 3079-3086.

222. Glanville, S. H., V. Bekiaris, E. J. Jenkinson, P. J. Lane, G. Anderson, and D. R. Withers. 2009. Transplantation of embryonic spleen tissue reveals a role for adult non-lymphoid cells in initiating lymphoid tissue organization. *Eur. J. Immunol.* 39: 280-289.

223. Zhang, J., R. Cao, Y. Zhang, T. Jia, Y. Cao, and E. Wahlberg. 2009. Differential roles of PDGFR-alpha and PDGFR-beta in angiogenesis and vessel stability. *FASEB J.* 23: 153-163.

224. Buckley, C. D., S. Halder, D. Hardie, G. Reynolds, R. Torensma, V. J. De Villeroche, D. Brouty-Boye, and C. M. Isacke. 2005. Report on antibodies submitted to the stromal cell section of HLDA8. *Cell Immunol.* 236: 29-41.

225. Halder, S., D. L. Hardie, D. Scheel-Toellner, M. Salmon, and C. D. Buckley. 2005. Generation and characterization of novel stromal specific antibodies. *Cell Res.* 15: 739-744.

226. Chen, C., J. L. Mobley, O. Dwir, F. Shimron, V. Grabovsky, R. R. Lobb, Y. Shimizu, and R. Alon. 1999. High affinity very late antigen-4 subsets expressed on T cells are mandatory for spontaneous adhesion strengthening but not for rolling on VCAM-1 in shear flow. *J. Immunol.* 162: 1084-1095.

227. Seemayer, C. A., S. Kuchen, M. Neidhart, P. Kuenzler, V. Rihoskova, E. Neumann, M. Pruschy, W. K. Aicher, U. Muller-Ladner, R. E. Gay, B. A. Michel, G. S. Firestein, and S. Gay. 2003. p53 in rheumatoid arthritis synovial fibroblasts at sites of invasion. *Ann. Rheum. Dis.* 62: 1139-1144.

228. Buckley, C. D., A. Filer, O. Haworth, G. Parsonage, and M. Salmon. 2004. Defining a role for fibroblasts in the persistence of chronic inflammatory joint disease. *Ann. Rheum. Dis.* 63 Suppl 2: ii92-ii95.

229. Bernstein, B. E., M. Kamal, K. Lindblad-Toh, S. Bekiranov, D. K. Bailey, D. J. Huebert, S. McMahon, E. K. Karlsson, E. J. Kulbokas, III, T. R. Gingeras, S. L. Schreiber, and E. S. Lander. 2005. Genomic maps and comparative analysis of histone modifications in human and mouse. *Cell* 120: 169-181.

Chapter Eight

Appendix

CHAPTER EIGHT

Appendix

Please see enclosed CD for appendix data.

8.1 Fibroblast low density array genes.

8.2 Fibroblast low density array normalised data.

8.3 Whole genome array genes and normalised results for all samples.

8.4 Gene expression that differed significantly from whole genome microarrays between peripheral and lymphoid samples.

8.5 Gene expression that differed significantly from whole genome microarrays between immortialised and *in vitro* cultured lymph node samples.

8.6 Site specific low density array genes.

8.7 Site specific low density array normalised data.

8.8 Ligand low density array genes.

8.9 Ligand low density array normalised data.

8.10 Gene expression that differed significantly from the ligand low density array between LTα treated and untreated stromal cell cultures.

Publications arising from this thesis

1. **Flavell,S.J.,** Hou,T.Z., Lax,S., Filer,A.D., Salmon,M., Buckley,C.D. Fibroblasts as novel therapeutic targets in chronic inflammation. *Br J Pharmacol*. 2008; 153: S241-S246.
2. Hou,T.Z., Mustafa,M.Z., **Flavell,S.J.,** Barrington,A.F., Jenkinson,E.J., Anderson,G., Lane,P.J., Withers,D.R., Buckley,C.D. Splenic stromal cells mediate IL-7 independent adult lymphoid tissue inducer cell survival. *Eur J Immunol*. 2009; 10.1002/eji.200939776